CRITICAL REVIEW

Check for updates

Latest technological advances and insights into capture and removal of hydrogen sulfide: a critical review

Muhammad Syahir Aminuddin, [iD] *[ab] Mohamad Azmi Bustam[ab] and Khairiraihanna Johari [iD] *[ac]

Hydrogen sulfide is an extremely toxic, poisonous and flammable gas often found in natural gas streams and crude oil reservoirs. Due to its hazardous and corrosive nature, it must be effectively removed to protect human health and for economic reasons. To overcome these issues, various technologies and methods have been implemented for efficient capture of H_2S. This work presents a comprehensive review of various up-to-date technologies and materials such as ionic liquids, deep eutectic solvents, carbon-based adsorbents, zeolites, metal organic frameworks, membranes and composite materials. Furthermore, an in-depth discussion for each technology and class of material is also included. Besides, potential opportunities and limitations are also identified to further enhance the development in future research. By evaluating eco-friendly and cost-effective techniques, our work contributes to reducing harmful emission of H_2S, protecting air quality and promoting cleaner industries. Our work aligns with the UN's sustainable development goals, specifically SDG 7 (affordable and clean energy) and SDG 13 (climate action), by advocating for a cleaner and more sustainable energy sector, as well as SDG 9 (industry, innovation, and infrastructure) through innovative solutions for cleaner industrial processes.

Sustainability spotlight

To minimize the impact of global climate change and environmental degradation, it is of paramount importance to address the urgent need to capture and remove hydrogen sulfide, an extremely toxic and pollutant gas. Our review paper provides a comprehensive analysis of cutting-edge methods that promise sustainable solutions for this critical issue. By evaluating eco-friendly and cost-effective techniques, our work contributes to reducing harmful emission of H_2S, protecting air quality and promoting cleaner industries. Our work aligns with the UN's sustainable development goals, specifically SDG 7 (affordable and clean energy) and SDG 13 (climate action), by advocating for a cleaner and more sustainable energy sector, as well as SDG 9 (industry, innovation, and infrastructure) through innovative solutions for cleaner industrial processes.

1. Introduction

Hydrogen sulfide (H_2S) conversion and capture has presented a persistent economic and environmental challenge throughout the last century.[1] H_2S is a noxious, foul-smelling, and toxic substance that frequently contaminates crucial fuel gases.[2] It is essential to eliminate this compound from these streams due to both economic and safety concerns. The natural tendency of H_2S to create acidic solutions when combined with water leads to corrosive damage in equipment and pipelines.[3] Additionally, the presence of H_2S in fuel gases diminishes the heating value[4] and causes catalyst poisoning.[4] Notably, the combustion of H_2S generates sulfur dioxide and other harmful sulfur oxides, which contribute to acid rain.[5] Furthermore, as indicated in Table 1, H_2S is a toxic gas that poses hazards even at low concentrations.[6,7] Prolonged exposure to around 5 ppm causes irritation of the eyes and respiratory system, while concentrations of 1000–2000 ppm result in immediate fatality. Hence, it is crucial to control and limit H_2S emissions to enhance worldwide atmospheric chemistry and improve overall life quality.[8]

Consequently, to utilize various fuel gases for generating energy or chemical manufacturing, it becomes necessary to purify them by eliminating and/or converting acid gases such as H_2S and CO_2. The acceptable level of H_2S in a gas stream relies on the specific intended use and local regulations. For instance, in the United States and Denmark, pipeline gas must contain less than 4 ppm of H_2S,[9] whereas fuel cell and reformer

[a]Department of Chemical Engineering, Universiti Teknologi PETRONAS, 32610 Bandar Seri Iskandar, Perak, Malaysia. E-mail: khairiraihana.j@utp.edu.my

[b]Centre of Research in Ionic Liquids (CORIL), Universiti Teknologi PETRONAS, 32610 Bandar Seri Iskandar, Perak, Malaysia

[c]CO₂ Research Centre (CO2RES), Universiti Teknologi PETRONAS, 32610 Bandar Seri Iskandar, Perak, Malaysia

Table 1 Acute health symptoms at various concentrations of H_2S[6,7]

Concentration (ppm)	Acute health symptoms
0.0001–0.0003	Standard ambient levels
0.01–1.5	Minimum limit where the distinctive smell of rotten egg becomes noticeable
2–5	Extended exposure might lead to headaches, nausea and insomnia
20	May cause fatigue, headache, appetite loss, forgetfulness, irritability and nausea
50–100	Irritation to respiratory tract and slight conjunctivitis "gas eyes" after 1 hour
	Might lead to loss of appetite and digestive upset
100–150	Eye irritation, coughing and loss of smell within 2 to 15 minutes
	Altered breathing and sleepiness after 15 to 30 minutes
	Sore throat after 1 hour
	The symptom severity increases steadily over several hours
	Death possibility after 48 hours
200–300	Evident conjunctivitis and irritation of breathing passages after 60 minutes
	Extended exposure may cause pulmonary edema to occur
500–700	Staggering, loss of coordination and collapse after 5 minutes
	Serious eye damage in 30 minutes
	Death within 30 to 60 minutes
700–1000	Death within several minutes due to respiratory paralysis
	Instant "knockdown" or collapse within a few breaths
1000–2000	Almost instant death

applications typically need lower than 1 ppm of H_2S.[10,11] The techniques for H_2S capture can be categorized into several classes such as absorption, adsorption, chemical conversion, membrane separation and cryogenic distillation. This extensive review focuses on the latest developments in each of these technologies, with a particular emphasis on advancements made within the past 5 to 15 years. Each technique has its own sets of advantages and disadvantages influenced by various aspects, which will be elaborated upon in the following sections. The summary of technology selection for this review is presented in Fig. 1.

2. Technologies for H_2S capture and removal

2.1. Absorption

Absorption is among the most established technologies in the oil and gas industry for removal of acid gases such as H_2S and CO_2 from natural gas streams using a liquid solvent.[12] H_2S absorption involves transfer of H_2S from the gas feed into the physical or chemical solvent in the packed or plated conventional absorption columns. In general, the reaction
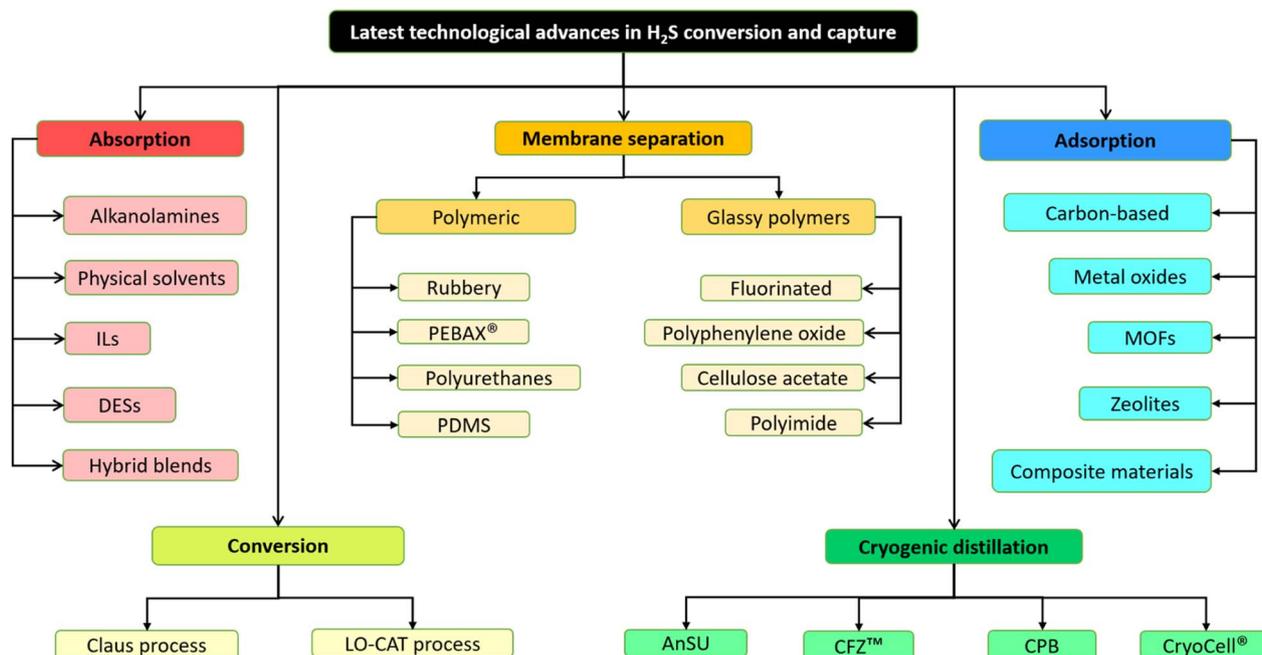

Fig. 1 The summary of technology selection for H_2S removal and capture.

mechanisms for the absorption process can be divided into two categories such as chemical and physical absorption, based on the interaction strength between the solvents and H_2S.

Chemical absorption involves strong chemical bonds that are difficult to break, whereas physical absorption involves weak intermolecular forces that are easier to overcome. Typically, chemical absorption operates at low pressure, while physical absorption requires high pressure to operate optimally. As a result, physical solvents are preferable as compared to chemical solvents under the conditions where the feed gas contains high H_2S concentrations and partial pressure. Physical solvent systems are identical to chemical solvent systems but are dependent on the gas solubility in the solvent instead of reaction stoichiometry.

The solubility of acid gases such as H_2S and CO_2 is heavily reliant on the gas partial pressure and reaction temperature of the system. Higher partial pressures lead to higher gas solubility. In contrast, low temperatures lead to higher gas solubility. However, in general, temperature is not as critical as pressure. Moreover, the solvents can be regenerated by adjusting the pressure and temperature.[13] Absorption methods can be classified into five major classes such as alkanolamines, physical solvents, ionic liquids (ILs), deep eutectic solvents (DESs) and hybrid blends. Table 2 provides the summary of recent studies on H_2S absorption using the different classes of solvents stated beforehand.

2.1.1 Alkanolamines. Alkanolamines are the most common chemical solvents for acid gas removal *via* absorption from natural gas streams.[43] Absorption by alkanolamines is also widely regarded as the most mature technology for acid gas removal due to their widespread applications in the oil and gas industry.[44,45] Alkanolamine solutions such as diisopropanolamine (DIPA), methyldiethanolamine (MDEA), diethanolamine (DEA), monoethanolamine (MEA), diglycolamine (DGA), triethanolamine (TEA) and 2-amino-2-methyl-1-propanol (AMP) are widely used as solvents for dissolving H_2S and CO_2 despite having different absorption performances.[46] Nonetheless, other types of solvents such as sodium hydroxide (NaOH), potassium carbonate (K_2CO_3), sodium carbonate (Na_2CO_3), sodium hypochlorite (NaClO) and piperazine (PZ) have also been used for H_2S absorption[14,47,48] in recent years.

Besides, there are also a large number of conventional solvents available for acid gas absorptive removal such as ADIP, ADEG. OASE, FLEXSORB, GAS/SPEC and UCARSOL series. Privately owned amine processes of low energy by oil companies such as Shell, *i.e.*, ADIP and Sulfinol;[49] and ExxonMobil, *i.e.*, FLEXSORB™SE[50] and OASE®sulfexx™[51] were able to selectively remove H_2S in the presence of CO_2 commercially. The long-established hot potassium carbonate (HPC) process was pioneered by Benson and Field, before being licensed by Universal Oil Products (UOP) as the UOP Benfield™ process.[52] On the other hand, the CATACARB® process which utilizes enhanced HPC technology is commercially proven, with over 150 plants in 30 different countries worldwide facilitating a variety of applications such as natural gas, ammonia, hydrogen and ethylene oxide.[52]

In chemical solvent processes, the acid gas feed enters the absorption columns at high pressure between 5 and 205 bar and low temperature between 35 and 50 °C, while the solvent enters the regenerator at high temperature between 115 and 130 °C and low pressure between 1.4 and 1.7 bar.[53] Generally, primary amines (MEA) and secondary amines (DEA) are more reactive towards acid gas, whereas tertiary amines (MDEA) and sterically hindered amines (AMP) are less reactive but possess higher selectivity towards H_2S.

MEA is the most widely used alkanolamine for removal of acid gas due to certain factors such as low cost, low hydrocarbon solubility, high reactivity and ease of recovery. However, MEA suffers from various drawbacks such as strong affinity towards CO_2, zero selectivity towards H_2S, stable carbamate formation, and highly volatility, corrosivity and degradability, thus limiting its absorption potential.[54,55] Similarly, DEA has advantages comparable to those of MEA but is less corrosive and has higher vapor pressure.[56] MDEA surpasses both DEA and MEA in performance and efficiency due to its high loading capacity, high selectivity towards H_2S, low vapor pressure, low corrosivity and high efficiency. Conversely, when MEA and DEA react with CO_2, they form stable carbamates, resulting in a reduced hydrolysis rate to bicarbonate, consequently leading to low absorption of H_2S into the amines.[57] In contrast, AMP reacts with CO_2 to form unstable carbamates, whereas MDEA does not form any carbamates, making them more favorable choices compared to MEA and DEA.[58]

Among these solvents, a combination of MEA and DEA is commonly used in the sweetening process of natural gas streams. Industrially, aqueous MDEA is mixed with primary or secondary amines such as 2-tertiarybutylamino-2-ethoxyethanol (TBEE), AMP, DGA, MEA, DEA and DIPA to obtain desirable performance and effects. Primary or secondary amines were used as they have higher reaction rates, whereas MDEA has a higher equilibrium capacity. It is also common that three different types of solvents were mixed to achieve the desired target. The blended solvents offer a combined effect of a high reaction rate and high equilibrium capacity. However, these multi-solvent systems involve very complex chemical reactions causing the solvents to be hard to regenerate. Moreover, the gas stripping process at elevated temperatures is an energy intensive process, leading to solvent losses due to thermal degradation and volatilization.[59]

Abdulrahman and Sebastine[60] investigated the best solvent for simultaneous removal of acid gases among MEA, DEA and MDEA. They suggested that 35 wt% DEA is the best and most cost-effective solvent for removal of both CO_2 and H_2S gases. Another study by Mandal *et al.*[61] revealed that MDEA performs slightly better as compared to AMP in H_2S absorption. Lu *et al.*[53] discovered that the performance of an aqueous blend consisting of 1.5 kmol m^{-2} of MDEA and 1 kmol m^{-2} of TBEE is far higher than that of 2.5 kmol m^{-2} of MDEA alone for selective removal of H_2S. The authors also deduced that both primary and secondary sterically hindered amines, *i.e.*, TBEE and AMP, exhibited comparable characteristics to tertiary amines such as MDEA. Moreover, Li *et al.*[19] and Du *et al.*[19] investigated the performance of AMP and 2-*tert*-butylamino ethanol (TBE) for

Table 2 Key findings on conventional H_2S removal technologies by absorption

Solvents	Feed gas	Operating conditions and H_2S partial pressure	Solubility/loading (mol mol^{-1})	H_2S removal efficiency	Reference
Alkanolamines					
30–50 wt% MDEA + 80 wt% MEA	Simulated coke oven gas	Temperature: 30–50 °C, partial pressure: 0.003–0.005 bar	0.022–0.096	93.6–95.9% (6 sieve trays)	14
3.5–11.6 wt% MEA	Gases: H_2S and CH_4	Temperature: 40–60 °C, partial pressure: 0–0.45 bar	−0.1–1.0	n/a	15
19.0–46.3 wt% MDEA		Partial pressure: 0.01–0.5 bar	−0.05–0.85	n/a	16
5.6 wt% MEA + 26.3 wt% MDEA + 3–7 wt% PZ		Partial pressure: 0.04–0.55 bar	−0.09–0.95	n/a	
20 wt% MDEA	Gases: H_2S and N_2	Temperature: 5–40 °C, partial pressure: 0.0003–0.01 bar	0.015–0.25	100%	
20 wt% MDEA + 80 wt% MEG		Temperature: 5 °C, partial pressure: 0.0003–0.01 bar	0.01–0.09	77%	
20 wt% MDEA + 80 wt% TEG			0.006–0.040	17%	
20 wt% t-BDEA			0.009–0.407	n/a	
20 wt% DIPA			0.012–0.185	n/a	
20 wt% TEA			0.013–0.165	n/a	
20–50 wt% DEAE-EO	Gases: H_2S and N_2	Temperature: 5–40 °C, partial pressure: 0.005–0.01 bar	0.094–0.416	100%	
20 wt% DEAE-EO + 80 wt% MEG		Temperature: 5 °C, partial pressure: 0.01 bar	0.280	76%	
20 wt% DEAE-EO + 80 wt% TEG			0.073	21%	
20–50 wt% 3DEA-1P	Gases: H_2S and N_2	Temperature: 5–40 °C, partial pressure: 0.005–0.01 bar	0.061–0.355	100%	
20 wt% 3DEA-1P + 80 wt% MEG		Temperature: 5 °C, partial pressure: 0.01 bar	0.193	57%	
20 wt% 3DEA-1P + 80 wt% TEG			0.080	24%	
MDEA + PZ	10 000 ppmv H_2S and remaining CO_2	Temperature: 30–45 °C, partial pressure: 1 bar	n/a	100%	17
10–30 wt% TBE	15 mol% H_2S and 85 mol% CO_2	Temperature: 25–45 °C, partial pressure: n/a	n/a	50–94%	18 and 19
10–30 wt% AMP			n/a	65–95%	20
ILs					
$[N_{2224}]_2$[maleate]	Gas: H_2S	Temperature: 40 °C, partial pressure: 1.1 bar	1.43	n/a	
$[N_{2224}]_2$[maleate] + maleic acid (1 : 1)		Partial pressure: 1.18 bar	1.30	n/a	
[BDMAEEH][NTf$_2$] + MAA (1 : 1)			0.8	n/a	
[BDMAEEH][MAA]			1.0	n/a	
[BDMAEEH][NTf$_2$]		Partial pressure: 1.1 bar	0.4	n/a	

Table 2 (*Contd.*)

Solvents	Feed gas	Operating conditions and H$_2$S partial pressure	Solubility/loading (mol mol^{-1})	H$_2$S removal efficiency	Reference
[DBNH][1,2,4-triaz]	Gas: H$_2$S	Temperature: 25 °C, partial pressure: 1 bar	1.4	n/a	21
		Temperature: 40 °C, partial pressure: 0.012–0.019 bar	0.253–1.198	n/a	
		Temperature: 60 °C, partial pressure: 1 bar	1.0	n/a	
[DBNH][1,2,3-triaz]	Gas: H$_2$S	Temperature: 60 °C, partial pressure: 0.016–1.089 bar	0.287–1.081	n/a	
[DBUH][1,2,4-triaz]		Partial pressure: 0.02–1.03 bar	0.447–1.174	n/a	
[DBUH][1,2,3-triaz]		Partial pressure: 0.02–1.03 bar	0.412–1.046	n/a	
[DBNH][Im]	Gas: H$_2$S	Temperature: 25 °C, partial pressure: 0.1 bar	1.18	n/a	22
		Partial pressure: 0.01–1 bar	0.63–1.36	n/a	
		Temperature: 40 °C, partial pressure: 0.1 bar	0.95	n/a	
		Partial pressure: 0.01–1 bar	0.40–1.26	n/a	
		Temperature: 60 °C, partial pressure: 0.01–1 bar	0.27–1.08	n/a	
[DBUH][Im]	Gas: H$_2$S	Temperature: 40 °C, partial pressure: 0.1–1 bar	0.98–1.26	n/a	
[DBNH][Pyr]			0.99–1.31	n/a	
[DBUH][Pyr]			0.95–1.17	n/a	
[TMGH][PhO]	Gas: H$_2$S	Temperature: 25 °C, partial pressure: 0.1 bar	0.69	n/a	23
		Partial pressure: 0.01–1 bar	0.38–0.97	n/a	
		Temperature: 40 °C, partial pressure: 0.1 bar	0.56	n/a	
		Partial pressure: 0.01–1 bar	0.20–0.85	n/a	
		Temperature: 60 °C, partial pressure: 0.1 bar	0.47	n/a	
		Partial pressure: 0.01–1 bar	0.08–0.78	n/a	
[DBUH][PhO]		Temperature: 40 °C, partial pressure: 0.1–1 bar	0.6–0.8	n/a	
[Hmim][PhO]			0.59–0.84	n/a	
[P$_{4444}$][PhO]			0.62–0.88	n/a	
40–70 wt% [BDMAEE][Ac]		Temperature: 25 °C, partial pressure: 1 bar	0.950–1.044	n/a	24
[NEMH][Bu]		Temperature: 25 °C, partial pressure: 0.035–1.056 bar	0.012–0.156	n/a	25
		Temperature: 35 °C, partial pressure: 0.056–1.07 bar	0.008–0.114	n/a	
		Temperature: 45 °C, partial pressure: 0.03–1.05 bar	0.007–0.098	n/a	

Table 2 (*Contd.*)

Solvents	Feed gas	Operating conditions and H$_2$S partial pressure	Solubility/loading (mol mol^{-1})	H$_2$S removal efficiency	Reference
[NEMH][Ac]		Temperature: 25 °C, partial pressure: 0.04–1.06 bar	0.009–0.127	n/a	
[NEMH][Pro]			0.011–0.151	n/a	
[NEMH][MoAc]			0.010–0.142	n/a	
[TEAH][Bu]		Partial pressure: 0.04–1.1 bar	0.009–0.135	n/a	
[TEAH][MoAc]		Partial pressure: 0.06–1.02 bar	0.010–0.138	n/a	
[C$_4$Py][BF$_4$]	Gas: H$_2$S	Temperature: 40 °C, partial pressure: 1 bar	0.07	n/a	26
[C$_4$Py][SCN]		Partial pressure: 1 bar	0.1	n/a	
[Emim][BF$_4$]		Temperature: 25 °C, partial pressure: 0.003–14 bar	0–1.46	n/a	27
		Temperature: 40 °C, partial pressure: 0.003–18.4 bar	0–1.26	n/a	
		Temperature: 60 °C, partial pressure: 0.003–18.2 bar	0–0.674	n/a	
		Temperature: 80 °C, partial pressure: 0.003–17.6 bar	0–0.425	n/a	
DESs					
ChCl-urea (1 : 1.5)		Temperature: 40 °C, partial pressure: 0.11–2.02 bar	0.0037–0.055	n/a	28
		Temperature: 50 °C, partial pressure: 0.11–2.01 bar	0.0025–0.046	n/a	
		Temperature: 60 °C, partial pressure: 0.10–2.02 bar	0.0021–0.037	n/a	
		Temperature: 80 °C, partial pressure: 0.1–1.98 bar	0.0014–0.023	n/a	
ChCl-urea (1 : 2)		Temperature: 40–80 °C, partial pressure: 0.10–2.02 bar	0.0015–0.046	n/a	
ChCl-urea (1 : 2.5)		Temperature: 40–80 °C, partial pressure: 0.10–2.01 bar	0.0011–0.035	n/a	
TBAB-ProH (1 : 1)	Gas: H$_2$S	Temperature: 25 °C, partial pressure: 2.45–4.96 bar	0.40–0.60	n/a	29
TBAB-AcH (1 : 1)		Partial pressure: 2.25–5.11 bar	0.32–0.59	n/a	
TBAB-ForH (1 : 1)		Partial pressure: 1.78–5.06 bar	0.21–0.55	n/a	
ChCl-ProH (1 : 2)		Partial pressure: 1.84–5.40 bar	0.13–0.44	n/a	
ChCl-AcH (1 : 2)		Partial pressure: 2.49–5.22 bar	0.16–0.33	n/a	
ChCl-ForH (1 : 2)		Partial pressure: 2.62–5.10 bar	0.12–0.25	n/a	
[C$_4$-TMHDA][Cl]-Im (1 : 2)	Gases: H$_2$S, CH$_4$, and CO$_2$	Temperature: 30 °C, partial pressure: 1 bar	0.99	n/a	30
[C$_4$-TMPDA][Cl]-Im (1 : 2)			0.48	n/a	
[C$_4$-TMEDA][Cl]-Im (1 : 2)			0.36	n/a	
[C$_4$-TMEDA][Cl]-1,2,4-triaz (1 : 2)			0.27	n/a	
[C$_4$-TMEDA][Cl]-1,2,3-triaz (1 : 2)			0.24	n/a	

Table 2 (*Contd.*)

Solvents	Feed gas	Operating conditions and H$_2$S partial pressure	Solubility/loading (mol mol^{-1})	H$_2$S removal efficiency	Reference
[C$_4$-TMHDA][Cl]-Im (1:2)		Temperature: 40 °C, partial pressure: 1 bar	0.71	n/a	
[C$_1$-TMHDA][Ac]-MDEA (1:2)	Gases: H$_2$S, CH$_4$, and CO$_2$	Temperature: 40 °C, partial pressure: 1 bar	1.44	n/a	31
[C$_1$-TMHDA][Ac]-pyrol (1:2)			1.17	n/a	
[C$_1$-TMHDA][Ac]-AA (1:2)			1.09	n/a	
[C$_1$-TMHDA][Ac]-Im (1:2)			1.02	n/a	
Hybrid blends					
30–50 wt% MDEA + 2.5–7.5 wt% [N$_{1111}$][Arg]	Simulated coke oven gas	Temperature: 30–50 °C, partial pressure: 0.003–0.005 bar	0.039–0.143	100% (requires 4 sieve trays)	32
30–50 wt% MDEA + 2.5–7.5 wt% [N$_{1111}$][Gly]	Simulated coke oven gas	Temperature: 30–50 °C, partial pressure: 0.003–0.005 bar	0.035–0.98	100% (requires 6 sieve trays)	14
30–50 wt% DIPA + 5–50 wt% [Bmim][Ac]	30 mol% CO$_2$ and H$_2$S	Temperature: 50–75 °C, partial pressure: 0.46–6.68 bar	0.010–0.153	n/a	33
Benchmarks					
Dimethyl sulfoxide (DMSO)	Gas: H$_2$S	Temperature: 25 °C, partial pressure: 1 bar	0.123	n/a	34
N-methyl-2-pyrrolidone (NMP)	Gas: H$_2$S	Temperature: 25 °C, partial pressure: 1 bar	0.013	n/a	35
Sulfolane	Gas: H$_2$S	Temperature: 25 °C, partial pressure: 1 bar	0.072	n/a	36
		Temperature: 40 °C, partial pressure: 1 bar	0.043	n/a	
50 wt% MDEA	Gas: H$_2$S	Temperature: 25 °C, partial pressure: 1 bar	0.944	n/a	37
		Temperature: 40 °C, partial pressure: 0.1–1 bar	0.3–0.85	n/a	
	Gases: CH$_4$ and H$_2$S	Temperature: 50 °C, partial pressure: 0.026–1.78 bar	0.084–0.775	n/a	38
[Bmim][PF$_6$]	Gas: H$_2$S	Temperature: 25–130 °C, partial pressure: 0.69–96.30 bar	0.016–0.875	n/a	39
Methanol	Gas: H$_2$S	Temperature: 25 °C, partial pressure: 1 bar	0.027	n/a	40
[TEGDME]		Partial pressure: 14 bar	0.8	n/a	41
	Gas: H$_2$S	Temperature: 40 °C, partial pressure: 1 bar	0.162	n/a	42

selective removal of H_2S from a feed gas that contains 15% H_2S and 85% CO_2. AMP has a higher performance and selectivity towards H_2S at low amine concentrations, whereas TBE performs better at high amine concentrations and displayed slightly higher selectivity towards H_2S as compared to AMP. Nevertheless, both AMP and TMP have a similar removal efficiency for H_2S.

An activator is typically added to the aqueous amine blend as an additive to enhance the base amine performance. Piperazine (PZ) is an example of a commonly used activator in amine blends because of its high resistance to oxidative and thermal decomposition.[62] Sheng et al.[63] and Lin et al.[64] recorded a higher reaction rate of PZ with CO_2 as compared to that of other conventional solvents such as MEA, DEA, MDEA and AMP. Nguyen et al.[65] and Dash et al.[66] reported that the blends of amines and PZ possess lower volatility than the amines alone as the blends typically form non-ideal solutions. On the other hand, Yunhai et al.[15] evaluated the performance of MEA, MDEA, a mixture of MEA and MDEA and a mixture of MEA, MDEA and PZ for H_2S capture from natural gas streams. They reported that the performance of MEA was the highest followed by the mixture of MEA, MDEA and PZ, the mixture of MEA and MDEA and MDEA, respectively. The results proved that PZ could improve the loading capacity of H_2S but possesses lower selectivity towards H_2S in the presence of CO_2. Meanwhile, Zhan et al.[17] investigated an aqueous blend of MDEA and PZ for H_2S absorption under different conditions. It was observed that PZ has a higher reaction rate with CO_2 as compared to MDEA. In addition, it was also noticed that a higher concentration of PZ has led to higher CO_2 removal but a lower H_2S removal efficiency. Similarly, Haghtalab and Izadi[67] also recorded a lower H_2S loading capacity with the addition of PZ to each aqueous solution of MDEA and DIPA, respectively.

Lee et al.[48] performed simultaneous absorption and desorption of H_2S and CO_2 from a feed gas containing 50 ppmv H_2S, 35% CH_4, and 15% CO_2 with the remainder being N_2 using a total of 11 aqueous blends containing 4.5 wt% MDEA and 5 wt% activator. The activators used are AMP, PZ, bis(3-aminopropyl)amine (APA), diethylenetriamine, tetraethylenepentamine, 1-dimethylamino-2-propanol, 2-amino-1-butanol, 5-amino-1-pentanol, dibutylamine, N-propylethylenediamine and 1,4-diaminobutane. PZ was found to be the best activator for CO_2 absorption but poor for H_2S absorption. On the other hand, APA demonstrated excellent performance for H_2S absorption but does not show any selectivity towards H_2S when CO_2 is present.

On the other hand, Zhan et al.[17] discovered that when the MDEA concentration rose above 1.68 mol L^{-1} in the aqueous blend of MDEA and PZ, the removal efficiency of CO_2 and H_2S declined sharply. Fu et al.[68] and Foo et al.[69] also stated that higher concentration of MDEA led to an increase in viscosity, which resulted in lower diffusivity of amine molecules in the solvent. Consequently, it led to lower capacity and absorption rate of the amine solvents. Similarly, Tian et al.[70] recorded a decreasing performance of MEA and DEA blends as the concentration of MDEA increases at low partial pressure of H_2S. Thus, it can be deduced that there should be an optimal concentration of MDEA that could lead to the highest performance in any solvent containing MDEA. The viscosity of the solvent also has a great impact on CO_2 absorption as compared to H_2S absorption. Generally, H_2S absorption is restricted by the gas mass transfer, whereas the absorption of CO_2 is restricted by reaction kinetics and liquid mass transfer.[53,61,71]

Alkanolamines are extensively utilized for acid gas removal via absorption methods due to their efficiency and versatility. Despite their wide applications in the natural gas industry, alkanolamine-based processes suffer from several drawbacks such as alkanolamine degradation, losses due to volatility, water presence in outlet gas and being energy intensive.[72] These limitations cause alkanolamine-based processes to be uneconomic and unsustainable, which has led to limited adoption outside the natural gas industry.

2.1.2 Physical solvents. In the chemical engineering context, physical solvents refer to substances used for acid gas or contaminant removal from the gas stream through the physical absorption principle, where the solvents physically interact with the polar CO_2 and H_2S molecules to capture and separate them from the gas stream without involving any chemical reaction. Generally, physical solvents operate at low temperatures and often require additional cooling, and operate at high pressures reaching up to 50 bar with H_2S partial pressures exceeding 3 bar. Physical solvents are often used when the pressure of the acid gas in the feed is above 3.45–4.14 bar, at low concentrations of heavy hydrocarbons, when there is a requirement for bulk removal of acid gas and when high selective removal of H_2S is needed. In addition, physical solvents can also remove organic sulfides, heavy hydrocarbons and carbonyl sulfide (COS). Nevertheless, physical solvent processes are only regarded as economical when the H_2S concentration is high, and the gas treatment is conducted at high pressure.[73]

There are several processes that employ physical solvents for H_2S absorption such as Selexol, Rectisol, Purisol, Fluor, Genosorb, Morphysorb, and Coastal AGR II processes. Selexol, Genosorb and Coastal AGR II use dimethyl ethers in polyethylene glycol (PEG), Rectisol uses methanol, Fluor uses propylene carbonate, Morphysorb uses N-formylmorpholine and morpholine derivatives, whereas Purisol process uses sulfolane and N-methyl-2-pyrrolidone (NMP) as solvents, respectively.[13,74] Among the listed processes, Rectisol and Selexol are the most outstanding due to their capability of acid gas deep removal and reducing the concentration of COS and H_2S to 0.01 ppm and 1 ppm, respectively. This makes Rectisol suitable for chemical synthesis applications which require less than 1 ppm of sulfur compounds. However, Rectisol is an energy-intensive process and uneconomic as the recovery process of the methanol solvent used needs a high cooling duty and large volume of water for washing. In addition, the methanol used is also highly volatile and has a low selectivity towards H_2S over CO_2. In contrast, the Selexol process exhibits exceptional selectivity for H_2S, low vapor pressure, and demonstrates high thermal and chemical stability. The only downside to the Selexol process is its high viscosity at low temperature, which contributes to lower efficiency and mass transfer rates.

By comparing all conventional physical solvents, Purisol demonstrated the highest selectivity towards H_2S in the presence of CO_2, making it highly viable for selective removal of H_2S. In addition, Purisol also possess a higher vapor pressure compared to Fluor and Selexol. Nevertheless, similar to Rectisol, Purisol needs water for washing in order to recover the spent solvents. Fluor is suitable for CO_2 bulk removal from feed gas containing a low content of H_2S with minimum loss of solvents. Moreover, Morphysorb is also excellent for selective removal of H_2S but suffers from high volatility.[75] The performance of physical solvent processes in H_2S absorption can be improved by increasing the gas pressure, as the solubility of H_2S in the solvent is directly proportional to its gas phase partial pressure.

Recently, nanofluid application for gas absorption has gained increasing attention. Nano-sized particles such as alumina, silica, graphene oxide and carbon nanotubes (CNTs) were mixed with solvents such as MEA, DEA and MDEA[76] to improve the mass transfer coefficient in three-phase systems which consist of gas, liquid and solid phases. The gas adsorption by nanoparticles aids in sustaining the flow of gas from areas of high concentration to areas of low concentration, a phenomenon commonly referred to as the shuttle effect. The collision between the gas–liquid interface and the nanoparticles causes the diffusion boundary layer to become thinner and inhibits bubble coalescence, resulting in higher contact surface area between the gas and liquid interface. The performance of Fe-5MEA-DES systems for H_2S removal was quite promising; nevertheless, the H_2S removal efficiency dropped to below 50% after the third regeneration cycle.[77] This showed the need to find better ILs which can maintain high desulfurization performance and H_2S removal efficiency after multiple regeneration cycles.

2.1.3 Ionic liquids. Ionic liquids (ILs) are liquid salts with a melting point lower than 100 °C.[78] They are a new class of environmentally friendly solvents and are gaining widespread recognition as novel solvents in chemistry due to their unique properties attractive to a variety of applications including in gas solubility, separations, catalysis, extraction, reaction media and high-temperature pyrochemical processing.[26,79,80] ILs possess various intrinsic properties such as good thermal stability, tunable viscosity and miscibility with organic solvents and water, as well as good extractability for various metal ions and organic compounds, which are highly dependent on their special structures.[81] ILs possess an extremely low or negligible vapor pressure because ILs have charged anions and cations that are held very strongly by coulombic interactions and are very difficult to break. This causes ILs to have a very low vapor pressure and remain in the liquid state without evaporating, even at high temperatures up to 400 °C.[82]

In general, ILs consist of bulky, nonsymmetrical organic cations such as imidazolium, pyrrolidinium, pyridinium, ammonium or phosphonium and various different inorganic or organic anions such as chloride and tetrafluoroborate anions. Compared to conventional solvents, ILs have many fascinating properties that make them unique. Generally, ILs are colorless liquids possessing relatively high viscosities. Under ambient

conditions, ILs exhibit very low vapor pressures contributing to their effective non-volatile nature. Due to their non-volatility, ILs have been advertised as green solvents.[83] Additionally, ILs are excellent solvents for a wide spectrum of organic, inorganic and polymeric materials and are immiscible with numerous organic solvents. The wide usage of ILs in various extraction processes as organic solvent replacements is considered a hot and interesting research topic.[84] The fact that ILs are not flammable and volatile makes them highly desirable for safer process development. Moreover, IL physicochemical properties such as hydrophobicity, polarity, viscosity and others can be tuned[85] by interchanging their constituent cations and anions. ILs are often regarded as "designer solvents" due to their tunable nature, which increases their potential uses.[86] Generally, ILs can be further divided into two major classes, ordinary ILs and task-specific ILs.

Among the first to study H_2S absorption using ILs, Jou and Mather[39] prepared [Bmim][PF$_6$] and classified it as a physical absorbent. They also deduced that ILs could be used for bulk removal of acid gas at high pressures. Pomelli et al.[41] investigated the H_2S solubility in [Bmim][NTf$_2$] and recorded a low correlation between H_2S solubility and Kamlett–Taft parameters. They deduced that the strength of anion interactions with H_2S is similar to that of hydrogen bonds and the H_2S solubility in ILs is less affected by the cations. Furthermore, the capacity and regenerability of any particular IL can be tuned by changing the anions of the IL. Wang et al.[26] found out that pyridinium-based ILs performed excellently for selective absorption of H_2S over CO_2 due to the presence of hydrogen protons in H_2S molecules. The solubility of H_2S and CO_2 was also found to have increased as the length of alkyl chains of cations increased. The solubility of H_2S increases in the following order of [BF$_4$], [C$_4$Py], [C$_4$Py][NO$_3$], [C$_4$Py][SCN], [C$_6$Py][SCN] and [C$_8$Py][SCN], respectively. By comparing the anions with similar cations, [SCN]$^-$ displayed the highest H_2S over CO_2 selectivity value of 8.99 at 30 °C. which is far higher than that of imidazolium-based ILs. On the other hand, Jalili et al.[27] reported that [Emim][BF$_4$] possesses similar absorption capacity for H_2S to that of other [BF$_4$]-based ILs and similar selectivity to other types of ILs such as [Emim][eFAP],[87] [C$_4$mim][PF$_6$],[88] [C$_8$mim][NTf$_2$][89] and [C$_8$mim][PF$_6$].[90] Nevertheless, conventional ILs act as physical absorbents and exhibit reduced absorption capacities for H_2S and CO_2 under low to moderate pressures.

To mitigate current deficiencies of ordinary ILs, new subcategories of ILs are introduced known as task-specific ionic liquids (TSILs). TSILs are specifically designed for a particular purpose of reaction such as for H_2S absorption applications.[91] Typically, TSILs are prepared by tethering one or more functionalized groups that could improve their physicochemical properties.[92] As a result, their chemical interactions with H_2S can be tailored to improve the absorption capacity of TSILs, exceeding that of ordinary ILs. Huang et al.[93] synthesized 1-alkyl-3-methylimidazolium carboxylates as TSILs for H_2S absorption. The TSILs exhibited a higher solubility of H_2S than ordinary ILs, reaching up to 0.6 mol mol^{-1} at room temperature and pressure. Nonetheless, the H_2S selectivity over CO_2 is unsatisfactorily low reaching only 1.0 at 30 °C. Consequently,

Huang et al.[94] also synthesized dual Lewis based-ILs (DLB-ILs) for selective H_2S capture over CO_2. [N_{2224}][IMA] exhibited a H_2S solubility of 0.85 mol mol^{-1} and selectivity of 10 for H_2S over CO_2 at standard temperature and pressure. Despite their advantages, DLB-ILs arevery viscous with over 2500 cP at room temperature and require complex synthesis procedures.

Furthermore, Huang et al.[95] prepared protic ionic liquids (PILs) by combining alkanolamines such as MDEA and DMEA with acetic and formic acids for selective removal of H_2S over CO_2. The synthesized PILs displayed a high selectivity of 8.9 to 19.5, and absorption capacities of 0.04 to 0.16 at 30 °C and 1 bar.[96,97] Additionally, they are also less viscous as compared to the common ILs. Zhao et al.[25] synthesized ten carboxylate-based PILs and recorded low viscosities of 4.3 cP at 25 °C and high absorption capacities of H_2S. However, these PILs are not thermally stable as most of them can be easily decomposed below 50 °C, making them unsuitable for regeneration and H_2S removal at higher temperatures. Similarly, Huang et al. prepared hydrophobic PILs functionalized with tertiary amines for selective removal of H_2S. The results showed that these PILs are highly selective towards H_2S with minimum absorption of CO_2. Consequently, Huang et al.[98] attempted to create hydrophilic PILs by replacing the tertiary amines with carboxylate groups. They observed that the solubilities of the hydrophilic PILs increases in the following order from [BMEE][Ac] to [TMEDA][Ac], [TMPDA][Ac] and [BDMAEE][Ac], respectively. As the concentration of PILs and temperature increased, the solubilities of H_2S and CO_2 were also found to have increased. Moreover, these PILs can be diluted by mixing with water.[99] Despite having a high H_2S absorption capacity of 1.044 mol mol^{-1}, aqueous PILs have a low selectivity of 1 to 2 only.

Huang et al.[23] also studied the selectivity and solubility of phenolic ILs for selective removal of polar gases, e.g., CO_2 and H_2S over non-polar gases, e.g., CH_4. They found out that the ILs are more soluble towards polar gases as compared to non-polar gases, leading to higher selectivity of H_2S and CO_2 over CH_4.[100] In addition, phenolic ILs also exhibited a decent absorption capacity of 0.6 mol mol^{-1} at 0.1 bar, which increases slightly to 0.85 mol mol^{-1} at 1 bar. Among all phenolic ILs, [TMGH][PhO] demonstrated the highest selectivity of 9.4 for H_2S absorption over CO_2. Nevertheless, phenolic ILs possess several drawbacks such as the toxic nature of phenolic compounds and high viscosities between 125.7 and 435.1 cP at 30 °C. Zhang et al.[21] studied four azole-based PILs for simultaneous removal of CO_2 and H_2S at 30 °C and 1 bar. [DBNH][1,2,4-triaz] has a high potential of becoming an excellent absorbent for H_2S due to its high absorption capacity of 1.2 mol mol^{-1} and a rather low viscosity of 42.6 cP at 40 °C. On the other hand, Xiong et al.[22] prepared four superbase PILs (SPILs) such as [DBUH][Im], [DBUH][Pyr], [DBNH][Im] and [DBNH][Pyr] for acid gas removal from natural gas.[101] SPILs possess low viscosity at 40 °C and demonstrated a remarkable H_2S absorption capacity of 6.81 mol kg^{-1} and excellent selectivity of H_2S and CO_2 over CH_4, respectively. However, their low thermal decomposition temperatures of around 80 °C hinder their regeneration capabilities and absorption at high temperatures. For example,

[DBNH][Im] lost 25% of its original absorption capacity after being regenerated four times.

Most of the ILs reported so far did not undergo a rigorous selection process to select the best IL for the H_2S absorption process but mostly rely on the trial-and-error method.[102] This is not only ineffective but failed to identify better possible combinations of anions and cations. In addition, the selection process via experimental methods is not realistic considering the huge amount of time and costs needed for completion.[103] Thus, a preliminary screening to identify desirable physical and thermodynamics properties is necessary to narrow down the selection of ILs from a vast array of possible ILs. One of the most effective ways of finding the most optimal ILs is by using a predictive model based on computational chemistry such as conductor-like screening model for real solvents (COSMO-RS). Mortazavi-Manesh et al.[104] used a COSMO-RS approach[105,106] and the Peng–Robinson equation of states[107] to screen 425 ILs for selective removal of H_2S over CO_2. From their findings, cations such as PMG, TMG and N_{4111} and anions such as CH_3SO_4, NO_3 and BF_4 were suggested as the best IL candidates. Zhao et al.[108] also utilized COSMO-RS to screen over 10 000 ILs but not for absorption of H_2S. Santiago et al.[109] integrated Aspen Plus with COSMO-RS to select from over 700 ILs with absorption process simulation using the selected ILs. The authors identified [Emim][DCN] as the IL with the highest absorption performance. By using similar methods, Lemus et al.[110] found out that hybrid blends of 75 wt% [Emim][DCN] and 25 wt% [Bmim][Ac] were able to recover over 98% of H_2S at 10 bar.

Apart from IL screening, several researchers compared industrial processes with IL-based processes to study the potential commercialization of ILs in industrial applications. Kazmi et al.[111] performed comparisons of imidazolium-based ILs with aqueous MDEA for simultaneous removal of acid gas from natural gas at a high pressure of 68 bar and 30 °C. The activation energies of ILsbased processes and MDEA were determined to be around 3981 kW and 18 619 kW, respectively. A huge reduction in activation energy of the IL-based processes was found to significantly reduce thermal energy usage by 78.6% and total annual cost by 59.8%. Additionally, the ILs are recoverable by passing through flash drums while removing the absorbed CO_2 and H_2S completely. However, the maximum absorption capacity of the ILs was not determined, making the performance hard to assess realistically. Wang et al.[112] and Yang et al.[113] compared the Rectisol process with [Bmim][NTf$_2$] for simultaneous removal of acid gas from syngas. They discovered that the process utilizing ILs is far better in terms of solvent recovery, cooling energy consumption and CO_2 capture. Based on a review by Haider et al.,[114] there is promising potential for applications of ILs in acid gas removal at lower cost as compared to the conventional methods.

It is very clear that ILs have huge potential as both CO_2 and H_2S absorbents due to their remarkable properties. The only drawbacks hindering them from being used in industries are the scalability costs and the commercialization of processes based on ILs due to their high costs of production, complex synthesis procedures, high viscosity, toxicity, etc. High viscosity is the main limitation of ILs,[115] as it limits the gas–liquid mass

transfer and decreases the diffusion rates of gases across the liquid. As a result, the process requires a longer reaction time and larger size of the absorption column. Furthermore, high viscosity requires high pumping power and initial cost of storage for the solvent. Thus, it is necessary to find solutions to lower the viscosity of ILs. One such way is by mixing ILs with low-cost solvents to reduce the viscosity of ILs significantly and efficiently.[116] Other concerns regarding ILs are their high toxicity and poor regeneration capability that lead to additional losses as the spent ILs could not be recovered and will lead to environmental pollution. These issues can be tackled by further investigating and designing ILs that could function not only as solvents, but also as catalysts that can be regenerated multiple times without needing to be discarded. Finding an ideal balance between viscosity, regeneration capability and ease of synthesis should definitely be research goal to further enhance the development of ILs for adoption in the oil and gas industry.

2.1.4 Deep eutectic solvents. Deep eutectic solvents (DESs) are a relatively new class of solvents,[117,118] with significantly reduced melting points as compared to its constituent components. DESs have emerged as potential alternatives to ILs in various fields of applications.[119] Typically, DESs consist of hydrogen bond donors (HBDs) and acceptors (HBAs).[120] DESs share many positive traits with ILs such as many possible combinations of liquids, high thermal stability, low volatility, excellent tunability, *etc.* Nevertheless, DESs are more advantageous as compared to ILs since DESs are much easier to synthesize, cheaper, more environmentally friendly and biodegradable.[118,121] In general, DESs are less toxic and in some cases, their toxicity is still unknown as compared to ILs.[122] So far, DESs have been widely used for ammonia, sulfur dioxide and CO_2 capture.[123,124] However, DESs are rarely used for H_2S capture applications.

Liu *et al.*[28] prepared a series of DESs using choline chloride (ChCl) and urea in various ratios, such as 1.5, 2 and 2.5 for the concurrent removal of H_2S, CH_4 and CO_2. They found that these DESs undergo physical absorption and as the ratios between ChCl and urea decreases, the solubility of H_2S also decreases. They also discovered that selectivity of H_2S and CO_2 over CH_4 is easily tunable by changing the ChCl and urea ratios. The DES is also rather stable thermally with a decomposition temperature of 176.85 °C. Wu *et al.*[29] prepared two types of DESs by mixing tetrabutylammonium bromide (TBAB) and ChCl with carboxylic acids (CA) for H_2S capture. Both DESs were acting as physical absorbents with similar trends. TBAB-CA performed better as compared to ChCl-CA due to strong hydrogen bond interactions in ChCl-CA contributing to its lower free volume for absorption. The carboxylic acid-based DESs also outperformed other reported DESs[28] and many ordinary ILs.

Similar to TSILs, DESs can also be functionalized to create more chances of chemisorption to increase the selectivity and absorption capacity. The functionalized DESs are known as task-specific deep eutectic solvents (TSDESs). Shi *et al.*[30] developed five TSDESs of quaternary ammonium salts with tertiary amines and azoles. Among them, only [C_4-TMEDA][Cl]-1,2,3-triaz has a viscosity below 100 cP at 40 °C making them unfavorable for industrial applications. Despite this, these TSDESs

showed a high selectivity towards H_2S ranging from 5.2 to 12.1. Nonetheless, [C_4-TMHDA][Cl]-[Im] displayed the highest absorption capacity of 0.996 mol mol^{-1} at room temperature and pressure. Moreover, [C_4-TMHDA][Cl]-[Im] also can be regenerated five times while retaining 92% of its capacity at 69 °C and 0.1 bar. Shi *et al.*[31] also prepared a series of TSDESs containing chemical dual sites such as acetate and ternary amine anions to form dual chemisorption sites with H_2S. [C_1-TMHDA][Ac]-[MDEA] exhibited the highest absorption capacity for H_2S followed by [C_1-TMHDA][Ac]-[Pyrol], [C_1-TMHDA][Ac]-[AA] and [C_1-TMHDA][Ac]-[Im], respectively. These TSDESs also displayed a high selectivity for H_2S over CO_2 ranging from 6.9 to 9.3 and can be regenerated up to six times while maintaining their absorption capacity of 92%. Furthermore, [C_1-TMHDA][Ac]-[Pyrol] and [C_1-TMHDA][Ac]-[Im] possess viscosities lower than 75 cP at 40 °C, increasing their potential for industrial applications.

Another method to evaluate the interactions between DESs and H_2S molecules is by computational methods such as *ab initio* calculations, and molecular dynamics (MD), Monte Carlo (MC) and COSMO-RS simulations. These methods could prove useful in cases where there is a lack of experimental data. Karibayev *et al.*[125] applied *ab initio* calculations and MD simulations to evaluate the interactions in four DESs made up of TBAB, tetrabutylammonium chloride (TBAC), caprolactam (CPL), ChCl, urea, MEA and methyltriphenylphosphonium bromide (MTPB) to form TBAB-CPL, TBAC-CPL, ChCl-urea and MTPB-MEA. The authors discovered that the TBAB-CPL DES demonstrated stronger affinity towards H_2S over CH_4, due to stronger interactions between CPL and H_2S as compared to CH_4. As a result, TBAB-CPL can selectively remove H_2S efficiently from CH_4. However, these DESs require a high pressure of 10 bar to operate optimally. Salehi *et al.*[126] predicted the solubilities of H_2S, CO_2, H_2 and N_2 in ChCl-ethylene glycol and ChCl-urea DESs by MC simulations. Their results showed that both DESs are highly soluble in H_2S followed by CO_2, CH_4, CO, H_2 and N_2. On the other hand, Stupek *et al.*[127] predicted the thermodynamic properties of 23 cost-effective DESs for biogas upgrading using COSMO-RS. ChCl-urea and ChCl-oxalic acid were found to be the best DESs to remove CO_2, H_2S and siloxanes effectively.

DESs are an interesting class of solvents with high potential to replace traditional solvents in various applications both from economics and sustainability viewpoints. Nonetheless, the applications of DESs in H_2S capture are still at the grassroots level and require further research to address issues such as high viscosities[124] and low H_2S absorption capacities.[128] Overcoming these limitations would make DESs highly viable for industrial adoption. TSDES development has demonstrated that chemisorption can be initiated to achieve greater absorption capacity and reduced viscosity. TSDESs have been applied for removal of other contaminant gases but are yet to be explored for H_2S absorption.[129–131] Therefore, more studies should be carried out in this area to further enhance the potential of TSDESs in the near future.

Despite their significant potential for H_2S removal applications, DESs are showing concerning signs of toxicity and

ecotoxicity. Recent studies by Jung et al.[132] have revealed that ChCl-based DESs with urea contain ammonia, which contributes to their toxic effects. Similarly, Lomba et al.[122] also concluded that the individual toxicity of the initial components cannot serve as a predictive factor of DES ecotoxicity. Furthermore, Hayyan et al.[133] discovered that the cytotoxicity of DESs was much higher than that of their individual components such as ChCl and glycerine, indicating that their toxicological behavior is different. These findings highlight the importance of assessing the safety and environmental impact of DESs before their widespread adoption. Further research is crucial to thoroughly investigate the potential risks associated with DES usage, particularly focusing on safety and ecotoxicity, in order to ensure their responsible and sustainable application in H_2S removal processes.

2.1.5 Hybrid blends. As elaborated previously in Sections 2.1.1 to 2.1.4, different classes of absorbents possess different benefits and limitations. Their limitations can be overcome by mixing them together to form a hybrid blend.[134] Hybrid blends refer to a combination of two or more different types of solvents, resulting in a new blend that exhibits a higher performance for H_2S absorption than the constituent solvents. By combining physical and chemical solvents to form a hybrid blend, various added advantages of both solvents can be achieved such as a shorter separation column, lower energy requirement for solvent recovery, and higher absorption capacity and higher removal efficiency for acid gas and sulfur compounds. Some of the conventional hybrid blends widely used are Sulfinol-D (water, DIPA and sulfolane) and Sulfinol-M (water, MDEA and sulfolane) developed by Shell, Amisol (methanol and alkanolamine) developed by Lurgi and Flexsorb PS (physical solvent, sterically hindered amine and water) developed by ExxonMobil.[74]

The limitations of most ILs such as high viscosity and cost can be overcome by blending the ILs with more affordable solvents, i.e., physical solvents and alkanolamines, to decrease the viscosity of ILs and enhance mass transfer. Several researchers[14,32,70] studied the effect of additional activators such as $[N_{1111}][Arg]$, $[N_{1111}][Gly]$ and MEA within 7.5 to 30 wt% on the performance of MDEA solution for H_2S removal at low partial pressure. All activators were observed to enhance the MDEA solution capacity for absorbing H_2S due to the increased availability of interaction sites. $[N_{1111}][Arg]$ recorded the highest removal efficiency and capacity followed by $[N_{1111}][Gly]$ and MEA, respectively. On the other hand, Afsharpour and Hagthalab[33] prepared a hybrid blend of [Bmim][Ac] with DIPA for simultaneous removal of CO_2 and H_2S. They noticed that both solvents are highly selective towards H_2S, thus leading to higher solubilities of H_2S at high pressures. Moreover, Lemus et al.[110] discovered that a hybrid blend of 75 wt% TEGDME and 25 wt% [Bmim][Ac] displayed an excellent removal performance of H_2S due to low viscosity of TEGDME and high absorption capacity of [Bmim][Ac].

2.1.6 Summary of absorption. The advantage of H_2S removal via the absorption process is it can produce a combined effect of a high reaction rate and equilibrium capacity by blending the solvents together. Nevertheless, the absorption

processes suffer from a few disadvantages such as being energy intensive and high operation and regeneration costs due to loss of solvents via thermal degradation and evaporation. Furthermore, these alkanolamine-based solvents are also expensive, corrosive, highly toxic and pose environmental threats. Some of these solvents are also non-regenerable. Besides, the application of a multi-solvent system can lead to the formation of very complex chemical reactions causing the solvent to be hard to regenerate and equipment failure due to corrosion.[46–48,59]

Chemicals not adhering to green chemistry principles can cause significant negative environmental impacts throughout their lifecycle, from production to disposal. Many conventional solvents like chlorinated solvents (e.g., dichloromethane and chloroform), aromatic solvents (e.g., benzene and toluene), and volatile organic compounds (VOCs) contribute to air pollution,[135] soil and water contamination,[136] and harm wildlife.[137] Long-term exposure to certain solvents can lead to health risks such as respiratory issues, neurological disorders, and cancer.[138] Some toxic solvents can severely impact ecosystems, leading to soil and water contamination, disrupting ecosystems, and harming aquatic life. Improper disposal of solvents containing heavy metals can lead to environmental contamination, affecting soil quality and agricultural productivity. Highly toxic metals such as mercury and lead can pose serious health risks to humans, especially through food and water contamination.[139]

Therefore, adopting sustainable and environmentally friendly alternatives is crucial. Green solvents[140–142] such as ILs and DESs offer advantages such as enhanced selectivity, improved absorption capacity, reduced environmental impact, and alignment with green chemistry principles, which aim to minimize hazardous substance use and generation, thereby reducing environmental pollution and protecting human health and ecosystems. A summary of conventional H_2S removal absorption processes is provided in Table 3.

2.2 Adsorption

Adsorption is a process in which the molecules of a fluid are adhered to a solid surface.[152] The molecules that adhere to the surface are referred to as adsorbates, whereas the surface where the molecules accumulate is the adsorbent. Adsorption can be divided into two different classes such as physisorption and chemisorption.[153,154] Physisorption, also known as physical adsorption, is a rather weak interaction where the molecules of adsorbates were adhered to the surface of the adsorbent by van der Waals forces, i.e., dipole–dipole interactions and London dispersion forces.[155] Physisorption involves rather low energy and gets stronger at lower temperatures. Furthermore, physisorption is a reversible process, which means that the adsorbates can be desorbed easily from the adsorbent surface by increasing the temperature or reducing the pressure. On the other hand, chemisorption or also known as chemical adsorption is a stronger interaction as compared to physisorption due to the formation of bonds such as covalent or ionic bonds between the adsorbate molecules and the adsorbent surface.[156] Generally, chemisorption requires an activation energy which is
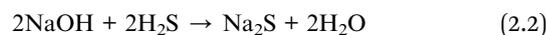
Table 3 The summary of conventional H_2S removal technology by absorption

Conventional technology	Feed gas composition	Operating conditions	Types of solvent used	H_2S removal efficiency	Reference
Selexol	44 mol% CO_2, 0.6 mol% H_2S, and 55.4 mol% CH_4	Temperature: −9.4 to 38 °C, pressure: 20–120 bar	Dimethyl ether of polyethylene glycol (DMPEG)	90%	143
Rectisol	Gas ratio: 6–7 mol% CO_2; 1 mol% H_2S	Temperature: −34 to −74 °C, pressure: 40–78 bar	Methanol	70%	144–146
Purisol	8 mol% H_2S, 18 mol% CO_2, 70 mol% CH_4, and 4 mol% N_2	Temperature: −15 °C, pressure: 32–35 bar	N-Methyl-2-pyrrolidone (NMP)	94%	74
ADIP	0.5 mol% H_2S, 5.5 mol% CO_2, and 94 mol% CH_4	Temperature: 100–150 °C, pressure: 4.1–24.8 bar	DIPA	75%	147
Sulfinol	15 mol% H_2S, 6 mol% CO_2, 57.69 mol% CH_4, 6.24 mol% C_2H_6, 7.57 mol% C_3H_8, and 7.5 mol% N_2	Temperature: 57–66 °C, pressure: 49.3–91.7 bar	Sulfolane® (tetra-hydrothiophene dioxide) and DIPA	70%	148
FLEXSORB™SE	1.8 mol% H_2S, 6.7 mol% CO_2, and 91.5 mol% CH_4	Temperature: 32 °C, pressure: 64.5 bar	MDEA	67%	50 and 149
OASE®sulfexx™	2 mol% H_2S, 10 mol% CO_2, and 88 mol% CH_4	Temperature: 45 °C, pressure: 64.5 bar	MDEA	81%	51 and 150
UOP Benfield™	2.65 mol% H_2S, 11.5 mol% CO_2, and 85.85 mol% CH_4	Temperature: 110–130 °C, pressure: 20.7 bar	Hot potassium carbonate, K_2CO_3	93.7%	151
CATACARB®	2.1 mol% H_2S, 6.7 mol% CO_2, and 91.2 mol% CH_4	Temperature: 153–204 °C, pressure: 20.7–56.5 bar	Hot potassium carbonate, K_2CO_3	38.7%	151

specific to both the adsorbate and the adsorbent. Unlike physisorption, chemisorption is mostly irreversible and needs high temperatures and drastic conditions to desorb the molecules from the adsorbent.

In general, gas adsorption by solid adsorbents was governed by five different mass transport mechanism stages such as external, pore, film, intraparticle and surface adhesive diffusion.[157] The process of H_2S adsorption from a gas stream is an exothermic process and occurs under dry conditions without requiring an extremely high temperature to operate. There are various adsorbent materials commonly used for large scale H_2S removal, including carbon-based adsorbents, zeolites, metal oxides, metal organic frameworks (MOFs) and composite materials. These materials were used mainly because of their high removal capacity, good selectivity and thermal and mechanical stability.[158,159] The removal efficiency of H_2S is significantly affected by the adsorbent properties such as porosity and surface chemistry; and operating parameters such as mixture gas concentration, temperature, gas hourly space velocity and relative humidity.[160]

2.2.1 Carbon-based adsorbents. Currently, porous carbon-based materials such as activated carbons (ACs) and biochar have been successfully applied for H_2S adsorption at the industrial level due to their green origins and low production costs as they are easily available from waste materials and biomass.[161] These materials have a large specific surface area of higher than 1000 $m^2 g^{-1}$,[162] high pore volume that promotes catalytic reactions and thermal stability. Besides, these materials also possess tunable surface chemistry and structural morphologies that facilitate effective sorption sites. The ACs were impregnated with alkaline chemicals such as sodium hydroxide (NaOH) or potassium hydroxide (KOH) to improve their catalytic properties, reduce porosity and increase H_2S adsorption.[163] The surface modification of ACs is to promote reactive adsorption and chemical bond formation with the adsorbate. H_2S removal occurred by H_2S dissociation into HS^- ions, and then oxidation by NaOH or KOH to form elemental sulfur or sulfuric acid. The surface reactions on the impregnated ACs were expressed using the following equations.[164]

$$NaOH + H_2S \rightarrow NaHS + H_2O \quad (2.1)$$

$$2NaOH + 2H_2S \rightarrow Na_2S + 2H_2O \quad (2.2)$$

$$NaHS + 0.5O_2 \rightarrow S + NaOH \quad (2.3)$$

$$Na_2S + 0.5O_2 + H_2O \rightarrow S + 2NaOH \quad (2.4)$$

$$2NaOH + H_2SO_4 \rightarrow Na_2SO_4 + 2H_2O \quad (2.5)$$

The exothermic reaction releases heat that may damage the adsorptive sites. H_2S oxidation is reported to be influenced by surface chemistry and local pH. An acidic carbon surface will result in higher yield of water-soluble products, but at the same time lower the total sorption capacity. When the adsorption performance of H_2S using impregnated ACs with various alkaline solutions such as K_2CO_3, Na_2CO_3, KOH and NaOH was compared, NaOH-activated carbons outperformed the other

alkaline solutions, despite the drawbacks mentioned earlier.[165] Recently, Ahmadi et al.[166] developed an N–S rich jute-derived nanoporous carbon activated by KOH; which possesses excellent gas adsorption capacity and high cycling performance. Meanwhile, Wang et al.[167] synthesized Cu-impregnated peanut shell-based AC for H_2S adsorption in an enclosed area, which displayed good regenerability with a 90% removal rate. A ZnO–MgO-based AC adsorbent investigated by Yang et al.[168] exhibited an impressive adsorption capability of 96.5 mg g^{-1} under dry conditions. Nevertheless, the regeneration capability of the adsorbent was not studied.

Yang et al.[169] also developed a $ZnFe_2O_4$-based AC adsorbent which demonstrated a 122.5 mg g^{-1} breakthrough capacity with an optimum loading of 10%, able to be regenerated three times with small capacity reduction after being treated thermally at 500 °C. Similarly, Yuan et al.[170] synthesized leftover rice-based ACs that displayed a 12.11 mg g^{-1} breakthrough capacity with 50 wt% loading. On the other hand, Pan et al.[171] prepared 2D nanostructures of CaO/CH carbonized at a temperature of 700 °C and above. CaO/CH-700 displayed the highest alkalinity, and a breakthrough adsorption capacity of 9.1 g g^{-1}. Nonetheless, CaO/CH-700 displayed a very low regeneration capability of lower than 0.2 g g^{-1} as the reaction between H_2S and CaO was irreversible.

In the last few years, N-rich carbon-based adsorbents are being developed as better alternatives to metal oxides, metal-doped carbons and caustic compounds for H_2S removal due to their high sustainability, safety and efficiency. Chen et al.[172] prepared N-rich porous carbons that shows higher breakthrough capacities as the CN/CS ratio increases from 0.5 to 1, which become lower after the ratio increases to 2. Furthermore, Fakhraie et al.[173] synthesized KOH-activated high N-doped ACs (HNAC) at 800 °C over 1 h. Among the synthesized adsorbents, HNAC-802 was proven to have the best adsorption capacity at 316.35 mg g^{-1} with a 2.17 selectivity for H_2S/CO_2. On the other hand, Yu et al.[174] used ZIF-8 to develop N-rich mesoporous carbon nanosheets (N-MCNS). Remarkably, N-MCNS have outperformed those in previous studies from Chen et al.[172] and Fakhraie et al.[173] by exhibiting an excellent adsorption capacity of 510 mg g^{-1} and a large surface area of 1937 $m^2 g^{-1}$. On the other hand, Wang et al.[175] integrated polyethyleneimine into MCNS to form MCNS-PEI with different loading percentages ranging from 0 to 65 wt%. MCNS-PEI 25 displayed a high breakthrough sulfur capacity of 13.68 mmol g^{-1} and regenerability without any performance drop within 6 cycles. Xu et al.[176] acquired N-doped porous carbons impregnated with KOH by treating them thermally with ammonia. The N-doped carbons managed to achieve over 85% conversion and 80% selectivity towards sulfur formation for 1 vol% of H_2S in the feed gas.

There are various kinds of functionalizations for synthesized carbon-based adsorbents such as impregnation, direct integration, heteroatom doping, or deposition–precipitation that has been studied up to now. Moreover, Ou et al.[177] synthesized granular ACs to remove H_2S with concentrations of 932 to 2060 ppm at 25 °C. The breakthrough capacity of the granulated ACs was found to be 745–1293 mg g^{-1} for low concentration (932–1560 ppm) and even lower capacity of 615–703 mg g^{-1} at

high concentration (1920–2060 ppm). However, no regeneration study of the adsorbent was conducted. Recently, Sawalha et al.[178] developed biochar from waste biomass materials such as eucalyptus barks, almond shells and used coffee grains to remove H_2S from biogas with an average concentration of 970 ppm. The adsorption capacity, breakthrough time and removal efficiency were observed to increase in the order of used coffee grains, almond shells and eucalyptus barks. Eucalyptus barks exhibited a capacity of 490 mg g^{-1}, which was the highest among all three but performed lower than the granular ACs in a study by Ou et al.[177] at the same temperature. Recently, Qi Dong et al.[179] developed a polyethylene polyamine impregnated carbon catalyst, exhibiting outstanding performance with a H_2S adsorption capacity of 1.58 g H_2S/g-catalyst at 30 °C. This achievement is credited to its optimal steric hindrance and enhanced stability during the H_2S adsorption–desorption cycle.

The development of carbon-based adsorbents that meets certain criteria such as cost-effectiveness, regenerability, sustainability and high capacity is in great demand nowadays. As a matter of fact, some of the adsorbents are capable of removing H_2S at low temperatures. Therefore, further research should be carried out to increase the regenerability of the adsorbents as most of the reactions involving carbon-based adsorbents are irreversible. More emphasis should also be placed on developing N-doped or metal oxide-doped porous carbons that are economic, sustainable and easy to synthesize. Despite the high-cost requirements to perform the functionalization of these adsorbents, it is noteworthy that their adsorption capacity and regeneration capability could be significantly improved making them excellent alternatives for removal of H_2S.

2.2.2 Metal oxide adsorbents. Metal oxides adsorbents have been extensively used for desulfurization at high temperatures primarily due to their strong affinity towards H_2S.[180,181] Several metal oxides[182] commonly used as catalysts for selective removal of H_2S at low temperatures are Cu, Co, Zn, Mn, Ca, Fe, etc. Major disadvantages of bulk metal oxides such as low porosity, dispersion and ratio of surface area to volume, often lead to poor desulfurization performance in these adsorbents. Therefore, porous metal oxides could be the alternatives since they possess wider surface area, extra adsorption sites, higher porosity and diffusivity.[183] Over the recent years, the development of mixed metal oxides is getting more emphasis due to their enhanced performance compared to that of single metal oxides alone.[184] The reaction mechanism of metal oxides is mainly chemisorption that produces sulfides, sulfates and elemental sulfur. Overall, metal oxides are more economic as compared to zeolites since the cost of materials is much lower and they possess higher adsorption capacities, but nonetheless, suffer from low regeneration capability.

Aside from this, the deployment of metal oxide adsorbents in industrial applications for H_2S capture such as iron oxide (FeO) adsorbents and mixed metal oxide-based adsorbents is getting recognition due to their capability of reducing H_2S concentration to 10 ppm while avoiding heat loss at high temperature.[185,186] FeO-based adsorbents such as SULFATREAT and SELECT FAMILY were developed by Schlumberger,[187] while

mixed-metal oxide adsorbents such as CuO/ZnO-based adsorbents, *i.e.*, PURISTAR® and alumina-based adsorbents, *i.e.*, Selexsorb® were developed by BASF. H_2S adsorption on a metal oxide reaches 95% even at high temperature and resulted in the formation of a solid or liquid phase containing sulfur and an adsorbent metal. Nonetheless, various studies have been conducted to harness their exceptional performance for H_2S capture. Hassankiadeh *et al.*[188] proposed the use of molybdenum oxide (MoO_2) nanoparticles for H_2S capture. Despite possessing a remarkable adsorptive capacity of 0.081 g of H_2S/g (non-spherical) and 0.074 g of H_2S/g (spherical) at 85 °C,[188] the adsorbent requires a high pressure of 16 bar with a low initial concentration of 43 ppm H_2S to operate optimally.

On the other hand, Orojlou *et al.*[189] developed nanocomposites such as NiO/TiO_2, CoO/TiO_2 and CuO/TiO_2 for H_2S capture at a very high temperature of 480 °C. The best nanocomposite at 480 °C was found to be CoO/TiO_2. However, the performance of these nanocomposites began to drop significantly at a temperature of 400 °C, indicating that these nanocomposites are not capable of operating optimally at low temperatures. A similar study was conducted by Pan *et al.*[190] who recorded a better performance of NiO/TiO_2 at 500 °C. Furthermore, Orojlou *et al.*[189] discovered that these nanocomposites can only be regenerated once before deteriorating in performance. Furthermore, Kim *et al.*[191] developed a Mn_2O_3/Fe_2O_3 nanocomposite to remove H_2S at room temperature. The adsorption capacity recorded was 11.97 mg g^{-1} which decreases as the flow rate of the feed gas increases. Regenerability performance of these nanocomposites should be further researched to improve their regeneration capability.

Wu *et al.*[192] prepared double metal oxides (DMOs) containing Zn and Fe with different molar ratios from 1 : 1 to 5 : 1 for H_2S capture at an elevated temperature ranging from 450 °C to 700 °C. DMO-5 exhibited the best performance at 550 °C with a breakthrough capacity of 250 mg g^{-1} and breakthrough time of 321 min. The Zn–Fe-based adsorbents can be fully regenerated at a temperature between 600 °C and 650 °C in the presence of 2 to 4% oxygen. On the other hand, Ahn *et al.*[193] synthesized acid mine drainage sludge (AMDS) which contains various types of metal oxides, and 56.6% of the sludge is iron oxide. AMDS demonstrated a breakthrough capacity of 8361 mg g^{-1} for removal of low concentration H_2S ranging from 110 ppmv to 126 ppmv.

Metal oxide adsorbents generally possess excellent adsorption capacities for H_2S. Nevertheless, they suffer from irreversible chemisorption, which leads to high replacement costs, and the spent adsorbents have to be disposed of. Another disadvantage of metal oxide adsorbents is the high temperature requirement to operate optimally, and a further increase in temperature might also lead to sintering of the adsorbents.[194] Furthermore, unsupported metal oxides may deteriorate with time due to rapid sintering and fail to be regenerated at high temperatures. In addition, metal oxide adsorbents also experience issues such as spalling and sublimation. The applications of metal oxide adsorbents is restricted by several factors, including low thermal and chemical stability at high temperatures, as well as limited surface areas at low temperatures.

2.2.3 Zeolites. Zeolites are a group of minerals found in nature or synthetically manufactured with a unique porous structure and they belong to a class of aluminosilicate glass minerals and are well-known as molecular sieves due to their capability of trapping and releasing molecules within their porous crystalline structures.[195] Zeolites offer various advantages due to their high thermal stability, large surface area and unique tunability of their structures making them widely used in various applications such as catalysts, adsorbents, ion exchangers, *etc.* Structurally, zeolites are made up of a three-dimensional (3D) tetrahedral framework which consists of Si, Al, P and O.[196] Different arrangements of the building blocks will lead to different types of unique 3D frameworks. Zeolites can be divided into two main categories such as natural and synthetic zeolites.[197] Natural zeolites occur naturally and possess porous structures similar to that of synthetic zeolites. There are many kinds of natural zeolites such as clinoptilolite, stilbite, chabazite, heulandite, natrolite, analcime, phillipsite, apophyllite, erionite and laumontite.[198] On the other hand, synthetic zeolites are engineered versions of natural zeolites tailored for specific industrial applications. Examples of synthetic zeolites include zeolite A (LTA), zeolite X and Y (FAU), ZSM-5 (MFI), beta zeolite (BEA), mordenite (MOR), chabazite (CHA), faujasite (FAU), silicalite (MFI), SSZ-13 (CHA) and offretite (OFF).[199] The suitability of zeolites for gas adsorption applications is typically determined by several criteria such as the type of framework, additional elements in the framework, framework structure and ratio of Si to Al in the zeolites. Zeolites with low ratios of Si to Al are more hydrophilic and highly selective towards polar molecules such as H_2S through chemisorption. Meanwhile, zeolites with high silica contents such as silicalite are hydrophobic and adsorb H_2S through physisorption.[200]

Ozekmekci *et al.*[201] determined that zeolite 13X (Na-X) and its derivatives have the highest performance in removing S compounds. Furthermore, Bareschino *et al.*[202] also investigated zeolite 13X for H_2S removal with concentrations ranging from 50 to 100 ppm. They discovered that H_2S adsorption is higher with the presence of water in the system and changes from physisorption to chemisorption at the end of the reaction. Similarly, Barelli *et al.*[203] synthesized a Cu-replaced 13X (Cu-Ex 13X) zeolite for removal of H_2S from biogas with concentrations between 200 and 1000 ppm. Cu-Ex 13X has a breakthrough time of 126 min and adsorption capacity of 11.46 mg g^{-1}. By comparison with the study carried out by Bareschino *et al.*,[202] it is noticeable that the presence of Cu^{2+} ions has led to an efficient adsorption process by the Cu-Ex 13X zeolite. Moreover, a higher H_2S concentration in the feed gas has led to a lower breakthrough time and adsorption capacity. On the other hand, Bahraminia *et al.*[204] prepared a nanozeolite of AgNaA for H_2S removal and reported a breakthrough time of 310 min and 33.24 mg g^{-1} capacity to obtain 1 ppmv H_2S at the outlet. The reported performance is far lower than that of commercial 4A and the pure NaA nanozeolite. Nonetheless, the AgNaA nanozeolite performed better than Cu-Ex 13X. Formation of water inside the zeolite indicated that H_2S chemisorption occurred

and led to higher performance. Additionally, the AgNaA zeolite can be regenerated with a 5% reduction of adsorption capacity for every cycle, probably because of the water loss during regeneration at high temperatures.

Currently, zeolite-based adsorbents are gaining worldwide attention for industrial adoption and being rigorously studied for H_2S capture purposes owing to their substantial surface areas and porosity. Jafari et al.[205] studied the effect of magnetite nanoparticle addition on the performances of Y and ZSM-5 zeolite substrates for removal of up to 120 ppm of H_2S at relatively high temperatures between 100 and 300 °C. Zeolite Y doped with 5% magnetite was found to have the highest adsorption capacity of 69.92 mg g^{-1} as the doping process has improved the specific surface area and increased the number of micropores and mesopores. Meanwhile, Florent and Bandosz[206,207] synthesized a new biosolid-based adsorbent incorporated with pluronic surfactant F127 for H_2S removal from air. The surfactant-added adsorbent displayed a 250% increase in H_2S removal efficiency compared to the adsorbent without surfactant addition. The surfactant addition increased the mesopore volume and carbon content, leading to higher catalytic center dispersion and carbon structural order which resulted in the conversion of H_2S into elemental sulfur.

Yan et al.[208] screened 95 different types of silica zeolites for removal of toxic gases such as H_2S, NO, NO_2, NH_3, SO_2 and CO using grand canonical ensemble Monte Carlo simulations. According to their prediction results, the top 10 adsorbents for H_2S removal showed a higher capacity towards NH_3 as compared to H_2S. Zeolites AFY, MER and PAU are found to be the best H_2S adsorbents with loading capacities of 7.8, 5.4 and 5.4 mmol g^{-1}, respectively. For adsorption that involves all gases, zeolite RWY showed an outstanding performance with a H_2S adsorption capacity of 17.74 mmol g^{-1}. Similarly, Song et al.[206] discovered that the CHA zeolite displayed the best adsorption capacity and decent H_2S selectivity, whereas LTA and FAU zeolites exhibited excellent H_2S selectivity but suffered from poor adsorption capacities. Georgiadis et al.[209] used an industrial molecular sieve with a ratio of 0.97 between Si and Al that resembles the LTA zeolite. The molecular sieve exhibited an adsorption capacity of 193.59 mg g^{-1} for 10 000 ppmv of H_2S and can be regenerated up to 15 times without any significant loss in its capacity at 200 °C. The adsorption capacity was also found to decrease to 164.5 mg g^{-1} after H_2S concentration increases to 30 000 ppmv.

One of the major disadvantages of zeolites is their high temperature requirement for regeneration, which hinders them from being widely implemented in industrial applications, especially for H_2S adsorption. Among all classes of commercial adsorbents, only zeolites are able to be regenerated. Another drawback commonly faced by zeolites is low selectivity towards H_2S in the presence of other gases, i.e., CO_2, SO_2 and NH_3. There are a few ways to boost the development of zeolites for H_2S adsorption such as by implementing more feasibility studies of the newly developed zeolites and changing the research approach to focus on developing new structures and frameworks.

2.2.4 Metal organic frameworks. Metal–organic frameworks (MOFs) are a class of highly porous crystalline hybrid materials with organic and inorganic structures, arranged systematically between metal cations and organic ligands. The arms of the organic ligands are attached to the nodes created by the metal cations forming a hollow cage-like structure.[210] Consequently, MOFs possess an exceptionally large internal surface area ranging from 1000 up to 10 000 m^2 g^{-1}.[211] In addition, MOFs are thermally and chemically stable, besides having a high tunability of their pore size.[212] Due to their remarkable properties, MOFs are excellent candidates for gas storage and separation applications.[213] MOFs are widely used as gas storage media for H_2 and CH_4 for clean energy production and as high-capacity adsorbents for separation of various gases, i.e., NH_3, H_2S, SO_2 and CO_2.

Gupta et al.[214] developed Cu-based MOFs such as CuBTC, CuBDC and CuBDC-N for H_2S capture at 25 °C. It was observed that CuBDC with the smallest ratio of Cu^+ to Cu^{2+} ions possesses the best adsorption capacity of 105.6 mg g^{-1}. Gupta et al.[215] also prepared $Cu(BDC)_{0.5}(BDC-NH_2)_{0.5}$ and noticed that a higher adsorption capacity of 128.4 mg g^{-1} was recorded for 500 ppm of H_2S inlet. The presence of moisture has appeared to affect the MOFs adversely by reducing their performance. The authors have attempted a methanol and UV-aided regeneration process but are unable to fully regenerate the MOF, with only 9.9 mg g^{-1} of adsorption capacity being recorded after three regeneration cycles. Further characterization conducted confirmed that the UV-regeneration method has damaged the internal structure of the studied MOF. On the other hand, Zarate et al.[216] used MIL-53(Al)-TDC to remove 5 vol% of H_2S in the inlet gas under ambient conditions and reported an extremely high adsorption capacity of 618 mg g^{-1}. Additionally, MIL-53(Al)-TDC can be regenerated up to 5 times in a temperature range of 65 to 200 °C, without losing any capacity.

Similarly, Flores et al.[217] developed MFM-300(Sc) for removal of 10 vol% of H_2S in the feed gas and recorded a high adsorption capacity of 565 mg g^{-1} at room temperature. Nevertheless, the MFM-300(Sc) zeolite was unable to be regenerated completely as the adsorption capacity dropped to 344 mg g^{-1} after being regenerated once. The capacity reduction was attributed to the irreversible chemisorption and formation of polysulfides from H_2S molecules. Grape et al.[218] prepared $Bi_2O(H_2O)_2(C_{14}H_2O_8)\cdot H_2O$ (SU-101) to remove 4.3 vol% of H_2S from the feed gas under room temperature conditions. The adsorption capacity recorded was 543.6 mg g^{-1}, almost similar to that of MFM-300(Sc) despite having smaller surface area. SU-101 also exhibited a notable decrease in capacity after the initial regeneration cycle, attributed to an irreversible chemisorption process. Even though both MFM-300(Sc) and SU-101 could not be regenerated, they have huge potential in the MOF-based Li–S battery industry[219] due to their capability of strong polysulfides formation and high stability.

Ngo and Chiang[220] compared H_2S removal performance using zeolite, calcined dolomite, and activated carbon in a hot gas cleaning system at 250 °C, with simulated synthesis gas containing 200 ppm of H_2S. The results showed that activated

carbon exhibited the highest removal efficiency and adsorption capacity, followed by calcined dolomite and zeolite. The adsorption capacities were 5.88 mg S g^{-1} for activated carbon, 3.16 mg S g^{-1} for calcined dolomite, and 2.22 mg S g^{-1} for zeolite. Calcined dolomite displayed poor adsorption–regeneration ability due to H$_2$S deactivation, while zeolite and activated carbon were fully regenerated at 350 °C over four cycles.

Zeolitic imidazolate frameworks (ZIFs) are a unique subclass of MOFs which possess structural similarity to zeolites with the presence of imidazolate-based ligands.[221] In ZIFs, the imidazolate ligands coordinate with metal ions forming a high porosity crystalline network. Consequently, ZIFs possess both added advantages of MOFs and zeolites.[222] In general, ZIFs are more stable chemically and thermally as compared to MOFs, and more porous as compared to zeolites. Their unique features have led to much research for potential applications in various fields, especially for CO$_2$ capture and storage. Nevertheless, similar applications for H$_2$S removal are still limited. On the other hand, Jameh et al.[223] developed a zeolitic imidazolate framework (ZIF-8) functionalized with ethylenediamine (ED) for effective removal of H$_2$S from natural gas streams. The ED-functionalized ZIF-8 showed remarkable improvements in terms of breakthrough time and adsorption capacities compared to the pure ZIF-8 adsorbent. Nevertheless, the adsorption performance after regeneration was not reported. Another study by Liu et al.[224] reported the usage of ZIF-67 for H$_2$S removal. Despite having high removal efficiencies, ZIF-67 was facing structural collapse after the reaction, and no data on the adsorption capacity were reported.

In general, MOFs suffer from structural collapse in the presence of certain chemicals and gases, especially H$_2$S. Commonly used metals such as Fe, Zn and Cu were reported for H$_2$S adsorption but were unstable. Meanwhile, metals such as Zr, V, Al, Ni. Ti and Mg displayed strong reactivity towards H$_2$S but were still rarely used.[225,226] Moreover, the stability of ZIFs is also affected by the linkers and their functionalization.[227] Additionally, the high cost of MOFs hinders their adoption in industrial applications. To mitigate the structural collapse in MOFs, higher emphasis should be given for designing linkers and metal nodes with higher stability, developing post-synthetic stabilization procedures and mixing the MOFs with metals that could enhance their stability. Besides, researchers should also focus on developing MOFs at much more affordable prices. Despite their limitations, MOFs have huge potential in H$_2$S adsorption applications and there is still much to explore and uncover in this regard.

2.2.5 Composite materials. Composite materials are a combination of two or more distinctive adsorbent materials with different physical or chemical properties that when combined, create a material with unique characteristics.[228] These materials are designed to harness the advantageous properties of their individual components while mitigating their individual weaknesses.[229] Composite materials are widely used in various industries due to their versatility, strength, and tailored properties. In addition to this, composite materials can be effectively applied for H$_2$S adsorption applications to improve the adsorption performance, capacity and cost-

effectiveness.[230,231] There are various kinds of composite materials that can be employed for H$_2$S adsorption applications such as AC-based composites, MOF-based composites, nanocomposites, polymer-based composites and natural fiber composites.

Gupta et al.[232] developed Zn-MOFs/ZnO nanocomposites such as ZnBDC/N/ZnO, ZnBDC/ZnO and ZNBTC/ZnO for H$_2$S adsorption at 25 °C. ZnBTC/ZnO demonstrated a 14.2 mg g^{-1} capacity followed by ZnBDC/ZnO and ZnBDC-N/ZnO. Zn-HKUST1 performed lower than the nanocomposites indicating that the presence of ZnO in the MOFs is crucial for excellent adsorption of H$_2$S. The nanocomposites could only be regenerated twice by using methanol and UV-based methods before showing a major decline in their adsorption capacity. Similarly, Wu et al.[233] prepared nanocomposites of ZnO mounted on MCM-41 and MCM-48. The optimum temperatures for ZnO/MCM-41 and ZnO/MCM-48 to achieve the highest performance were 500 °C and 600 °C, respectively. It was observed that the addition of ZnO into the nanocomposites provided more active sites for adsorption to occur, thus increasing the reaction rate of the adsorbents. Nevertheless, metal oxides are prone to conversion into metal sulfides which are larger in size, causing the pore structure to expand and might cause structural collapse. Similarly, Lin et al.[234] synthesized a series of cuprous chloride/copper chloride hydroxide composites (CCCCHs) and recorded a high H$_2$S adsorption capacity of 259.5 mg g^{-1}. Upon reaction with H$_2$S, the CCH surface undergoes decomposition, generating CuCl$_2$·2H$_2$O and reducing Cu^{2+} to Cu$^+$, leading to the oxidation of H$_2$S to elemental sulfur and sulfate.

Okonkwo et al.[235–237] studied SBA-15 based nanocomposites of sterically hindered and unhindered amines for H$_2$S removal under humid and dry conditions. Only (tertbutylaminopropyl) methoxysilanes (TBAPS) and (N,N-dimethylaminopropyl)trimethoxysilane (DMAPS) were selected to study the effect of humidity on H$_2$S adsorption performance in a feed gas containing 1 vol% of H$_2$S. Under humid conditions with 45% relative humidity, DMAPS/SBA-15 displayed a higher adsorption capacity as compared to TBAPS/SBA-15. In addition, TBAPS/SBA-15 was found to be the most selective towards H$_2$S in the presence of other gases such as CO$_2$ and CH$_4$.[237] After desorption at 120 °C, the capacity of both materials decreased sharply as the desorption process could not be completed under dry conditions. However, when subjected to desorption at 80 °C under humid conditions, both DMAPS/SBA-15 and TBAPS/SBA-15 displayed a minor decline in performance in the first cycle and it remained constant for the second and third cycles.[237] This probably occurred because the chemisorption bond was likely reversible under humid conditions. As a result, this could lead to further research for reversing the chemisorption bonds under such conditions. Nonetheless, the regeneration process under humid conditions demands extra energy and water resources, potentially making it economically impractical.

Generally, composite materials could offer a versatile and effective approach for H$_2$S adsorption applications due to the added advantages of the combined materials. By tailoring their composition and structures in order to be adapted for specific process requirements, researchers can design composite

Table 4 The summary of conventional H_2S removal technology and latest studies on adsorption

Adsorbent	Adsorption conditions	Initial concentration of H_2S	Breakthrough time, concentration of H_2S and capacity	BET surface area ($m^2\ g^{-1}$)	Reference
Conventional adsorbents					
SULFATREAT	Temperature: 100 °C, pressure: 20–120 bar	Pure	Time1–2 min, capacity: 150 mg g⁻¹	n/a	13
SELECT FAMILY	Temperature: −34 to −74 °C, pressure: 40–78 bar		n/a	n/a	13
PURISTAR®	Temperature: −15 °C, pressure: 32–35 bar		n/a	n/a	74
Selexsorb®	Temperature: 100–150 °C, pressure: 4.1–24.8 bar		Capacity: 8 mg g⁻¹	n/a	13
Carbon-based adsorbents					
AC	Gases present: H_2S, O_2, N_2, and H_2O, temperature: 30 °C	850 mg m⁻³	Concentration: 0.1 ppmv, capacity: 3.4 mg g⁻¹	1120	168
Mg–Ac			Capacity: 32.7 mg g⁻¹	366	
Zn–Ac			Capacity: 38.5 mg g⁻¹	769	
$Mg_{0.2}Zn_{0.8}$-AC			Capacity: 113.4 mg g⁻¹	653	
Cu-Ac	Gases present: H_2S, O_2, N_2, and H_2O, temperature: 30 °C	100 ppmv	Concentration: saturated, capacity: 129.2 mg g⁻¹	559	239
Zn–Ac			Capacity: 30.9 mg g⁻¹	n/a	
$Cu_{0.5}Zn_{0.5}$-AC			Capacity: 118 mg g⁻¹	570	
COF	Gases present: H_2S, CO_2, O_2, and N_2, temperature: 25 °C, pressure: 1 bar	970 ppm	Concentration: saturated, capacity: 22 mg g⁻¹	n/a	178
ALM			Capacity: 230 mg g⁻¹		
EUC			Capacity: 460 mg g⁻¹		
GAC	Gases present: H_2S, CO_2, CH_4, and O_2, temperature: 20–25 °C, pressure: 1 bar	932–2350 ppm	Concentration: 100 ppm, capacity: 615–1293 mg g⁻¹		177
Alkaline graphene aerogel	Gases present: H_2S, O_2, and N_2, temperature: 30 °C	1000 ppmv	Concentration: 50 ppm, capacity: 3190 mg g⁻¹	40	240
CaCO₃/CH-600	Gas present: H_2S Temperature: 30 °C	1000 ppmv	Concentration: 50 ppmv Capacity: 99 mg g⁻¹	22	171
CaO/CH-700			Capacity: 9100 mg g⁻¹	162	
CaO/CH-800			Capacity: 4400 mg g⁻¹	203	
CaO/CH-900			Capacity: 2380 mg g⁻¹	312	
N-rich mesoporous carbon nanosheets, NMCNS-0-5	Gases present: H_2S, N_2, O_2, and H_2O Temperature: 25 °C, pressure: 1 bar	1000 ppm	Concentration: 250 ppm	1389	174
$(NaCO_3)_{0.2}$/NMCNS-0-5			Capacity: 48 mg g⁻¹	n/a	
NMCNS-50-8			Capacity: 65 mg g⁻¹	1937	
$(NaCO_3)_{0.2}$/NMCNS-50-8			Capacity: 510 mg g⁻¹	983	
KOH-activated, Cu-impregnated peanut shell derived-ACs	Temperature: 25–110 °C, humidity: 60%	200–1000 ppm	Capacity: 1370 mg g⁻¹ Capacity: 34.4–97.6 mg g⁻¹	1326–1523	167

Table 4 (*Contd.*)

Adsorbent	Adsorption conditions	Initial concentration of H_2S	Breakthrough time, concentration of H_2S and capacity	BET surface area (m^2 g^{-1})	Reference
Cu-modified AC fiber (ACF)	Temperature: 25–110 °C, mass: 0.5 g	30 ppm	Capacity: 22.4–75.9 mg g^{-1}	980.8–1768.9	241
$CuSO_4$, $ZnAc_2$, KOH, KI, Na_2CO_3-modified coconut shell-derived AC (CAC)	Temperature: 25 °C, pressure: 1 bar, mass: 32–155 g, flowrate: 1.5–5.5 L min^{-1}	1000–5000 ppm	Time: 63–68 min, capacity: 0.673–1.83 mg g^{-1}	39.8–901.6	242
$ZnAc_2$-CAC	Gases present: H_2S, N_2, temperature: 25 °C, pressure: 1 bar	5000 ppmv	Concentration: 5–10 ppmv, capacity: 2.37 mg g^{-1}	620.6	243
Thermally treated biowaste residues	Temperature: 25 °C, mass: 26.7–168.8 g, flowrate: 1 L min^{-1}	1700 ppm	Capacity: 3.1–171.8 mg g^{-1}	3–919	244
Rice-based ACs, RBC-500	Gases present: H_2S, O_2, N_2, and H_2O, temperature: 25 °C	300 ppm	Concentration: 270 ppm, capacity: 12.11 mg g^{-1}	2.76	170
50 wt% $ZnFe_2O_4$-loaded biochar, RZF-500-1:1			Capacity: 228.29 mg g^{-1}	1065	
Maize cob waste (MCW)-based ACs	Temperature: 25 °C, pressure: 1 bar, mass: 0.5 g, particle size: 1–3 mm, flowrate: 400 cm^3 min^{-1}	1100–1800 ppm	Time:11–629 s, capacity: 0,25–15.5 mg g^{-1}	8–820	245
BAX-1520 (commercial AC)	Gases present: H_2S, O_2, N_2, and H_2O, temperature: 25 °C, pressure: 1 bar	1000 ppm	Concentration: 100 ppm, capacity: 5.6 mg g^{-1}	2158	169
10 wt% $ZnFe_2O_4$-BAX-1520			Capacity: 122.5 mg g^{-1}	1403	
Porous carbons (PC)	Gases present: H_2S, O_2, N_2, and H_2O, temperature: 30 °C	1000 ppmv	Concentration: 50 ppmv, capacity: 12.5 mg g^{-1}	1340	172
N-rich carbons			Capacity: 19.5 mg g^{-1}	187	
N-rich PC (0.5)			Capacity: 119.1 mg g^{-1}	2459	
N-rich PC (1)			Capacity: 426.2 mg g^{-1}	1839	
N-rich PC (1.5)			Capacity: 334.5 mg g^{-1}	1274	
N-rich PC (2)			Capacity: 267.2 mg g^{-1}	1048	
N-rich hierarchical PC, NHPC-802	Gas present: H_2S, temperature: 30 °C, pressure: 1–10 bar	Pure	Concentration: saturated, capacity: 284.1 mg g^{-1} (1 bar), 669.7 mg g^{-1} (10 bar)	1544	173
NHPC-812			Capacity: 316.5 mg g^{-1} (1 bar), 613.8 mg g^{-1} (10 bar)	1477	
AN-OMC-700	Gases present: H_2S, O_2, and N_2, temperature: 25 °C, pressure: 1 bar	5000 ppm	Concentration: saturated, capacity: 276.21 mg g^{-1}	1538	246
N-OMCS-700	Gases present: H_2S, O_2, and N_2, temperature: 0 °C, pressure: 1 bar		Capacity: 456.94 mg g^{-1}	1575	247
N-OMCS-800			Capacity: 371.69 mg g^{-1}	1201	
N-OMCS-900			Capacity: 303.49 mg g^{-1}	1202	
N-PCNF-1/2-700	Gases present: H_2S, O_2, N_2, and H_2O, temperature: 25 °C, pressure: 1 bar, humidity: 70%	1000 ppm	Concentration: 50 ppm, capacity: 1490 mg g^{-1}	1279	248

Table 4 (*Contd.*)

Adsorbent	Adsorption conditions	Initial concentration of H$_2$S	Breakthrough time, concentration of H$_2$S and capacity	BET surface area (m^2 g^{-1})	Reference
N-PCNF-1/2-800			Capacity: 1840 mg g^{-1}	1308	
40 wt% N-PCNF-1/2-800			Capacity: 3340 mg g^{-1}	n/a	
N-MCNS-PEI-25	Gases present: H$_2$S, O$_2$, and N$_2$, temperature: 25 °C; Gases present: H$_2$S, CO$_2$, O$_2$, and N$_2$, temperature: 25 °C	1000 ppm	Concentration: 50 ppm, capacity: 466.23 mg g^{-1}; Capacity: 436.82 mg g^{-1}	193	175
D-glucose and D-fructose-based PC	Temperature: 25 °C, pressure: 1 bar, mass: 100 mg, flowrate: 0.2 L min^{-1}	20 ppm	Time:18–68.2 min, capacity: 6.32–25.7 mmol g^{-1}	229–3217	249
ZnO-supported N-modified ACs	Temperature: 25 °C, pressure: 1 bar, flowrate: 100 mL min^{-1}	400 ppm	Time: 105–345 min, capacity: 24.2–62.5 mg S g^{-1}	495–816	250
Jute-derived NPC	Temperature: 25 °C, pressure: 1–10 bar (pure H$_2$S), 35 bar (mixed gas), mass: 1 g	Pure and mixed with He (20 : 80 vol% H$_2$S/He)	Capacity: 6.45–19.10 mmol g^{-1} (1 bar), 12.8–32.6 mmol g^{-1} (10 bar), 16.2–45 mmol g^{-1} (35 bar)	1065–2580	166
KOH-modified waste oil fly ash derived ACs	Temperature: 1–50 °C, pressure: 1.38–3.45 bar, mass: 1 g, flowrate: 0.2–0.8 L min^{-1}	50 and 100 ppm	Time: 25–120 min, capacity: 3.5–8.5 mg g^{-1}	35.24	251
Metal oxides					
ZnO	Gases present: H$_2$S, CO$_2$, CO, H$_2$, N$_2$, and H$_2$O, temperature: 400–600 °C	100 ppmv	Concentration: 20 ppmv, capacity: 10 mg g^{-1} (400 °C)	2–3	190
28 wt% Ni–ZnO			Capacity: 210 mg g^{-1} (400 °C), 178 mg g^{-1} (500 °C), 117 mg g^{-1} (600 °C)		
28 wt% Co–ZnO			Capacity: 184 mg g^{-1} (400 °C), 177 mg g^{-1} (400 °C), 145 mg g^{-1} (400 °C)		
28 wt% Cr–ZnO			Capacity: 48 mg g^{-1} (400 °C)		
28 wt% Fe–ZnO			Capacity: 101 mg g^{-1} (400 °C)		
CuO/TiO$_2$	Gases present: H$_2$S and N$_2$, temperature: 400–480 °C	2000 ppm	Concentration: saturated, capacity: 40–300 mg g^{-1}	44.34	189
CoO/TiO$_2$			Capacity: 100–410 mg g^{-1}	45.92	
NiO/TiO$_2$			Capacity: 100–580 mg g^{-1}	52.77	
Mn$_2$O$_3$/Fe$_2$O$_3$	Gas present: H$_2$S, temperature: 25 °C, pressure: 1 bar	500 ppm	Concentration: 400 ppm, capacity: 11.97 mg g^{-1}	6.19	191
CaO–Fe$_2$O$_3$	Gases present: H$_2$S, CO$_2$, NH$_3$, and H$_2$, temperature: 850 °C	230 ppmv	n/a	1.50	252
ZnFe$_2$O$_4$	Gases present: H$_2$S, O$_2$, N$_2$, and H$_2$O, temperature: 25 °C, pressure: 1 bar	1000 ppm	Concentration: 100 ppm, capacity: 1.6 mg g^{-1}	16	169
MoO$_2$	Temperature: 65–89 °C, pressure: 10–19 bar, Mass: 1 g	38–73 ppm	Time: 78–85 min, capacity: 0.03–0.08 g S g^{-1}	48–65	188

Table 4 (Contd.)

Adsorbent	Adsorption conditions	Initial concentration of H_2S	Breakthrough time, concentration of H_2S and capacity	BET surface area (m^2 g^{-1})	Reference
Acid mine drainage sludge (AMDS)	Gases present: H_2S and N_2, temperature: 25 °C, pressure: 1 bar	110–126 ppmv	Concentration: 5.5–6.3 ppmv, capacity: 8361 mg g^{-1}	155.65	193
		1000 ppmv	Concentration: 50 ppmv, capacity: 0.23–0.31 mg g^{-1}	155.65	
ZnFe-DMO-5	Gases present: H_2S, CO_2, CO, N_2, and H_2, temperature: 550 °C	2000 ppmv	Concentration: 100 ppmv, capacity: 250 mg g^{-1}	27	192
NaMnO-D	Gases present: H_2S, N_2, and H_2O, temperature: 25 °C, pressure: 1 bar	500 ppm	Concentration: 400 ppm, capacity: 439.2 mg g^{-1}	1.77	253
NaMnO-T			Capacity: 818.7 mg g^{-1}	2.56	
NaCo$_{0.7}$O$_{2.4}$-D	Gases present: H_2S and N_2, temperature: 25 °C	500 ppm	Concentration: 10 ppm, capacity: 154.6 mg g^{-1}	1.15	254
NaCo$_{1.1}$O$_{3.3}$-T			Capacity: 168.2 mg g^{-1}	1.90	
Zeolites					
NaA	Gases present: H_2S and N_2, temperature: 25 °C, pressure: 1 bar	15 ppmv	Concentration: 1 ppmv, capacity: 13.95 mg g^{-1}	263.35	204
AgNaA			Capacity: 33.24 mg g^{-1}	201.79	
NaX	Gases present: H_2S and N_2, temperature: 25 °C, pressure: 1 bar	110–126 ppmv	Concentration: 5.5–6.3 ppmv, capacity: 277.86 mg g^{-1}	515	193
FeX			Capacity: 10.01 mg g^{-1}	350	
Magnetite-supported Y and ZSM-5 zeolites	Temperature: 100, 200, and 300 °C, pressure: 1 bar, mass: 0.5 g, flowrate: 1 L min^{-1}	30, 60, 90 and 120 ppm	Time: 120–330 min, capacity: 14.7–69.9 mg g^{-1}	332.6–550.1	205
Industrial molecular sieve (IMS)	Gases: H_2S and Ar, temperature: 25 °C, pressure: 1 bar	200 and 10 000 ppmv	Concentration: saturated, capacity: 32 mg g^{-1} (200 ppmv), 194 mg g^{-1} (10 000 ppmv)	590	209
MOFs					
UiO-66	Gases: H_2S and N_2, temperature: 30–50 °C	4000 ppm	Concentration: saturated, capacity: 50–80 mg g^{-1}	1351	255
		4500 ppm	Concentration: 2250 ppm, capacity: 51.1–95.4 mg g^{-1}		256
UiO-66-NH$_2$	Gases: H_2S and N_2, temperature: 25 °C, pressure: 1 bar	10 ppmv	Concentration: 1 ppmv, saturated, capacity: 0.04 mg g^{-1} (1 ppmv), 0.07 mg g^{-1} (saturated)	963	257
MOF-5			Capacity: 1.2 mg g^{-1} (1 ppmv), 4.97 mg g^{-1} (saturated)	424	
MOF-199			Capacity: 40 mg g^{-1} (1 ppmv), 69 mg g^{-1} (saturated)	725	
CuBDC	Gases: H_2S, N_2, and H_2O, temperature: 25 °C	500 ppm	Concentration: 400 ppm, capacity: 105.6 mg g^{-1}	218	
CuBDC-N			Capacity: 1.3 mg g^{-1}	38	
CuBTC			Capacity: 27.1 mg g^{-1}	317	

Table 4 (Contd.)

Adsorbent	Adsorption conditions	Initial concentration of H_2S	Breakthrough time, concentration of H_2S and capacity	BET surface area (m^2 g^{-1})	Reference
	Gases: H_2S and N_2, temperature: 25 °C	500 ppm	Concentration: saturated, capacity: 77.1 mg g^{-1}	231.9	258
	Gases: H_2S and N_2, temperature: 25 °C, pressure: 1 bar	99.6 ppm	Concentration: 5 ppmv, capacity: 17.1–56.3 mg g^{-1}	434–1380	259
$Cu(BDC)_{0.5}(BDC\text{-}NH_2)_{0.5}$	Gases: H_2S and N_2, temperature: 25 °C	500 ppm	Concentration: 50 ppm, capacity: 128.4 mg g^{-1}	19.4	215
MFM-300(In)	Gases: H_2S and N_2, temperature: 25 °C, pressure: 1 bar	10 vol%	Concentration: saturated, capacity: 310 mg g^{-1}	1060	217
MFM-300(Sc)			Capacity: 564 mg g^{-1}	1360	216
MIL-53(Al)-TDC	Gases: H_2S and N_2, temperature: 30 °C, pressure: 1 bar	5 vol%	Concentration: saturated, capacity: 606–654 mg g^{-1}	1150	216
ZIF-8	Gases: H_2S, CO_2, CH_4, and He, temperature: 25 °C, pressure: 2–10 bar	3 vol%	Time: 190–400 s, concentration: 1500 ppmv, capacity: 3299 mg g^{-1}	412–1389	223
$Bi_2O(H_2O)_2(C_{14}H_2O_8) \cdot nH_2O$	Gases: H_2S and N_2, temperature: 25 °C, pressure: 1 bar	4.3 vol%	Concentration: saturated, capacity: 543.58 mg g^{-1}	412	218
Porous organic polymers					
Hierarchical porous polymers (HPP)	Gas: H_2S, temperature: 25 °C, pressure: 1 bar	Pure	Concentration: saturated, capacity: 94 mg g^{-1}	1605	260
N-HPP-pyridine			Capacity: 170 mg g^{-1}	792	
N-HPP-bipyridine			Capacity: 188 mg g^{-1}	1350	
N-HPP-3-aminophenol			Capacity: 153 mg g^{-1}	1229	
N-HPP-HMTA			Capacity: 198 mg g^{-1}	1397	
N-HPP-p-phenylenediamine			Capacity: 177 mg g^{-1}	1186	
Pluronic® F127-modified biosolid-derived	Temperature: 25 °C, volume: 2 cm^3, particle size: 425–600 μm	1000 ppm	Time: 120–325 min, capacity: 89.1–221.2 mg g^{-1}	110–180	207
CBAP-1-EDA	Gases: H_2S and N_2, temperature: 25 °C, pressure: 1 bar	10 ppmv	Concentration: 1 ppmv, saturated, capacity: 0.033 mg g^{-1} (1 ppmv), 0.12 mg g^{-1} (saturated)	672	257
CBAP-1-DETA			Capacity: 0.026 mg g^{-1} (1 ppmv), 0.1 mg g^{-1} (saturated)	667	
Composite materials					
ZnBDC/ZnO	Gases: H_2S and N_2, temperature: 25 °C	500 ppm	Concentration: 400 ppm, capacity: 13.6 mg g^{-1} (moist), 10.6 mg g^{-1} (dry)	12.4	232
ZnBDC-N/ZnO			Capacity: 9.4 mg g^{-1} (moist), 7.9 mg g^{-1} (dry)	15.0	
ZnBTC/ZnO			Capacity: 7.8 mg g^{-1} (moist), 14.3 mg g^{-1} (dry)	20.6	
ZnO/MCM-41	Temperature: 50, 175, and 300 °C	5000 ppm	Time: 119–850 min	254–739	261
20 wt% ZnO/MCM-41	Gases: H_2S, N_2, and H_2O, temperature: 25 °C	500 mg m^{-3}	Concentration: 1.5 mg m^{-3}, capacity: 54.9 mg g^{-1}	686	262
30 wt% ZnO/MCM-41	Gases: H_2S, CO_2, CO, H_2, and N_2, temperature: 500 °C	2000 ppmv	Concentration: 100 ppmv, capacity: 84 mg g^{-1}	459	233

© 2024 The Author(s). Published by the Royal Society of Chemistry

Table 4 (Contd.)

Adsorbent	Adsorption conditions	Initial concentration of H_2S	Breakthrough time, concentration of H_2S and capacity	BET surface area (m^2 g^{-1})	Reference
20 wt% ZnO/SBA-15	Gases: H_2S, N_2, and H_2O, temperature: 25 °C	500 mg m^{-3}	Concentration: 1.5 mg m^{-3}, capacity: 41 mg g^{-1}	213	262
30 wt% ZnO/MCM-48			Capacity: 53.2 mg g^{-1}	323	
30 wt% ZnO/MCM-48	Gases: H_2S, CO_2, CO, H_2, and N_2, temperature: 500 °C	2000 ppmv	Concentration: 100 ppmv, capacity: 54 mg g^{-1}	459	233
ZnO/SiO$_2$	Gases: H_2S and N_2, temperature: 30 °C	850 mg m^{-3}	Concentration: 0.15 mg m^{-3}, capacity: 28.6–108.9 mg g^{-1}	106.3–168.5	263
Co$_3$O$_4$/SiO$_2$			Capacity: 114.3 mg g^{-1}	n/a	
CuO/SiO$_2$			Capacity: 145.6 mg g^{-1}	n/a	
	Gases: H_2S and N_2, temperature: 150 °C, pressure: 1 bar	100 ppm	Concentration: 5 ppm, capacity: 32–363 mg g^{-1}	13.44–175.75	264
HKUST-1/GO-PEI	Gases: H_2S and N_2, temperature: 25 °C, pressure: 1 bar	99.6 ppm	Concentration: 5 ppmv, capacity: 30.7–55.6 mg g^{-1}	56–489	259
SBA-15/PEI-25	Gases: H_2S, N_2, and O_2, temperature: 25 °C, pressure: 1 bar	1000 ppm	Concentration: 50 ppm, capacity: 26.6 mg g^{-1}	495	
UiO-66/GO	Gases: H_2S and N_2, temperature: 30–50 °C	4500 ppm	Concentration: 2250 ppm, capacity: 115.9–296.5 mg g^{-1}	1002–1432	256
1 wt% TiO$_2$/UiO-66		4000 ppm	Concentration: saturated, capacity: 180–210 mg g^{-1}	1171	255
3 wt% TiO$_2$/UiO-66			Capacity: 140–180 mg g^{-1}	986	
5 wt% TiO$_2$/UiO-66			Capacity: 80–130 mg g^{-1}	652	
5 wt% TiO$_2$/GO	Gases: H_2S and N_2, temperature: 220 °C, pressure: 1 bar	4400 ppm	Concentration: 2200 ppm, capacity: 200 mg g^{-1}	154	265
5 wt% N–TiO$_2$/GO			Capacity: 250 mg g^{-1}	145	

materials that are durable, cost-effective and highly efficient for specific H_2S removal applications. Nevertheless, it is rather challenging to select the right combination of materials and modifications to enhance the overall performance due to limited adjustability of the main adsorbent component and lack of understanding of the reaction mechanisms for each component within the composite materials.

2.2.6 Summary of adsorption. In general, adsorbents can be divided into two major classes, adsorbents with high performance and adsorbents with high regenerative capability. Adsorbents with high performance usually have high adsorption capacity and selectivity towards H_2S by a partially or fully irreversible chemisorption mechanism. As a result, they tend to face structural collapse and could not be regenerated within a few cycles. These adsorbent materials, *i.e.*, ACs and metal oxides are much lower in price and commonly used in the second purification step after primary treatment for thorough removal. In contrast, adsorbent materials that possess high regenerative capability *via* physisorption tend to possess lower capacity for H_2S. These materials, *i.e.*, zeolites are higher in price and commonly utilized in applications that prioritize regeneration. Nonetheless, MOFs do not belong to any of the classes, as they are very costly and unable to be regenerated. As a result, MOFs are inconvenient for industrial adoption.

There are a few advantages of the adsorption process such as low cost, energy-efficiency, easy operation and simple design besides having a high temperature variation.[185,186,188] However, there are various drawbacks associated with the adsorption process such as high-pressure steam requirement to desorb high molecular weight pollutants and a gas stream pre-filter to prevent any particles from clogging the adsorbent bed.[238] In general, the adsorption process requires high temperature and pressure to operate optimally.[188] Moreover, the capacity of adsorbents gradually deteriorates as the number of cycles increases, and a steam or vacuum source is required to regenerate the adsorbent. Nonetheless, some adsorbents are non-regenerable, resulting in a huge volume of sulfide wasted. In addition, the product recovery might require a special expensive distillation or extraction. The spent absorbent is often considered as hazardous waste as some contaminants might undergo an exothermic reaction with the adsorbent leading to explosion. The existing conventional technologies and recent research findings on H_2S capture through adsorption are summarized in Table 4.
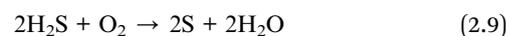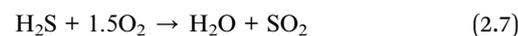
2.3 Chemical conversion

There are two major conventional technologies for H_2S removal by chemical conversion into elemental sulfur such as Claus and LO-CAT processes.

2.3.1 Claus process. The Claus process is a technology patented for H_2S conversion into elemental sulfur and water. This process typically occurs in a sulfur recovery unit (SRU) and plays a significant role in global sulfur production. The production of elemental sulfur from H_2S is a crucial industrial process. Besides, it is essential to comply with stringent environmental regulations regarding H_2S emissions.[266] Carl

Friedrich Claus developed the Claus process under a British patent in 1883 which underwent transformation in the 1930s by Baehr in 1938, but it was not developed further until the 1950s.[267]

The Claus process was further improved to enhance the overall sulfur recovery up to 97% of inlet sulfur.[268] The feed gases for the majority of Claus process applications typically originate from absorption units, and they primarily consist of H_2S, H_2O, and CO_2 as major components, along with minor components such as NH_3, N_2 and hydrocarbons.[269] By utilizing amine extraction, H_2S is absorbed from the absorption unit gas stream and channeled into the Claus unit. The furnace and waste heat boiler are usually considered as a single unit. The process of H_2S conversion in Claus technology involves two main steps such as thermal oxidation and catalytic reaction. The two-step process is described using eqn (2.7) and (2.8); meanwhile, eqn (2.9) is the overall reaction of the Claus process.[182]

$$H_2S + 1.5O_2 \rightarrow H_2O + SO_2 \tag{2.7}$$

$$2H_2S + SO_2 \rightarrow 3S + 2H_2O \tag{2.8}$$

$$2H_2S + O_2 \rightarrow 2S + 2H_2O \tag{2.9}$$

The Claus process combines multiple thermal and catalytic steps.[270] One third of the feed gas containing H_2S is burned in a furnace with oxygen from air to give sufficient SO_2 at 823 K in the thermal step as in eqn (2.7). In the presence of a catalyst based on alumina- or titanium dioxide, the remaining H_2S undergoes further reaction with SO_2 to produce water and elemental sulfur in the catalytic steps as described in eqn (2.8). However, since O_2 in eqn (2.9) is limited, H_2S is not fully converted.[271] Hence, the treatment of tail gas is required to comply with the environmental regulations.

Nearly all refinery plants require above 99% sulfur recovery from SRUs to meet the strict SO_X emission laws. The Claus process is only able to attain 97% of sulfur recovery even with 3 catalytic reactors. Since H_2S is not converted fully in the Claus process, its tail gas requires an additional sulfur recovery unit for tail gas treatment to meet environmental regulations regardless of the plant capacity. Three main methods of tail gas treatment that are available at the commercial scale are sub dew point, selective or direct catalytic oxidation and reduction–absorption.[272] The sub dew point process uses a special alumina-based catalyst to process H_2S and SO_2 in the tail gas from the Claus reactor at or below the sulfur dew point in a liquid system to produce more elemental sulfur at a low temperature. Nevertheless, the catalyst is vulnerable to deactivation due to deposition of liquid elemental sulfur on its surface and requires occasional replacements.[182]

The advantages of the Claus process are it is convenient for a high percentage of H_2S conversion and a well proven process technology for desulfurization. The disadvantages of the Claus process are the process is not economical and might not operate after H_2S concentration falls below 20%. In addition to this, the catalyst tends to deactivate because of liquid elemental sulfur
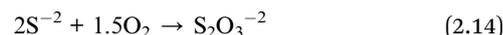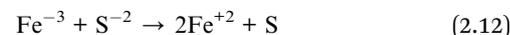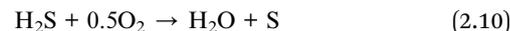
deposition on its surface. The presence of heavy hydrocarbons will lead to catalyst fouling and deactivation, resulting in a lower quality sulfur product.[273] Besides, the Claus process is an energy intensive process and requires a significant investment in capital equipment, and high operating costs due to the need for high-temperature combustion and the use of a catalyst.[274] There are also safety concerns as the process requires careful handling of high-temperature and high-pressure gases, which can pose safety risks if not managed properly. Last but not least, the process has a limited operating range and may not be effective for gas streams with low H_2S concentrations or high levels of other impurities.[275]

2.3.2   LO-CAT process. Liquid oxidation catalyst (LO-CAT) technology was developed to offer an isothermal, cost-effective method for conducting the modified Claus reaction. Humphreys and Glasgow first developed the LO-CAT process in 1965 as a chelated iron process. Ethylene diamine tetra acetic acid (EDTA) was employed to retain the iron in solution. In 1972, ARI Technologies Inc. began work on developing a H_2S removal process from air circulation and managed to overcome the main stability issue of the chelated iron compound by adding polyhydroxylated sugar (type B chelating agent) to EDTA (type A chelate). In 1980, a patent was granted to Thompson for his work. The outcome of this development was named the LO-CAT (liquid oxidation-catalytic) process.[276] In 1977, the first LO-CAT system was installed at the Plateau Refining Co. in Bloomfield, NM. The system uses a catalytic reagent called ARI-300. Eventually, a more stable catalytic reagent, ARI-310 was introduced in 1982.

The LO-CAT technology was first used commercially in 1980. Commencing with the oil and gas industry, the LO-CAT process has been persistently upgraded and modified from time to time to allow for extended usage in other industrial segments and markets such as petrochemicals, metals, water and wastewater treatment and last but not least, CO_2-based products such as food and beverages. More recently, alternative and conventional energy sources such as stranded offshore gas, shale gas, gasification syngas and biogas have also successfully utilized LO-CAT technology for sulfur recovery.[276] The LO-CAT process involves an exclusive liquid redox catalyst that converts H_2S to elemental sulfur by carrying out direct oxidation of H_2S.

The LO-CAT process uses iron(III) chelate catalytic solution as a catalyst reagent to promote the overall reaction.[276] In the absorber, the sulfide ions are oxidized by the iron ions. Eqn (2.10) and (2.11) represent H_2S absorption into the aqueous, chelated iron (Fe) solution and its subsequent ionization. Eqn (2.12) represents the S^{-2} ion oxidation to elemental sulfur and reduction of Fe^{3+} to Fe^{2+}. In the oxidizer, the reduced iron ions are regenerated by oxidation in dissolved oxygen for reuse as expressed in eqn (2.13). The function of organic chelating agents is to inhibit the precipitation of ferric hydroxide or ferrous sulfide. The Fe^{+2}/Fe^{+3} reactions are very rapid so minimum excess S^{2-} ions are carried over into the oxidizer. Eqn (2.12) and (2.14) occur very fast. Hence, the unwanted byproduct, thiosulfate salts are not formed by the side reaction. Eqn (2.13) and (2.14) represent the oxygen absorption from surrounding air into the aqueous solution followed by Fe^{2+} to

Fe^{3+} oxidation. However, eqn (2.10) and (2.13) are quite slow and become the rate controlling steps in a LO-CAT process.[276]

$$H_2S + 0.5O_2 \rightarrow H_2O + S \tag{2.10}$$

$$H_2S \rightarrow 2H^+ + S^{-2} \tag{2.11}$$

$$Fe^{-3} + S^{-2} \rightarrow 2Fe^{+2} + S \tag{2.12}$$

$$2Fe^{+2} + 0.5O_2 + H_2O \rightarrow 2Fe^{+3} + 2OH^- \tag{2.13}$$

$$2S^{-2} + 1.5O_2 \rightarrow S_2O_3^{-2} \tag{2.14}$$

Also, excess dissolved O_2 is limited by the presence of Fe^{+2} ions in the regenerated solution. The presence of high partial pressures of CO_2 in the process gas stream leads to pH reduction of the LO-CAT solution. Thus, a buffer solution such as ammonium, sodium or potassium carbonate is added. Since the reaction of H_2S absorption is very fast compared with CO_2 absorption, high selectivity of H_2S removal can be attained. Fe was chosen for the LO-CAT process mainly because it is safe to operate and inexpensive, even though there are many metals that are able to perform similar functions. The iron(III) chelate catalytic solution does not participate in the reaction. Its role is just to retain Fe ions in solution because both Fe^{2+} and Fe^{3+} ions are not very stable and soluble in aqueous solutions.[276,277] Usually at low concentrations, Fe will form precipitates as either ferrous sulfide, FeS or ferric hydroxide, $Fe(OH)_3$. The chelating agents are organic compounds that wrap around the Fe ions to prevent them from precipitating and holding them in solution throughout the operation.

LO-CAT has been developed into an adaptable processing technology for treating gas streams containing any percentage of H_2S. Among the advantages of LO-CAT include the ability to treat both aerobic and anaerobic streams of gases, high efficiencies of H_2S removal and production of only safe products and byproducts. Elemental sulfur recovered by the LO-CAT technology is totally different from sulfur produced by other processes. Compared to the sulfur generated by other methods, LO-CAT sulfur particle sizes are finer, within a range of 8 to 45 microns.[278]

There are a few advantages of the LO-CAT process such as easily obtainable and cheap catalysts besides being stable at any pH, low catalyst consumption and tolerating CO_2, NH_3 and other gas contaminants. The LO-CAT process almost ensures complete H_2S removal from acid gas streams with low H_2S content. The process operates under mild reaction conditions and does not require high temperatures or pressures, resulting in lower energy consumption compared to other processes.[279] However, there are also a few disadvantages associated with the LO-CAT process such as the catalyst reagent used is slightly corrosive, and therefore, equipment cannot be fabricated from carbon steel. Besides, the process has a limited operating range, and its performance can be affected by variations in operating conditions such as gas composition and temperature.[280] Furthermore, the degradation of chelated iron and the formation of sulfur-oxo-acid salts reduce the concentration of iron(III) chelate in the solution, hence limiting the sulfur production to

1050 kg h^{-1}.[281] Additionally, the LO-CAT catalyst needs to be periodically regenerated, which requires additional equipment and chemicals. Furthermore, the LO-CAT catalyst is proprietary, which can limit the availability and increase the cost of the catalyst.[280]

2.4 Membrane separation

Membrane separation is an industrially established technology in various industrial processes and has several advantages over other technologies such as absorption and adsorption due to its high modularity, large surface area of the membrane per unit module, smaller footprint and simple operation.[282] In addition, membrane separation can optimize the gas separation processes by lowering the energy requirement in the presence of pressurized gas, reducing the size of equipment and capital costs and improving the process safety, and it does not require a complex system to operate.[283] Besides, H_2S removal can be accomplished effectively *via* membrane separation at low cost at both offshore and remote areas.[284] Nonetheless, current research and development of membranes were focusing mainly on CO_2 removal instead of H_2S. There was a higher emphasis on membrane development for various industrial gases such as light hydrocarbons, CO_2, N_2, O_2 and H_2 based on review papers to date.[285–288] Only a few reviews[289,290] reported the development of polymeric membranes for H_2S removal due to high purification requirements (<4 ppm) and the toxic nature of the gas. Essentially, the membrane separation process uses a physical porous barrier where selective gas transport *via* permeation occurs due to transmembrane pressure. The gas separation of these membranes is influenced by the permeability–selectivity relationship while the gas permeability is controlled by the solution–diffusion mechanism. In recent years, membrane materials have been engineered to cater to the need for higher performance, efficiency and economy by optimizing several criteria such as selectivity, permeability, and chemical and mechanical stability.[291]

The application of membrane separation technology is mostly overshadowed by polymeric membranes as inorganic membranes are expensive and difficult to manufacture.[292] The only disadvantage of polymeric membranes as compared to inorganic membranes is their inability to operate under high temperature conditions. Nonetheless, polymeric membranes have proven to be one of the most successful membranes in industrial applications for H_2S separation due to their high chemical stability, ability to operate under harsh conditions and very efficient pretreatment for other technologies to purify streams containing high level of H_2S.[291] Such polymeric membranes include cellulose acetate-based membranes, *i.e.*, Schlumberger Cynara® [293] and UOP Separex™ [293] and polyimide-based membranes, *i.e.*, Air Liquide MEDAL™.[294] In general, polymeric membranes are used for natural gas sweetening processes which contains 10–20% or higher of H_2S concentration and are driven by the selectivity of H_2S over CO_2 and CH_4, respectively. Despite having similar operating conditions to biogas separation, the performances of these membranes for H_2S removal from biogas are rarely reported. This is due to the

membrane material failure to withstand acidic properties of H_2S in the gas streams and since they are only capable of removing very low concentrations of H_2S (<1%) efficiently.

Membrane-based gas separation operates through a pressure-driven mechanism as the gases flow through a thin selective membrane capable of separating different chemicals species. The process is driven by the pressure difference from high to low pressure across the membrane which allows the gas molecules to pass through the membrane layer. The rate of gas permeation is highly dependent on diffusivity, membrane thickness, partitioning of chemical species in the feed-membrane phase and the interactions between the molecules and the membranes. A higher gas solubility and diffusivity rate will result in a higher flow rate of gases passing through the membrane at a certain membrane thickness and pressure gradient.

The key factors contributing to the performance of polymeric membranes in gas separation are permeability and selectivity. Permeability is defined as the rate at which a chemical species penetrates through a membrane, whereas selectivity is the membrane's ability to effectively select the desired product with high purity and recovery. According to Robeson,[295] there is an inverse relationship between permeability and selectivity. A higher permeability will lead to a lower selectivity and *vice versa*. To achieve the optimal separation conditions and highest performance using polymeric membranes, a reasonable balance between both parameters must be obtained. Additionally, high durability with high chemical and thermal stability must be present in polymeric membranes to withstand harsh operating conditions during application.

2.4.1 Polymeric membranes. Materials with high permeability and selectivity to obtain the desired products are widely sought after over recent years.[296] Among these, polymeric membranes are gaining more attention as they are easily manufactured due to low material and manufacturing cost. Furthermore, they exhibit closely arranged and densely compacted polymer chains that offer flexibility, durability and distinctive chemical functionality. Continuous research has been carried out to fabricate a long-lasting, plasticization resistant, thermally and chemically stable membrane that can withstand the acidic nature of acid gases.[297] Besides, polymeric membranes are ideal for acid gas removal as they are highly soluble and permeable in acid gases as compared to other gases with less condensability such as CH_4, H_2, O_2 and N_2. There are a few issues related to acid gas separation using polymeric membranes such as competitive absorption, plasticization and aging that could deteriorate the performance of a membrane over time. Various methods have been implemented to overcome these issues such as using a facilitated transport membrane, base material modification *via* coupling and cross-linking with other fillers to form a mixed matrix or hybrid membranes which are more resilient and selective towards the desired gas. In a matrix membrane, the polymer serves as the matrix or continuous phase in which other components, such as additives or fillers, may be dispersed. The structure of matrix membranes typically consists of a dense polymer layer that provides selective transport properties, allowing certain molecules or ions to pass

through while rejecting others based on size, shape, polarity, or other physicochemical characteristics.

2.4.2 Classification of polymeric membranes. In general, polymeric membranes can be categorized into two different types based on their glass transition temperature (T_g).[290] Polymeric membranes with T_g higher than room temperature are known as glassy polymers, whereas polymeric membranes with T_g lower than room temperature are known as rubbery polymers. Each polymeric membrane has different structures, bonds and functional groups which influence their T_g and also affect their mechanical properties.

2.4.3 Rubbery polymers. Rubbery polymers are soft and flexible as compared to glassy polymers as their chains are highly mobile and easily rotatable around the main axis. As a result, they have many free spaces between the chains contributing to their high permeability but rather low selectivity for gas separation application.[298] Since H_2S is more soluble compared to other gases, rubbery polymers are excellent choices for H_2S removal.[299] Rubbery polymers that are widely used for gas separation purposes include polyurethanes, PEBAX and polydimethylsiloxane (PDMS) due to their excellent permeability.[290]

Rubbery polymers have low glass transition temperatures, are flexible under ambient conditions and rely mainly on solubility for transport across rubbery membranes,[300] thus making them favorable for H_2S removal from CH_4 which is influenced by solubility.[301] Furthermore, the performance of a polyethylene glycol (PEG)-based membrane[302] can be tuned by changing the crosslinking density and polymer crystallinity. Membrane rigidification was found to be effective in resisting the strong effect of plasticization and improving the overall diffusion in a solubility-controlled membrane, contributing to outstanding H_2S/CH_4 and CO_2/CH_4 selectivity of higher than 110 and 60, respectively.[302] Nevertheless, polydimethylsiloxane (PDMS) was found to be the most permeable rubbery polymer compared to the rest of the polymeric membranes.[303]

2.4.4 Polyether block amide (PEBAX®). Polyether block amide, also well known as PEBAX®, is a commercial thermoplastic polymer widely used for gas separation purposes.[304] PEBAX is synthesized by linking together two of its main components, *i.e.*, polyether and polyimide chains by copolymerization. The properties of PEBAX are affected by its chemical properties and the ratios of both segments. The polyether chains have a high selectivity towards acid gases,[305] especially CO_2, whereas the polyimide chains provides structure stability that prevents the polyether chains from crystallizing. Amo *et al.*[306] discovered that a PEBAX 4011 membrane possesses the highest selectivity for H_2S over CO_2 (>15) and CH_4 (>70) after comparison with several materials. On the other hand, Vaughn and Koros[307] investigated the permeability of the PEBAX membrane for acid gas, *i.e.*, CO_2 and H_2S removal at 35 °C and different pressures. The permeability for both gases was found to increase as the pressure increases from 1.0 to 6.98 bar due to the high chain mobility and diffusivity coefficient of acid gases across the membrane. H_2S solubility was also found to increase in PEBAX membranes as they are amide-based and have strong affinity towards H_2S.

2.4.5 Polyurethanes. Polyurethane membranes are synthetic elastomers composed of polyurethane polymers, which are formed by the reactions between polyols and isocyanates.[308] The ratio of polyols to isocyanates, known as the NCO/OH ratio, is an important criterion to achieve desirable properties of polyurethane membranes. The ratio affects the extent of crosslinking, mechanical properties, flexibility, and other characteristics. Careful consideration and optimization of this ratio are essential to achieve the desired balance between flexibility and strength. Their high selectivity towards H_2S over CH_4 has sparked various studies on their suitability for natural gas sweetening processes. Chatterjee *et al.*[309] developed poly(ether urethanes) and poly(ether urethane ureas) that demonstrated high permeability to H_2S as compared to CO_2 and CH_4 at both low pressure and high pressure up to 10 bar for both pure and mixed gas feeds. Their results also agreed with those of Mohammadi *et al.* which stated that permeability is affected by the solubility of the gas, and it increases as the temperature and pressure of the gas feed increases.

2.4.6 Polydimethylsiloxanes (PDMSs). A polydimethylsiloxane (PDMS) membrane is a silicone-based polymer commonly used for gas separation application due to its unique properties.[310] The glass transition temperature of PDMS typically ranges from around −125 °C to −120 °C.[298] This low T_g is a result of the flexible and highly mobile nature of the silicone polymer's molecular structure, which allows the chains to move easily even at relatively low temperatures. As a result, PDMS has a high permeability and good selectivity towards CO_2 and CH_4, making them suitable for natural gas purification applications.[311] However, less emphasis has been given towards H_2S removal purposes.

According to Robb,[312] the H_2S presence could significantly increase the elasticity of PDMS membranes leading to a very high permeability of 10 000 Barrer for H_2S as compared to CO_2 (3250 Barrer) and CH_4 (900 Barrer). Besides, the permeability of the PDMS membrane is also observed to be very high in acidic compounds, with a selectivity of 3 and 10 for H_2S/CO_2 and H_2S/CH_4, respectively. However, no plasticization effect was observed as the permeability coefficients remain unchanged despite the increase in feed pressure. Several authors[313,314] discovered that a PDMS membrane is more permeable in H_2S compared to CO_2. Meanwhile, Bhide *et al.*[313] determined that the permeability of the PDMS membrane is 1000 Barrer at 25 °C, whereas Merkel *et al.*[314] obtained a value of 5100 Barrer at 23 °C.

A similar observation was also reported by Merket and Toy. A study revealed that the applied PDMS coating layer on the crosslinked 6FDA-DAM/DABA polyimide hollow fiber membranes successfully enhanced membrane performance. The selectivity of H_2S to CH_4 was in the range of 22 to 29 under demanding sour gas feed conditions, such as a 20% H_2S concentration and very high pressures ranging from 34.47 to 48.26 bar.[315] It was anticipated that the PDMS coating layer assisted in sealing and leveraging the morphological defects present in the crosslinked polyimide fibers, which could potentially worsen under such harsh conditions.

Table 5 Summary of the latest H_2S separation findings by using membranes

Membrane	Feed composition	Membrane separation conditions	H_2S permeability (mol m^{-2} s^{-1} Pa^{-1})	H_2S/CO_2 selectivity	H_2S/CH_4 selectivity	Reference
PEBAX 3533 SA00	1.3 mol% H_2S, 27.9 mol% CO_2, and 70.8 mol% CH_4	Temperature: 35 °C, pressure: 10 bar	2.97×10^{-13}	3.65	21	309
PEBAX 4033 SA00			1.04×10^{-13}	3.7	24	
PEBAX 6333 SA00			1.26×10^{-14}	5.11	20	
PEBAX 7233 SA00			2.54×10^{-15}	1.85	15	
PEBAX MX 1041			5.85×10^{-14}	4.41	49	
PEBAX MX 1657			8.3×10^{-14}	3.59	50.6	
PEBAX MX 1074	12.5 mol% H_2S, 18.1 mol% CO_2, and 69.4 mol% CH_4		1.85×10^{-13}	4.53	54	
			2.33×10^{-13}	4.48	50.4	
PEBAX SA01 MV3000	Pure	Temperature: 35 °C, pressure: 1.17 bar	1.75×10^{-13}	4.87	50.48	307
		Pressure: 2 bar	2.1×10^{-13}	5.83	60.43	
		Pressure: 2.76 bar	2.25×10^{-13}	5.83	67.32	
		Pressure: 3.45 bar	2.42×10^{-13}	6.49	64.94	
PDMS	Pure	Temperature: 35 °C, pressure: 1.1 bar	1.68×10^{-12}	3.08	10	314
PDMS + PEG + Psf (glycerol)		Temperature: 25 °C,	n/a	1.8	6.5	348
		Temperature: 25 °C,	n/a	5.7	140	317
Cytop	15 mol% H_2S and 10.5 mol% CO_2	Temperature: 37 °C, pressure: 4.4 bar	n/a	n/a	n/a	314
Silica-rich CHA-type zeolite	0.3 mol% H_2S, 2.13 mol% CO_2, and 97.57 mol% CH_4	Temperature: 25 °C, pressure: 1 bar	1.70×10^{-8}	n/a	3.24	349
Amine-based CNT butylamine, sec-butylamine, dodecylamine, and octadecylamine	0.5, 1.2, and 2.5% (6000, 12 000, 2 and 5 000 ppm of H_2S, remaining gas is CH_4)	Temperature: 25 °C, pressure: 4 bar	$(6.2–7.6) \times 10^{-7}$	n/a	:	350
		Temperature: 30 °C Pressure: 1–5 bar	$(3.2–4.1) \times 10^{-7}$		7–8.4	
			$(4.7–5.7) \times 10^{-7}$		3.9–4.8	
			$(2.9–3.6) \times 10^{-7}$		5.5–7	
					3.5–4.5	
Cellulose acetate (CA)	20 mol% H_2S, 20 mol% CO_2, and 60 mol% CH_4	Temperature: 35 °C, pressure: 34 bar	2.91×10^{-15}	1.01	30.5	342
		Pressure: 35 bar	n/a	n/a	30	
		Pressure: 48 bar	1.33×10^{-14}	1.44	27.5	
	6 mol% H_2S, 29 mol% CO_2, and 65 mol% CH_4	Pressure: 10.8 bar	n/a	0.88	19	309
Modified CA	20 mol% H_2S, 20 mol% CO_2, and 60 mol% CH_4	Temperature: 35 °C, pressure: 34 bar	6.82×10^{-14}	1.58	34.3	342
		Pressure: 48 bar	6.36×10^{-14}	1.40	27.5	
CTA	1000 ppm H_2S and remaining N_2	Temperature: 25–80 °C, pressure: 1–9 bar	$(1.57–3.41) \times 10^{-15}$	n/a	n/a	351
CTA hollow fiber	20 mol% H_2S, 5 mol% CO_2, 3 mol% C_2H_6, 3 mol% C_2H_8, 100–300 ppm toluene, and remaining CH_4	Temperature: 35, 50 °C, pressure: 6.9–31.3 bar	4.69×10^{-14}	n/a	28	345

Table 5 (Contd.)

Membrane	Feed composition	Membrane separation conditions	H_2S permeability (mol m^{-2} s^{-1} Pa^{-1})	H_2S/ CO_2 selectivity	H_2S/CH_4 selectivity	Reference
6FDA-DAM. 6FDA-DAM/DABA (3 : 2)	(i) 0.5 mol% H_2S, 20 mol% CO_2, and 79.5 mol% CH_4 (ii) 5 mol% H_2S, 45 mol% CO_2, and 50 mol% CH_4 (iii) 20 mol% H_2S, 20 mol% CO_2, and 60 mol% CH_4	Temperature: 35 °C, pressure: 7–46 bar	$(6.93\text{-}36.4) \times 10^{-14}$, $(7.63\text{-}29.3) \times 10^{-15}$	n/a	14–38.7, 18.8–49.1	301
6FDA-DAM/6FpDA (1 : 3), 6FDA-DAM/CARDO (1 : 3), 6FDA-DAM/ABL-21 (1 : 3), 6FDA-DAM/6FDA-CARDO (1 : 1)	20 mol% H_2S, 10 mol% CO_2, 57–59 mol% CH_4, 1–3 mol% C_2H_6, and 10 mol% N_2	Temperature: 22 °C, pressure: 24,35, 46 bar	$(1.76\text{-}2.28) \times 10^{-14}$, $(7.83\text{-}8) \times 10^{-15}$, $(1.05\text{-}1.1) \times 10^{-14}$, $(3.85\text{-}6.03) \times 10^{-14}$	n/a	19.7–21.2, 15.2–15.9, 15.2–15.9, 23–25	352
Crosslinked telechelic PEG	5 mol% H_2S, 3 mol% CO_2, and 92 mol% CH_4	Temperature: 25 °C, pressure: 55.2 bar	$(0.027\text{-}8.37) \times 10^{-15}$	n/a	65–116	302
Vinyl-added polynorbornene (VAPNB) membranes	(i) 5 mol% H_2S, 3 mol% CO_2, and 92 mol% CH_4 (ii) 20 mol% H_2S, 10 mol% CO_2, 57 mol% CH_4, 3 mol% C_2H_6, and 10 mol% N_2	Temperature: 25 °C, pressure: 55.2 bar	3-Gas mixture: $(1.51\text{-}2.01) \times 10^{-12}$ 5-Gas mixture: $(2.01\text{-}2.34) \times 10^{-12}$	n/a	6–45 9–40	353
6FDA-HAB-DAM	1000 ppm H_2S and remaining N_2	Temperature: 25, 35, 55, 75 °C, pressure: 2–9 bar	$(5.19\text{-}5.69) \times 10^{-14}$	n/a	n/a	354
6FDA-HAB-DAM-DABA 6FDA-DAM:DABA (3 : 2)	10 mol% H_2S, 20 mol% CO_2, and 70 mol% CH_4	Temperature: 35 °C, pressure: 6.7 bar Pressure: 20.8 bar Pressure: 41.3 bar Pressure: 62 bar	$(4.35\text{-}5.02) \times 10^{-14}$ 3.88×10^{-15} 5.15×10^{-15} 7.26×10^{-15} 9.77×10^{-15}	0.21 n/a n/a n/a	9.0 10.3 13.2 15.6	334
6F-PAI 1	Pure Pure	Pressure: 2 bar Temperature: 35 °C, pressure: 4.5 bar	1.0×10^{-14} 2.07×10^{-15}	0.29 0.19	10 8.1	355
6F-PAI 2 6F-PAI 3		Pressure: 10 bar Pressure: 30 bar	1.0×10^{-15} 1.67×10^{-15}	0.21 0.23	10.3 10.9	
PPO	0.4 mol% H_2S and 99.96 mol% CH_4	Temperature: 22 °C, pressure: 4.5 bar	n/a	n/a	3.1	339
PPOP	Pure	Temperature: 30 °C, pressure: 2.1 bar	4.01×10^{-15}	2.5	10	356
Polyester urethane urea (PEUU) + Teflon	3 mol% H_2S, 5.4 mol% CO_2, and 91.6 mol% CH_4	Temperature: 35 °C, pressure: 10 bar Pressure: 30 bar Temperature: 55 °C, pressure: 10 bar Pressure: 30 bar	n/a n/a n/a n/a	3.79 2.72 3.91 1.9	43 27 43 12	357

Table 5 (Contd.)

Membrane	Feed composition	Membrane separation conditions	H_2S permeability (mol m^{-2} s^{-1} Pa^{-1})	H_2S/CO_2 selectivity	H_2S/CH_4 selectivity	Reference
PPO hollow fiber, PEUU	101, 198, 401, 968, 3048, and 5008 ppm H_2S in CH_4, and real natural gas concentration: 3360 ppm H_2S	Temperature: 22, 40 °C, pressure: 3.45, 5.17, 6.89 bar	PPO:$(0.5-2.44) \times 10^{-14}$; PEUU: 1.67×10^{-15}	n/a	1.34-4.1; 3.25-3.43	358
PPG-PEU (PU1)	1.3 mol% H_2S, 27.9 mol% CO_2, and 70.8 mol% CH_4	Temperature: 35 °C, pressure: 10.8 bar	8.0×10^{-14}	3.0	21	309
	12.5 mol% H_2S, 18.1 mol% CO_2, and 69.4 mol% CH_4		6.12×10^{-14}	4.28	22.6	
PPG-PEUU (PU2)	1.3 mol% H_2S, 27.9 mol% CO_2, and 70.8 mol% CH_4		2.05×10^{-13}	3.1	19	
	12.5 mol% H_2S, 18.1 mol% CO_2, and 69.4 mol% CH_4		2.07×10^{-13}	3.17	18	
PEG-PEU (PU3)	1.3 mol% H_2S, 27.9 mol% CO_2, and 70.8 mol% CH_4		9.07×10^{-14}	4.6	58	
	12.5 mol% H_2S, 18.1 mol% CO_2, and 69.4 mol% CH_4		9.37×10^{-14}	4.5	54.9	
PEG-PEUU (PU4)	1.3 mol% H_2S, 27.9 mol% CO_2, and 70.8 mol% CH_4		6.66×10^{-14}	4.45	74	
	12.5 mol% H_2S, 18.1 mol% CO_2, and 69.4 mol% CH_4		7.46×10^{-14}	4.39	66	
PVDC	Pure	Temperature: 30 °C, pressure: 0.93 bar	n/a	n/a	n/a	356
PVDF + [Bmim][BF$_4$]	Pure	Temperature: 35-65 °C, pressure: 4 bar	$(0.54-3.68) \times 10^{-13}$	n/a	130-260	359 and 360
PVDF + [Bmim][BF$_4$]		Temperature: 40 °C, pressure: 1 bar	1.36×10^{-12}	3.7	36.6	361
PVDF + [Bmim][PF$_6$]			6.38×10^{-13}	3.7	29.8	362
PVDF + [Bmim][AC]			2.44×10^{-12}	11.7	136	
PVDF + [Bmim][NTf$_2$]			8.7×10^{-13}	2.1	19.8	
PVDF + [Bmim][CF$_3$SO$_3$]			1.44×10^{-12}	4.0	50.7	
PVTMS	Pure	n/a	1.17×10^{-13}	n/a	1.59	362
PVTFA	Pure	Temperature: 30 °C, pressure: 1 bar	n/a	n/a	n/a	363
PTBP		Pressure: 2.1 bar	5.35×10^{-15}	0.94	9.4	356
PDTBP			6.69×10^{-15}	0.74	4	
PVBTAF	10.5 mol% H_2S and 89.5 mol% CH_4	Temperature: 30 °C, pressure: 1.2 bar	n/a	n/a	7000	364
	10 mol% CO_2	Pressure: 1.1 bar	n/a	10.8	3300	
	10.3 mol% H_2S	Pressure: 8.5 bar	n/a	8.7	2100	
	79.7 mol% CH_4	Pressure: 5 bar	n/a	n/a	950	
Nafion NE111	Pure	Temperature: 20 °C, pressure: 1 bar	1.87×10^{-13}	n/a	n/a	365
Nafion NE117			7.56×10^{-13}	n/a	n/a	

Table 5 (*Contd.*)

Membrane	Feed composition	Membrane separation conditions	H_2S permeability (mol m^{-2} s^{-1} Pa^{-1})	H_2S/CO_2 selectivity	H_2S/CH_4 selectivity	Reference
Aquivion®	10 mol% H_2S and 90 mol% CH_4	Temperature: 35 °C, pressure: 1 bar	1.07×10^{-14}	0.53	12	328
PBI composites	5.3 mol% H_2S, 5.1 mol% CO_2, and 89.6 mol% CH_4	Pressure: 2 bar; Temperature: 50 °C, pressure: 1.2 bar	1.26×10^{-13}; 2.72×10^{-13}	0.93; 7.5	28; 140	366
TEGMC : 6FDA-DAM/DABA (3 : 2) with/without PDMS	(i) 5 mol% H_2S, 45 mol% CO_2, and 50 mol% CH_4 (ii) 20 mol% H_2S, 20 mol% CO_2, and 60 mol% CH_4	Temperature: 35 °C, pressure: 6.9–48.3 bar	$(3.18–6.7) \times 10^{-15}$	n/a	With PDMS: 20–29 Without PDMS: 12–20	315

2.4.7 Classification of glassy polymers. Glassy polymers are rather different from their counterparts by having high selectivity and lower permeability as they possess fewer mobile chains and fewer free spaces between them.[316] The rigid and hard structures of glassy polymers enable selectivity-based diffusion to occur based on the different kinetic diameters of the compounds. For example, CH_4 which has a larger kinetic diameter than the acid gases, *i.e.*, CO_2 and H_2S, can be separated easily by the selectivity-based diffusion mechanism.[317] High partial pressure of the feed gas might affect the membrane performance due to the plasticization effect.[318] Another weakness of glassy polymers is the aging effect which causes the membranes to lose permeability to acid gases and a drop in performance over time.[319] There are a few categories of glassy polymers that are commonly used for gas separation such as polyimide, polyphenylene oxide, cellulose acetate and fluorinated polymers.

2.4.8 Fluorinated polymers. Fluorinated polymers, also known as fluoropolymers, are a class of synthetic polymers that contain fluorine atoms within their molecular structure.[320] They are known to be chemically and thermally stable, which makes them well-suited for gas separation applications.[321] However, they possess several undesirable properties which hinder their development as membrane materials such as high costs, difficulty synthesis and rigid crystalline and semi-crystalline structures.[322] Their high permeability and solubility towards H_2S have encouraged many researchers to develop ideal fluorinated polymers membranes well-suited for gas separation. There are a few types of fluorinated polymers commonly used for natural gas separation such as perfluorosulfonic acid (PFSA), polytetrafluoroethylene (PTFE) and polyvinylidene fluoride (PVDF).

Based on a comparison between different types of fluorinated and non-fluorinated polymers, Merkel and Toy[323] found out that both Cytop and Teflon membranes were capable of absorbing more CO_2 than H_2S. These results also indicate that fluorinated polymers are more plasticization-resistant as compared to non-fluorinated polymers as they are highly resistant to chemical degradation which allows them to withstand acidic conditions without a decrease in performance. On the other hand, perfluorosulfonic acid (PFSA) such as Aquivion and Nafion exhibited a glassy behavior under dry conditions and increasing permeability under humid conditions. Several authors[324–326] reported that the PFSA membranes are showing glassy behavior under dry conditions, the gas permeation is dependent on the solution–diffusion and their performance is affected by the kinetic diameter of the reactants. However, PFSA membranes were found to have a low permeability which makes them undesirable for gas separation purposes under dry conditions.[327] Nonetheless, PFSA membranes demonstrated outstanding performances and strong affinity towards polar compounds when being used under humid conditions. By increasing the relative humidity of the feed gas at 35 °C, PFSA membranes exhibited increasing permeability from 32 to 370 Barrer and from 40 to 250 Barrer for H_2S and CO_2, respectively.[328]

2.4.9 Polyimide polymers. Polyimide polymers are a class of high-performance polymers known for their exceptional

mechanical strength, thermal and chemical stability and high resistance to corrosion.[329] Due to their high selectivity, permeability and resistance to plasticization, polyimides are excellent choices as membrane materials for gas separation applications. Matrimid® is a well-known commercial polyimides polymer widely used for various applications. However, Matrimid is not widely used as a membrane for mixture gas separation.[330] Scholes et al.[331] reported that the permeability of a Matrimid membrane is rather low after being tested with mixture gases of H_2S and CO_2 due to the presence of competitive absorption between both gases.

Other polyimide membranes that are commonly used are semi-fluorinated modified polyimides such as 6FDA, 6F-PAI-1, 6FDA-HAB and 6FDA-DAM:DABA. These polymers are proven to have a high selectivity towards H_2S, and CO_2 as compared to CH_4 with a selectivity range of 10 to 16 for H_2S/CH_4 and 30 to 60 for CO_2/CH_4.[307,332,333] Kraftschik et al.[334] discovered that the plasticization effect of the 6FDA-DAM:DABA membrane can be minimized by thermal treatment when tested with binary mixture gases of H_2S and CH_4, and also ternary mixture gases of H_2S, CO_2 and CH_4. They found out that upon treatment, the permeability of H_2S has increased to 100 Barrer and the interactions between the reactant and polymers have increased the selectivity of membranes. On the other hand, Vaughn and Koros[307] investigated the performances of 6FDA and 6F-PAI-1 membranes for H_2S removal and discovered a selectivity of 10 for H_2S/CH_4.

2.4.10 Polyphenylene oxide polymers. Polyphenylene oxide (PPO), also known as polyphenylene ether (PPE), is a class of thermoplastic polymers that possesses a unique combination of properties such as high thermal and chemical stability and high permeability and selectivity which makes them an excellent choice for gas separation purposes which involves H_2S, CO_2 and CH_4.[335,336] The presence of phenyl rings inside PPO protects the chains from degradation under acidic and basic conditions.[337,338] According to Chenar et al.,[339] the H_2S permeability in a PPO hollow fiber module increases as the concentration and pressure of the feed gases increase except for CH_4 which was found to remain unchanged.[340] However, the permeability was found to increase for both H_2S and CH_4 as the temperature increases.

2.4.11 Cellulose acetate polymers. Cellulose acetate is a flexible thermoplastic polymer obtained from natural cellulose via a chemical modification process known as acetylation where acetates are introduced onto the cellulose polymer chains.[340] Cellulose acetate membranes are suitable for gas separation due to their tunable pore structure, easy to be modified, compatible with various gases, and cost-effective.[341] Besides, cellulose acetate membranes have a good selectivity value between 10 and 30 for H_2S/CH_4.[342] In addition, the presence of both H_2S and CO_2 gases, even at low concentration, was reported to decrease the plasticization of membranes that could lower the separation performance.[343]

In addition, Baker[344] discovered that the permeability of H_2S in cellulose acetate membranes become lower at higher relative humidity due to the hydrophilic nature of the membranes which lose their rigidity as they began to absorb water from the surroundings.[339] Due to these limitations, their application at the industrial level has been restricted to operating only in the presence of a little water in the feed gas to maintain a high level of permeability and selectivity. To improve the separation performance and mechanical resistance of the cellulose acetate membrane, various studies have been conducted to develop a better membrane by functionalizing the surface with specific groups such as vinyl methoxysilanes. The modified cellulose acetate membrane not only showed similar selectivity to the unmodified membrane but a significantly improved permeability up to 200 Barrer from 8.7 Barrer originally.[342]

On the other hand, Liu et al.[345] investigated the plasticization effect of CTA hollow fibers on the removal of acid gas from a feed stream containing a mixture of gases of H_2S, CO_2, CH_4, C_2H_6 and C_3H_8 at 35 °C. The CTA hollow fibers demonstrated a remarkably higher permeability towards H_2S and CO_2 as the feed gas pressure increases. As pressure increased from 5 to 30 bar, the permeability rose from 80 GPU to 140 and 120 GPU for H_2S and CO_2, respectively. This happened due to the competitive absorption between H_2S and CO_2 and also the plasticization effect of CTA hollow fibers at high temperature. Furthermore, Liu et al.[345] concluded that the plasticization effect of acid gases and high separation efficiency contributed to high selective removal of H_2S in the presence of CO_2.

2.4.12 Summary of membrane separation. Generally, various types of membranes were evaluated for their effectiveness and potential for H_2S removal in natural gas sweetening processes. These membranes were assessed to verify their durability and suitability for realistic and harsh condition operations, i.e., high concentrations of H_2S between 5 and 20% in the gas mixture. However, these membranes are known to have several drawbacks such as vulnerability to physical aging and plasticization in the presence of plasticizers, e.g., H_2S, CO_2, condensable aromatics such as benzene, toluene, ethylbenzene, xylene (BTEX); and highly pressured feed gas.[346] Other major issues associated with membrane technology is membrane fouling, which reduces the treatment efficiency, membrane life and requirement of high cost of energy and chemicals for backwashing.[347] Not to mention that these membranes are actually relying heavily on high pressure of the feed gas as high as 48 bar to operate optimally,[315] which is energy intensive and uneconomical. Another drawback of these polymeric membranes would be their low selectivity towards H_2S[302] in the simultaneous removal of acid gas, as they show higher affinity towards CO_2, favored by the diffusion-influenced and glassy polymeric membranes. Recent studies on H_2S separation by using a series of membranes are summarized in Table 5.

2.5 Cryogenic distillation

The distillation process has been used since the 19th and 20th centuries, specifically for separation of alcohol applications.[367] Frank Sherwood Taylor[368] pioneered the distillation concept in 1945 using laboratory apparatus such as condensing apparatus, a vessel and a receiver. In 1953, John M. Chambers[369] further developed the idea by creating a structured distillation column for the purification of fermented alcohols by taking into

consideration heat input and optimum reflux ratio factors. Since then, distillation technology has improved significantly and is well-suited for harsh operating conditions such as low and high temperatures, high pressure as well as vacuum conditions. A distillation column is widely used for separation of two or more components from the feed gas based on different boiling points and volatility of the respective components.[370] The component with a lower boiling point left the column as the top product, whereas the component with a higher boiling point remained as a liquid as the bottom product.

Cryogenic distillation technology is a process used to separate different components of a gas mixture by cooling the mixture to very low temperatures and then distilling it.[371] Cryogenic distillation technology is one of the most efficient methods used for the simultaneous removal of CO_2 and H_2S from natural gas streams.[372] Commercially, cryogenic separation is widely utilized for CO_2 separation to fulfill the pipeline requirements. There are a few advancements in cryogenic separation technology being implemented currently such as anti-sublimation unit (AnSU), controlled free zone (CFZ), cryogenic packed bed (CPB) and CryoCell®.

2.5.1 Anti-sublimation unit (AnSU). An anti-sublimation unit (AnSU) was developed by Clodic et al.[373] by using a series of expanders and evaporators for CO_2 capture on the low-temperature frost evaporators. AnSU uses CO_2 thermodynamics of anti-sublimation at room temperature by converting CO_2 directly into a solid from the gas phase at a point where the pressure is below the triple point pressure.[374] The AnSU consists of five stages such as moisture removal, water content reduction, cold energy supply, freezing process and finally the recovery of CO_2. AnSU uses liquefied natural gas (LNG) as its source of cooling energy.[375]

The advantage of the AnSU method is high purity of CO_2 which can be captured without the presence of any contaminants.[376] Clodic et al.[375] discovered that AnSU consumed a high level of energy for the removal of low CO_2 concentration and the energy consumption decreases as the concentration of CO_2 increases. On the other hand, Schach et al.[377] investigated and made a comparison between AnSU and the adsorption method in terms of energy consumption using ASPEN HYSYS simulation for CO_2 removal at 90% efficiency. The results showed that the energy consumption of AnSU is far lower at 178 MW as compared to the adsorption method using MEA at 208 MW.

Despite having high efficiency of CO_2 removal, AnSU has several drawbacks such as high costs for regular maintenance for the compression systems and high capital costs for AnSU since it requires five stages of separation mechanisms. Furthermore, the formation of a CO_2 frost layer on the surface of the heat exchanger affects its efficiency and thus, a better material is required for the heat exchanger with higher mechanical stress tolerance and thermal conductivity.[378] Moreover, simultaneous removal of CO_2 and H_2S using AnSU has not yet been investigated.

2.5.2 Controlled freeze zone (CFZ). Controlled freeze zone (CFZ™) technology was developed and patented by ExxonMobil in 1985 for H_2S and CO_2 separation from natural gas.[379] CFZ™ is integrated with cryogenic technology to form a single-step

cryogenic distillation for bulk removal of CO_2 from sour gases.[380] The CFZ™ process operates in a high-pressure range of 34.47 to 41.37 bar and allows CH_4 to vaporize at a temperature between −90 °C and −85 °C, and CO_2 to freeze at higher temperatures ranging between −62 °C and −42 °C.[381] Overall, CFZ™ has lower capital costs as compared to other conventional methods due to its less equipment, small footprint and since it does not require any solvent.[382] In 2007, ExxonMobil designed a commercial demonstration project (CDP) to evaluate the technological readiness level (TRL) of yjr CFZ™ method by processing 228.8 m^3 s^{-1} of natural gas with H_2S and CO_2 contents of 5% and 65%, respectively, at a high pressure of 41.37 bar.[383] The process managed to obtain 1.2 ppm H_2S and 680 ppm CO_2 as the top product, while the liquid product contained 0.23% H_2S and 4.1% CO_2 at the bottom.

CFZ™ technology is regarded as economically viable due to its capability of handling various compositions of H_2S and CO_2 in the feed stream. The discharge of both top and bottom products at relatively high pressure helps to minimize the recompression cost for delivery and reinjection of acid gas back to the reservoir. The acid gas injection (AGI) method is usually used to discard the separated H_2S and CO_2 from the feed gas. By combining the CFZ™ and AGI approaches, the geological sequestration of CO_2 could be facilitated using the high-pressure liquid stream released from the bottom column.[384] Furthermore, Northrop et al.[149] finalized the CDP of CFZ™ technology and concluded that the technology is ready for scale-up and commercialization for sour gas treatment up to 327 m^3 s^{-1}. However, CFZ™ application for simultaneous removal of H_2S and CO_2 is facing drawbacks as the presence of H_2S inhibits the freezing of CO_2.

2.5.3 Cryogenic packed bed (CPB). Cryogenic packed bed (CPB) is a combination of cryogenic and packed bed separation methods.[385] The CPB separation begins with the cooling of the packed bed column with liquid nitrogen until the temperature reaches −120 °C, switched with the sour gas feed after the cooling process is completed. After the packed bed is sufficiently cooled, crystals will be formed from the sublimation of H_2S and CO_2, and condensation of water molecules. After some time, the packed bed column will become saturated, and the crystals will continue to form and spread throughout the column leading to the formation of front frost. Once the packed bed is fully saturated, a regeneration process is required to recover CO_2 and water.[386]

One of the major advantages of this process is its ability to simultaneously remove H_2S, CO_2 and water from the sour gas based on their respective sublimation and dew points.[378] Additionally, the CPB process does not require chemical solvents and high pressure to operate, which in turn could save cost as the chemical solvents require regular replacement, which could lead to a higher capital cost.[387] The crystallization of H_2S, CO_2 and water only requires the cold energy provided by the packed bed materials without requiring high pressure.[387] Furthermore, the methane produced by the CPB process has a higher purity as compared to that produced by the PSA process. Ali et al.[388] compared the energy requirements between the CPB and conventional methods for the removal of 70% CO_2. The authors

found that CPB consumed lower energy at 810 kJ kg^{-1} of CO_2 as compared to the conventional cryogenic process which used 1472 kJ kg^{-1} of CO_2. On the other hand, Turnier et al.[389] concluded that the energy consumption by the CPB method was much lower at 2.9 MJ kg^{-1} of CH_4 as compared to the pressure swing adsorption (PSA) which used 3.7 MJ kg^{-1} of CH_4.

However, the CPB process faces several drawbacks such as limited availability of commercial thermal insulators that can maintain a very low temperature required by the process, loss of cold energy to the surroundings and high energy consumption for simultaneous removal of H_2S and CO_2.[390] The reason behind high energy requirement for simultaneous removal of H_2S and CO_2 is the requirement to reach the H_2S dew point at -150 °C. To achieve high removal efficiency of H_2S, the process requires long hours of operation at extremely low temperatures and leads to high costs of operation. Therefore, to minimize losses during the purification process, it is recommended to have a proper heat integration system between the LNG production and air separation unit.[391]

2.5.4 CryoCell®. CryoCell® is a new cryogenic technology developed in 2009 by Cool Energy Ltd. for feed gas treatment with high concentration of CO_2 using a similar approach of CO_2 sublimation applied in the CFZ™ process.[392] CryoCell® has a compact and portable design that allows this process to be used for offshore applications and CO_2 geo-sequestration by injecting the liquid CO_2 collected at the bottom product into the porous rock formations in geologic basins for storage.[393,394] CryoCell® is economically advantageous as compared to other conventional methods due to elimination of water, chemical and solvent requirements and minimum corrosion issues. This will further result in lower capital costs by 20 to 40% as compared to the conventional LNG methods.

The initial step of the CryoCell® process involves the treatment of feed gas, which has a high CO_2 content, by reducing its moisture level to as low as 5 ppm through a dehydration process.[388] After this, the dehydrated feed gas is cooled to a temperature above the freezing point of CO_2 at a constant pressure, condensing the gas mixture into a liquid phase. Subsequently, the liquid mixture undergoes expansion through a Joule–Thomson valve, while maintaining a constant enthalpy that induces a phase change in CO_2, into liquid, solid, and vapor phases which is later separated by a three-phase separator.[395] It is very critical to maintain a low CO_2 content in the vapor phase and high CO_2 level in the liquid product in the CryoCell® process. The solid CO_2 product will then be melted and mixed with the liquid product.

Cool Energy Ltd. collaborated with Shell Global Solutions and developed a commercial demonstration plant (CDP) in 2006 to investigate the viability of CryoCell® technology.[392] The CDP of CryoCell® was designed to process 60 mol% of CO_2 feed gas with the pressure ranging from 55 to 65 bar and feed flowrate between 600 and 1300 kg h^{-1}. The separator was designed to operate at 12, 16 and 19 bar whereas the reboiler was kept between -50 and -60 °C. The results from CDP showed that CryoCell® technology can remove up to 81% of CO_2 from natural gas. On the other hand, Hart and Gnanendran[392] performed a comparison between the CryoCell® and amine process for treatment of feed gas containing 20 mol% and 30 mol% of CO_2 using Aspen HYSYS simulation. Their results indicated that CryoCell® required a lower heat duty as low as 0.1 MW, as compared to the amine process which required between 19 and 35 MW. Nonetheless, the simulation data also revealed that the CryoCell® process requires more compression between 4.3 and 7.0 MW, as compared to the amine process which only requires 1.9 to 3.8 MW at higher CO_2 content in the feed gas.[392]

Based on initial testing through CDP and simulation data, it is expected that this technology can be commercialized and has huge potential for treatment of natural gas involving high CO_2 content and geo-sequestration of CO_2 for storage. Furthermore, Amin et al.[393] stated that the CryoCell® process can handle a diverse range of contaminants including H_2S and heavy hydrocarbons. Nevertheless, limited applications of CryoCell® technology for H_2S removal were reported. Besides, the CryoCell® process also faces several drawbacks such as uncontrollable freezing of CO_2 and poor handling of solids formed. Therefore, more research should be carried out for H_2S removal applications by benefiting from their progress for CO_2 purification.

2.5.5 Summary of cryogenic distillation. Despite excellent progress in cryogenic technology, the applications of cryogenic distillation process are currently limited to CO_2 separation, whereas the capture of H_2S is barely reported. Moreover, cryogenic technology is mostly suitable for bulk removal of CO_2 from an economic point of view. Cryogenic distillation technology is an effective method for H_2S removal, as it can achieve very high levels of purity, is able to handle large volumes of gas and is highly effective at removing even trace amounts of H_2S from natural gas streams.

In general, cryogenic distillation can achieve very high levels of sulfur recovery, up to 99% or higher, which means that almost all of the H_2S in the natural gas stream can be separated and recovered.[396] However, H_2S purification is an energy-intensive process and requires greater cooling duty to cool down H_2S to below its boiling point. As a result, H_2S removal by cryogenic separation is rarely reported as of now. In H_2S removal, the process starts with the compression of the gas stream to a high pressure and then cooling to a very low temperature below the boiling point of H_2S, typically around -50 °C.[397] This causes the H_2S gas to condense and form a liquid, which can be removed from the gas stream via the distillation method. The process requires a significant amount of energy to cool the natural gas stream to very low temperatures necessary for the H_2S to condense.[398] This leads to high operating costs, especially for large-scale industrial applications.

In addition, cryogenic distillation requires complex and expensive specialized equipment with high maintenance costs such as refrigeration units, distillation columns and heat exchangers.[371] Furthermore, there are also safety concerns regarding cryogenic distillation as the process involves handling extremely cold materials, which can be hazardous if not properly managed. There is also a risk of leaks or equipment failure, which could result in the release of toxic gases or other safety hazards. Besides, the effectiveness of cryogenic distillation for H_2S is limited by the feed gas composition. High levels

of other impurities such as CO_2 and N_2 will interfere with the separation process, reducing its efficiency and increasing the operation costs. Last but not least, the process also has a significant environmental impact due to the high energy consumption and the potential for leaks or release of toxic gases.[371]

3. Status, opportunities and challenges

There are various methods and materials being developed specifically for the purpose of H_2S capture from mainly gaseous streams. This emphasizes the significance and urgency of addressing this problem. The suitability of any method to a specific application is highly dependent on various factors such as cost, operating conditions, initial concentration of H_2S, gas volume, space and weight limitations, outlet specification and technological readiness level (TRL). Table 6 provides a general comparison between various techniques for H_2S removal. However, the general comparison used cannot be applied specifically for every material used under each technique category. For example, a technology with TRL of 9 is mainly because of its wide industrial application such as the wide usage of alkanolamines as absorbents. However, the same absorption method by using ionic liquids or deep eutectic solvents would only have a TRL of 2–4. Comparatively, an absorbent material with a TRL of 4 is more likely to be used for industrial application as compared to a membrane material with the same level of TRL. This is because the absorption technique has a higher TRL generally than membrane separation technology for selective removal of H_2S. This highlights the significance of the TRL as a systematic approach to assess the maturity level of a particular material and in technology development for any application, and the TRL is also crucial to determine the ease of its integration into the current industrial environment.

The determination of the TRL for a certain technology is carried out based on the economics and sustainability of a certain technology. The most widely used materials currently are activated carbons, aqueous amines, metal oxides, zeolites and chelated iron solution (LO-CAT process). Despite their disadvantages in certain criteria, most of these materials have been used in industrial applications for many decades. Nevertheless, low-cost and sustainable alternatives are yet to be discovered. ILs are widely known as sustainable solvents, but this was proven to be an overstatement for most conventional ILs. Protic ILs and DESs have shown potential as simpler, more sustainable and cheaper options as compared to the conventional ILs, but they are still more costly than amines. Over the recent years, MOFs have made a significant impact on adsorption applications. Despite comparable performances of MOFs to zeolites, MOFs suffer from high material costs as compared to zeolites and amines. Functionalized carbonaceous materials have shown promising development for H_2S removal ability, but still require further studies to explore various potential functionalization techniques. Generally, most of the adsorbents

were facing regeneration failure due to irreversible chemical reactions on the surface. Membrane separation technology presents numerous benefits and possibilities due to its lightweight and compact characteristics, making it well-suited for applications in remote areas and small-scale settings. However, they are not economical as standalone applications as they are mostly effective when being used together with other techniques such as adsorption or absorption where the main purpose of the membrane is to reduce the feed flowrates before entering the separation columns and helping to reduce the column size and energy requirements. Cryogenic distillation has huge potential for H_2S capture applications. Nevertheless, most of the available methods focus mostly on CO_2 capture and rarely focus on H_2S. Advancement of this particular technology for H_2S capture would be beneficial in terms of technical, economic and sustainability factors.

By taking into consideration all the provided information, a general comparison between technologies for H_2S capture could be represented clearly as shown in Table 6. The selection of a suitable technology to be used is highly dependent on the operational requirements and conditions of the specific process. For small-scale applications (associated gas, offshore, biogas, etc.), there is a requirement for processes with smaller footprints. For the required sulfur production between 0.5 and 20 tons per day, liquid redox processes such as the LO-CAT process is the best option. As the total gas flowrate got higher, a combination of H_2S removal methods which involves membranes and chemical solutions followed by catalytic adsorbents (impregnated ACs and metal oxides) may be adopted. As the H_2S partial pressure increases and the required sulfur production is above 20 tons per day, the absorption method is more suitable economically, possibly combined with the membrane separation method. For the operating pressures between 1 and 25 bar, chemical solvents are a viable option. When the operating pressure is between 15 and 40 bar, hybrid solvents are a better option as compared to chemical solvents. As the operating pressure exceeds 30 bar, especially at a very high pressure of 50 bar or even higher, physical solvents are probably a better option as compared to the latter. If there is an additional requirement for other products such as methane or other light gases, then cryogenic distillation could be the most effective economically compared to other methods. Generally, the adsorption method is mostly economic for removal of a low concentration of H_2S between 10 and 20 ppm as currently, most of the spent adsorbents cannot be regenerated and need to be disposed.

Recent development of hybrid and composite materials such as functionalized MOFs, supported IL membranes, functionalized mesoporous silica or activated carbons, and mixed matrix membranes based on zeolites are excellent examples of such development. However, these materials were mostly being developed for specific CO_2 removal applications and their use for H_2S capture is still at the grassroots level. It is also predicted that the development of a new generation of membranes, adsorbents, functionalized ILs and DESs will become the major focal points of H_2S capture research in the near future. The usage of computational tools to design the molecules and

Table 6 General comparison summary of conventional technologies for H$_2$S removal

Conventional technologies	Absorption	Adsorption	Conversion		Membrane separation	Cryogenic distillation
			Claus process	LO-CAT process		
Operating principle	Absorption of H$_2$S in a liquid solvent	Adsorption of H$_2$S onto a solid surface	Conversion of H$_2$S to elemental sulfur via chemical reactions	Catalytic oxidation of H$_2$S to elemental sulfur on a proprietary catalyst	Separation of H$_2$S from a gas stream by a semi-permeable membrane	Separation of H$_2$S from a gas stream by condensation and distillation
Reaction involved	Absorptive oxidation reaction	Adsorption reaction	Thermal oxidation and catalytic reaction	Liquid catalytic oxidation reaction	No chemical reaction involved	No chemical reaction involved
Phase separation	Gas–liquid phase	Gas–solid phase	Gas–liquid phase	Gas–liquid and liquid–solid phase	Gas phase	Gas–liquid phase
Sulfur recovery	92.8–94.8% of H$_2$S conversion	≤95% of H$_2$S conversion	95–97% of H$_2$S conversion	≥99% of H$_2$S conversion	0% (pre-treatment step before sulfur recovery)	≥99% of H$_2$S conversion
Advantages	• High removal efficiency • Simple process • Low capital cost • Can handle large gas volumes	• Easily regenerated • Designed for high selectivity	• High removal efficiency • Produces elemental sulfur as a byproduct • Proven technology	• Low energy consumption • High removal efficiency • Produces no waste products • Produces elemental sulfur as a byproduct • Compact design	• Simple process • No chemicals required • Compact design	• High purity separation • Low energy consumption for high flow rates • Proven technology • Can handle high gas volumes
Disadvantages	• High solvent consumption • Requires high temperature and pressure conditions • Requires regeneration of solvent • Potential solvent degradation	• Requires high temperature and pressure conditions • Requires frequent replacement or regeneration of the adsorbent • Potential for bed fouling • Limited capacity • Can be affected by other gases in the feed stream • Spent absorbent is considered as hazardous waste as some contaminants might undergo	• High capital and operating costs • Complex process • Requires additional equipment for sulfur recovery • Requires high temperature and pressure conditions	• Limited to low H$_2$S concentrations • Limited operating range • Requires careful temperature control and a proprietary catalyst • Require additional treatment for high H$_2$S concentrations • Formation of sulfur-oxo-acid salts that could lead to catalyst poisoning and degradation	• Limited to low H$_2$S concentrations • May require additional treatment for high H$_2$S concentrations • Limited by membrane selectivity • Potential for membrane fouling • High capital cost • Requires high temperature and pressure conditions	• High capital and operating costs • Requires high pressure and low temperature conditions • High energy consumption • Requires specialized equipment and expertise • Can be affected by other gases in the feed stream

Table 6 (*Contd.*)

Conventional technologies	Absorption	Adsorption	Conversion		Membrane separation	Cryogenic distillation
			Claus process	LO-CAT process		
		exothermic reaction with the adsorbent leading to explosion				
Capital costs	Medium to high	Medium to high	High	High	Medium to high	High
Operating costs	Medium to high	Medium to high	High	High	Medium	High
TRL	9	9	9	9	6	6

prediction of their physicochemical properties for IL and DES application such as a conductor-like screening model for real solvents (COSMO-RS) and process modeling is also expected to gain more interest and become a driving force in designing materials that are excellent in various criteria which includes economic, functionality and sustainability aspects.

The exploration of challenges and the way forward in industrial applications of H_2S removal, with a specific focus on large-scale adoption, deployment, and medium-scale application, is essential for advancing effective strategies and technologies in this domain. This involves addressing issues such as scalability, integration into existing infrastructure, cost-effectiveness, regulatory compliance, and ensuring optimal performance across diverse operational settings. Scalability remains a critical consideration, ensuring that solutions can be adapted to meet varying demands across different scales of operation. Integration into existing infrastructure is vital for seamless implementation, while cost-effectiveness is essential for widespread adoption. Regulatory compliance underscores the need for solutions that meet environmental standards. Operational performance across diverse settings, from energy production to wastewater treatment, requires robust technologies capable of consistent and reliable H_2S removal. Understanding these challenges and potential pathways forward is crucial for enhancing the efficiency, reliability, and sustainability of H_2S removal processes in various industrial contexts.

The cost of the material also plays a significant role in determining the suitability of materials for H_2S capture application. Usually, the cost of any material decreases as its TRL increases which eventually lead to a larger production of that specific material. The present state of lab-scale development discussed so far is still far from transcending them to a higher level of TRLs. Most of the experimental studies conducted so far have not considered the influence of realistic feed gas compositions on their performances. The presence of impurities in the feed gas such as CO_2 and water are recognized to impact the efficiency of H_2S removal. This work also addresses a clear gap between science and engineering. Almost all adsorbents and absorbents reported the performance of material in terms of breakthrough capacity or equilibrium, mostly focusing on maximizing their performance. Nonetheless, these parameters are insufficient to provide comprehensive data on the overall performance of the process. Many other critical process parameters have been overlooked such as selectivity, regenerability, reaction kinetics, purity and activation energy which could provide better understanding of the overall process and its cost of H_2S capture. Additionally, the specific challenges that need to be addressed by each class of materials are further elaborated in their individual sections to further accelerate the development of these materials.

4. E-factors

In the context of green chemistry, e-factors[399] refer to the environmental impact of chemical processes,[400] specifically the efficiency of resource utilization and the generation of waste. Green chemistry aims to design chemical products and

processes that minimize environmental pollution, reduce resource consumption, and promote sustainability.[401,402] E-factors serve as quantitative indicators of the environmental performance of chemical processes, providing insights into their sustainability and potential for improvement. The e-factor is defined as the ratio of the mass of waste generated by a chemical process to the mass of the desired product. It quantifies the efficiency of a chemical process in terms of waste generation, with lower e-factors indicating more sustainable practices. The e-factor can be expressed using the following equation:

$$\text{E-factor} = \frac{\text{total mass of waste generated(g)}}{\text{mass of desired product(g)}} \quad (4.1)$$

E-factors are used to evaluate the environmental impact of chemical processes and guide the development of greener alternatives. By assessing the amount of waste generated per unit of product, researchers and industrial players can identify opportunities to minimize waste and optimize resource utilization. The evaluation of e-factors relies on waste definition, encompassing non-recoverable starting materials, solvents, catalysts and undesired side products from reactions. Smaller e-factor means closer to zero waste. Similarly, the e-factor can be used to estimate the total waste generated by using the following expression:

$$\text{Amount of waste} = \text{e-factor} \times \text{amount of product} \quad (4.2)$$

Comparing the latest technological advances in H_2S removal, such as absorption, adsorption, conversion, membrane separation, and cryogenic distillation, regenerable solvents like ILs emerge as the most promising option with the lowest e-factors and highest efficiency for H_2S removal applications. This is because regenerable ILs produce minimal or zero waste as compared to their desired products.[81,403,404] Their high regenerability contributes to efficient H_2S removal, enabling multiple uses over a certain period. Emphasizing the high regenerability of materials used in other methods is essential to minimize e-factors. The high regenerability of materials leads to lower e-factors as it allows for the repeated use of the same materials in a chemical process.[405] When materials can be regenerated and reused multiple times, there is less need to produce new materials, resulting in reduced waste generation per unit mass of the desired product. This efficient recyclability of materials decreases the overall amount of waste generated during the process, thereby lowering the e-factor. Lower e-factors indicate higher efficiency in a chemical process, signifying less waste generated per unit mass of the desired product. In other words, a lower e-factor suggests that the process produces less waste relative to the amount of product obtained, aligning with sustainability goals and efficient resource utilization.

In regard to recyclability, ILs are well-known for their potential recyclability[406,407] due to their unique properties, such as low vapor pressure[408] and high stability.[409] In general, ILs can be recovered through processes like solvent regeneration or extraction. Plus, ILs are generally considered to be less prone to

leaching compared to traditional solvents due to their low vapor pressure, non-volatile nature and high chemical stability. However ILs still face the risk of contamination and should be monitored periodically, especially in long-term applications. Additionally, ILs can undergo degradation or deactivation over time,[410] leading to reduced efficiency in H_2S removal. However, proper selection of ILs and optimization of operating conditions can mitigate this issue. Some of the ILs were also reported to be non-regenerative and cannot be recycled.[411] These could lead to several drawbacks such as increased chemical consumption, waste generation, and higher operational costs. Additionally, disposal of used ILs may pose environmental concerns.

To date, e-factors are often overlooked in previous studies and should be given higher emphasis in future work. E-factors, which measure the mass of waste generated per unit mass of desired product, provide an excellent means to assess the efficiency of a chemical process by considering the amount of waste generated such as used solvents, reagents and catalysts, relative to the production amount of the desired product. While e-factors provide valuable insights into the environmental performance of chemical processes, challenges remain in their practical implementation and interpretation. Factors such as the definition of waste, the inclusion of energy consumption, and the consideration of life cycle impacts can influence e-factor calculations and their relevance to sustainability. In conclusion, e-factors play a crucial role in green chemistry by quantifying the environmental impact of chemical processes and guiding the development of more sustainable alternatives. By reducing waste generation, optimizing resource utilization, and promoting innovative synthesis strategies, green chemistry contributes to the transition towards a more sustainable and environmentally conscious chemical industry. As a result, a more holistic approach must be used to assess the properties of each material and their respective performances in H_2S capture.

5. Conclusion

Effective capture and removal of H_2S is very crucial to avert harmful consequences upon exposure to human beings, the environment and production facilities. To date, there are various conventional methods being implemented for H_2S capture on the commercial scale such as absorption, adsorption, conversion, membrane separation and cryogenic distillation. However, there is still huge room for improvements and optimizations for these processes, to achieve high efficiency and significant reduction in overall costs. Adsorption *via* metal oxide adsorbents is by far the most established method for fine H_2S removal. Meanwhile, absorption and membrane separation methods are primarily applicable for the bulk removal of acid gases, with alkanolamine solvents and polymeric membranes being the dominant choices for this purpose.

Highly regenerable solvents such as ILs emerge as highly promising candidates for H_2S removal, offering the potential for efficient and sustainable processes with a low environmental impact. Their high regenerability enables multiple uses over

time, contributing to lower e-factors by minimizing waste generation per unit mass of the desired product. The unique properties of ILs, such as low vapor pressure, high stability, and strong solvent power, inherently make them less prone to leaching compared to traditional solvents, further enhancing their appeal for environmentally conscious applications. However, challenges such as degradation or deactivation over time and the potential non-regenerability of some ILs highlight the importance of careful selection, optimization, and monitoring to ensure their continued effectiveness and sustainability. Addressing these challenges is crucial to fully capitalize on the potential of ILs in H_2S removal while also minimizing environmental risks and maximizing resource utilization.

Much on-going research is still conducted to develop novel materials by functionalization and molecular design to enhance their performance, whilst at the same time, being cost effective and environmentally friendly. Even though H_2S capture can be performed simultaneously with CO_2 efficiently using highly established carbon capture technologies with a high TRL, the selective removal of H_2S from CO_2 still requires deeper research. This would pave the road for further research on the recovery and separation of H_2S into valuable end-products such as elemental sulfur, hydrogen, mercaptan and other sulfur-containing materials which are highly lucrative for a circular economy.

Author contributions

Muhammad Syahir Aminuddin: conceptualization, writing – original draft, review & editing, visualization. Mohamad Azmi Bustam: supervision, Khairiraihanna Johari: supervision, writing – review.

Conflicts of interest

There are no conflicts to declare.

Acknowledgements

Notes and references

1 A. G. Georgiadis, N. Charisiou, I. V. Yentekakis and M. A. Goula, *Materials*, 2020, **13**, 3640.
2 S. Batterman, A. Grant-Alfieri and S.-H. Seo, *Crit. Rev. Toxicol.*, 2023, **53**, 244–295.
3 L. Zhang, Y.-Y. Qiu, K. R. Sharma, T. Shi, Y. Song, J. Sun, Z. Liang, Z. Yuan and F. Jiang, *Water Res.*, 2023, 120046.
4 N. N. Zulkefli, L. S. Mathuray Veeran, A. M. I. Noor Azam, M. S. Masdar and W. N. R. Wan Isahak, *Materials*, 2022, **15**, 5409.
5 D. S. Rathore, P. Singh, C. Misra, C. Chandel, S. Bugalia and K. S. Gupta, *Environ. Monit. Assess.*, 2023, **195**, 1–12.
6 O. S. a. H. Administration, *Safety and Health Topics/ Hydrogen Sulfide*, https://www.osha.gov/SLTC/ hydrogensulfide/hazards.html, (accessed 30th January, 2023).
7 M. D. Group, *The Dangers of Hydrogen Sulfide Exposure*, https://www.mdgbio.com/news/the-dangers-of-hydrogen-sulfide-exposure/, (accessed 18th February, 2023).
8 C. Secco, M. E. K. Fuziki, A. M. Tusset and G. G. Lenzi, *Energies*, 2023, **16**, 1759.
9 S. Mokhatab, W. A. Poe and J. Y. Mak, *Handbook of Natural Gas Transmission and Processing: Principles and Practices*, Gulf Professional Publishing, 2018.
10 R. Mohtadi, W.-K. Lee, S. Cowan, J. Van Zee and M. Murthy, *Electrochem. Solid-State Lett.*, 2003, **6**, A272.
11 Z. Du, C. Liu, J. Zhai, X. Guo, Y. Xiong, W. Su and G. He, *Catalysts*, 2021, **11**, 393.
12 K. Gonzalez, L. Boyer, D. Almoucachar, B. Poulain, E. Cloarec, C. Magnon and F. de Meyer, *Chem. Eng. J.*, 2023, **451**, 138948.
13 M. I. Stewart, in *Surface Production Operations*, ed. M. I. Stewart, Gulf Professional Publishing, Boston, 3rd edn, 2014, vol. 2, pp. 433–539.
14 X. Tian, L. Wang and D. Fu, *Energy Fuels*, 2019, **33**, 8413–8422.
15 S. Yunhai, L. Shan, L. Wei, L. Dong, G. Remy and D. JianPeng, *Int. J. Ind. Chem.*, 2016, **7**, 297–307.
16 U. Shoukat, D. D. Pinto and H. K. Knuutila, *Processes*, 2019, **7**, 160.
17 J. Zhan, B. Wang, L. Zhang, B.-C. Sun, J. Fu, G.-W. Chu and H. Zou, *Ind. Eng. Chem. Res.*, 2020, **59**, 8295–8303.
18 L. Du, H. Li, L. Li, J. Xu and Y. Li, *Pet. Sci. Technol.*, 2019, **37**, 56–60.
19 H. Li, L. Li, J. Xu and Y. Li, *Pet. Sci. Technol.*, 2019, **37**, 1825–1829.
20 X. Zhang, W. Xiong, M. Shi, Y. Wu and X. Hu, *Chem. Eng. J.*, 2021, **408**, 127866.
21 X. Zhang, W. Xiong, L. Peng, Y. Wu and X. Hu, *AIChE J.*, 2020, **66**, e16936.
22 W. Xiong, M. Shi, L. Peng, X. Zhang, X. Hu and Y. Wu, *Sep. Purif. Technol.*, 2021, **263**, 118417.
23 K. Huang, X.-M. Zhang, L.-S. Zhou, D.-J. Tao and J.-P. Fan, *Chem. Eng. Sci.*, 2017, **173**, 253–263.
24 K. Huang, J.-Y. Zhang, X.-B. Hu and Y.-T. Wu, *Energy Fuels*, 2017, **31**, 14060–14069.
25 T. Zhao, P. Li, X. Feng, X. Hu and Y. Wu, *J. Mol. Liq.*, 2018, **266**, 806–813.
26 X. Wang, S. Zeng, J. Wang, D. Shang, X. Zhang, J. Liu and Y. Zhang, *Ind. Eng. Chem. Res.*, 2018, **57**, 1284–1293.
27 A. H. Jalili, M. Shokouhi, G. Maurer, A. T. Zoghi, J. S. Ahari and K. Forsat, *J. Chem. Thermodyn.*, 2019, **131**, 544–556.
28 F. Liu, W. Chen, J. Mi, J. Y. Zhang, X. Kan, F. Y. Zhong, K. Huang, A. M. Zheng and L. Jiang, *AIChE J.*, 2019, **65**, e16574.
29 H. Wu, M. Shen, X. Chen, G. Yu, A. A. Abdeltawab and S. M. Yakout, *Sep. Purif. Technol.*, 2019, **224**, 281–289.

30 M. Shi, W. Xiong, Z. Tu, X. Zhang, X. Hu and Y. Wu, *Sep. Purif. Technol.*, 2021, **276**, 119357.

31 M. Shi, W. Xiong, X. Zhang, J. Ji, X. Hu, Z. Tu and Y. Wu, *Sep. Purif. Technol.*, 2022, **283**, 120167.

32 X. Tian, L. Wang, P. Zhang, D. Fu and Z. Wang, *Environ. Sci. Pollut. Res.*, 2021, **28**, 5822–5832.

33 A. Afsharpour and A. Haghtalab, *Int. J. Greenhouse Gas Control*, 2017, **58**, 71–80.

34 H. Renon, J. Y. Lenoir and P. Renault, *J. Chem. Eng. Data*, 1971, **16**, 340–342.

35 F. Murrieta-Guevara and A. Trejo Rodriguez, *J. Chem. Eng. Data*, 1984, **29**, 456–460.

36 F.-Y. Jou, R. Deshmukh, F. Otto and A. Mather, *Fluid Phase Equilib.*, 1990, **56**, 313–324.

37 F. Y. Jou, A. E. Mather and F. D. Otto, *Ind. Eng. Chem. Process Des. Dev.*, 1982, **21**, 539–544.

38 E. Skylogianni, I. Mundal, D. D. Pinto, C. Coquelet and H. K. Knuutila, *Fluid Phase Equilib.*, 2020, **511**, 112498.

39 F.-Y. Jou and A. E. Mather, *Int. J. Thermophys.*, 2007, **28**, 490–495.

40 K. Fischer, J. Chen, M. Petri and J. Gmehling, *AIChE J.*, 2002, **48**, 887–893.

41 C. S. Pomelli, C. Chiappe, A. Vidis, G. Laurenczy and P. J. Dyson, *J. Phys. Chem. B*, 2007, **111**, 13014–13019.

42 S. F. Sciamanna and S. Lynn, *Ind. Eng. Chem. Res.*, 1988, **27**, 492–499.

43 J. Xue, C. Yang, J. Fu, J. He and J. Li, *Processes*, 2022, **10**, 1795.

44 H. M. Polat, F. de Meyer, C. Houriez, C. Coquelet, O. A. Moultos and T. J. Vlugt, *Fluid Phase Equilib.*, 2023, **564**, 113587.

45 J. Mustafa, A. H. Al-Marzouqi, N. Ghasem, M. H. El-Naas and B. Van der Bruggen, *Desalination*, 2023, **548**, 116263.

46 N. Agarwal, L. Cao Nhien and M. Lee, *Energies*, 2022, **15**, 6817.

47 L. Li, *J. Chem. Eng. Jpn.*, 2022, **55**, 15–21.

48 W. Y. Lee, S. Y. Park, K. B. Lee and S. C. Nam, *Energy Fuels*, 2020, **34**, 1992–2000.

49 S. Energy, *Natural Gas Purification*, https://www.shell.com/business-customers/catalysts-technologies/licensed-technologies/gas-processing/natural-gas-purification.html, (accessed 7th March, 2023).

50 E. M. Corporation, *Selective H₂S removal (FLEXSORB™)*, https://www.exxonmobilchemical.com/en/catalysts-and-technology-licensing/gas-treating/flexsorb, (accessed 20th March, 2023).

51 E. M. Corporation, *Selective H₂S removal (OASE® sulfexx™)*, https://www.exxonmobilchemical.com/en/catalysts-and-technology-licensing/gas-treating/oase-sulfexx, (accessed 13th March, 2023).

52 K. H. Smith, N. J. Nicholas and G. W. Stevens, in *Absorption-Based Post-Combustion Capture of Carbon Dioxide*, ed. P. H. M. Feron, Woodhead Publishing, 2016, pp. 145–166, DOI: 10.1016/B978-0-08-100514-9.00007-X.

53 J.-G. Lu, Y.-F. Zheng and D.-L. He, *Sep. Purif. Technol.*, 2006, **52**, 209–217.

54 N. Upreti, S. Mohan and P. D. Vaidya, *Chem. Eng. Commun.*, 2023, 1–16.

55 A. Haghtalab and M. Dehghani Tafti, *Ind. Eng. Chem. Res.*, 2007, **46**, 6053–6060.

56 A. A. Abd, M. R. Othman, Z. Helwani and J. Kim, *Energy*, 2023, **272**, 127060.

57 N. Haimour and O. C. Sandall, *Chem. Eng. Commun.*, 1987, **59**, 85–93.

58 A. Vrachnos, G. Kontogeorgis and E. Voutsas, *Ind. Eng. Chem. Res.*, 2006, **45**, 5148–5154.

59 P. Pal and F. Banat, *J. Nat. Gas Sci. Eng.*, 2016, **29**, 479–487.

60 R. Abdulrahman and I. Sebastine, *J. Nat. Gas Sci. Eng.*, 2013, **14**, 116–120.

61 B. P. Mandal, A. Biswas and S. Bandyopadhyay, *Sep. Purif. Technol.*, 2004, **35**, 191–202.

62 M. Zamani, M. Shokouhi, H. Fatoorehchi and M. Vahidi, *J. Solution Chem.*, 2023, DOI: 10.1007/s10953-023-01342-8.

63 M. Sheng, C. Xie, X. Zeng, B. Sun, L. Zhang, G. Chu, Y. Luo, J.-F. Chen and H. Zou, *Fuel*, 2018, **234**, 1518–1527.

64 C.-C. Lin, Y.-H. Lin and C.-S. Tan, *J. Hazard. Mater.*, 2010, **175**, 344–351.

65 T. Nguyen, M. Hilliard and G. T. Rochelle, *Int. J. Greenhouse Gas Control*, 2010, **4**, 707–715.

66 S. K. Dash, A. N. Samanta and S. S. Bandyopadhyay, *Fluid Phase Equilib.*, 2011, **307**, 166–174.

67 A. Haghtalab and A. Izadi, *Fluid Phase Equilib.*, 2014, **375**, 181–190.

68 D. Fu, P. Zhang and C. Mi, *Energy*, 2016, **101**, 288–295.

69 C. Foo, C. Leo, R. Aramesh, M. Aroua, N. Aghamohammadi, M. Shafeeyan and A. Shamiri, *J. Mol. Liq.*, 2015, **209**, 596–602.

70 X. Tian, L. Wang, D. Fu and C. Li, *Energy Fuels*, 2018, **33**, 629–635.

71 X. Rozanska, A. Valtz, M. Riva, C. Coquelet, E. Wimmer, K. Gonzalez-Tovar and F. de Meyer, *Ind. Eng. Chem. Res.*, 2023, **62**, 11480–11490.

72 C. Chiappe and C. S. Pomelli, in *Ionic Liquids II*, Springer, 2017, pp. 265–289.

73 *Ludwig's Applied Process Design for Chemical and Petrochemical Plants*, ed. A. K. Coker, Gulf Professional Publishing, Boston, 4th edn, 2010, pp. 679–686, DOI: 10.1016/B978-0-7506-8366-1.10021-0.

74 A. L. Kohl and R. B. Nielsen, in *Gas Purification*, ed. A. L. Kohl and R. B. Nielsen, Gulf Professional Publishing, Houston, 5th edn, 1997, pp. 1187–1237, DOI: 10.1016/B978-088415220-0/50014-8.

75 B. Burr and L. Lyddon, A comparison of physical solvents for acid gas removal, in *Gas Processors' Association Convention*, Grapevine, TX, 2008.

76 X. Liu, B. Wang, X. Dong, Y. Qiu and Q. Meng, *J. Hazard. Mater.*, 2021, **419**, 126394.

77 X. Liu, B. Wang, Y. Qiu, X. Dong, Y. Song, Q. Meng and M. Li, *Environ. Sci. Pollut. Res.*, 2021, **28**, 38026–38033.

78 J. S. Wilkes, *Green Chem.*, 2002, **4**, 73–80.

79 X. Zhao, H. Xing, R. Li, Q. Yang, B. Su and Q. Ren, *Prog. Chem.*, 2011, **23**, 2258.

80 M. G. Cowan, M. Masuda, W. M. McDanel, Y. Kohno, D. L. Gin and R. D. Noble, *J. Membr. Sci.*, 2016, **498**, 408–413.

81 M. S. Aminuddin, M. A. B. Khalil and B. Abdullah, *RSC Adv.*, 2022, **12**, 11906–11912.

82 P. K. Mohapatra, *Dalton Trans.*, 2017, **46**, 1730–1747.

83 Z. Wang, S. He, V. Nguyen and K. E. Riley, *Eng. Sci.*, 2020, **11**, 3–18.

84 I. V. Vorotyntsev, A. A. Atlaskin, M. M. Trubyanov, A. N. Petukhov, O. R. Gumerova, A. I. Akhmetshina and V. M. Vorotyntsev, *Desalin. Water Treat.*, 2017, **75**, 305–313.

85 M. Han and R. M. Espinosa-Marzal, *ACS Appl. Mater. Interfaces*, 2019, **11**, 33465–33477.

86 T. Koishi, *J. Phys. Chem. B*, 2018, **122**, 12342–12350.

87 A. H. Jalili, M. Shokouhi, G. Maurer and M. Hosseini-Jenab, *J. Chem. Thermodyn.*, 2013, **67**, 55–62.

88 M. B. Shiflett and A. Yokozeki, *Fluid Phase Equilib.*, 2010, **294**, 105–113.

89 A. H. Jalili, M. Safavi, C. Ghotbi, A. Mehdizadeh, M. Hosseini-Jenab and V. Taghikhani, *J. Phys. Chem. B*, 2012, **116**, 2758–2774.

90 M. Safavi, C. Ghotbi, V. Taghikhani, A. H. Jalili and A. Mehdizadeh, *J. Chem. Thermodyn.*, 2013, **65**, 220–232.

91 B. A. Neto, A. A. Lapis and R. Y. Souza, *Encyclopedia of Ionic Liquids*, 2023, pp. 1273–1283.

92 M. Nisar, H. Y. Gondal, S. Munir, Z. M. Cheema, S. A. Alhussain and M. E. Zaki, *J. Saudi Chem. Soc.*, 2023, **27**, 101687.

93 K. Huang, D. N. Cai, Y. L. Chen, Y. T. Wu, X. B. Hu and Z. B. Zhang, *AIChE J.*, 2013, **59**, 2227–2235.

94 K. Huang, D. N. Cai, Y. L. Chen, Y. T. Wu, X. B. Hu and Z. B. Zhang, *ChemPlusChem*, 2014, **79**, 241–249.

95 K. Huang, X. M. Zhang, Y. Xu, Y. T. Wu, X. B. Hu and Y. Xu, *AIChE J.*, 2014, **60**, 4232–4240.

96 T. L. Greaves and C. J. Drummond, *Chem. Rev.*, 2008, **108**, 206–237.

97 T. L. Greaves and C. J. Drummond, *Chem. Rev.*, 2015, **115**, 11379–11448.

98 K. Huang, X. M. Zhang, X. B. Hu and Y. T. Wu, *AIChE J.*, 2016, **62**, 4480–4490.

99 C. F. Patzschke, J. Zhang, P. S. Fennell and J. M. Trusler, *J. Chem. Eng. Data*, 2017, **62**, 2075–2083.

100 L.-Y. Wang, Y.-L. Xu, Z.-D. Li, Y.-N. Wei and J.-P. Wei, *Energy Fuels*, 2018, **32**, 10–23.

101 C. Wang, H. Luo, D. E. Jiang, H. Li and S. Dai, *Angew. Chem.*, 2010, **122**, 6114–6117.

102 A. A. Sulaimon, P. I. Murungi and D. F. B. Mohshim, *Pet. Sci. Technol.*, 2023, **41**, 257–301.

103 M. Huo, X. Peng, J. Zhao, Q. Ma, R. Cai, C. Deng, B. Liu, C. Sun and G. Chen, *Int. J. Hydrogen Energy*, 2023, **48**(85), 33173–33185.

104 S. Mortazavi-Manesh, M. A. Satyro and R. A. Marriott, *AIChE J.*, 2013, **59**, 2993–3005.

105 L. S. Tomaník, L. R. Rulíšek and P. Slavíček, *J. Chem. Theory Comput.*, 2023, **19**, 1014–1022.

106 M. S. Aminuddin, Z. Man, M. A. Bustam Khalil and B. Abdullah, *E3S Web Conf.*, 2021, **287**, 02003.

107 M. Yazdani, E. Salehi, S. Zilabi and G. Nikravesh, *J. Chem. Thermodyn.*, 2023, 107092.

108 Y. Zhao, R. Gani, R. M. Afzal, X. Zhang and S. Zhang, *AIChE J.*, 2017, **63**, 1353–1367.

109 R. Santiago, J. Lemus, A. X. Outomuro, J. Bedia and J. Palomar, *Sep. Purif. Technol.*, 2020, **233**, 116050.

110 J. Lemus, R. Santiago, D. Hospital-Benito, T. Welton, J. P. Hallett and J. Palomar, *ACS Sustain. Chem. Eng.*, 2021, **9**, 2080–2088.

111 B. Kazmi, J. Haider, M. A. Qyyum, S. Saeed, M. R. Kazmi and M. Lee, *Int. J. Greenhouse Gas Control*, 2019, **87**, 89–99.

112 Y. Wang, X. Liu, A. Kraslawski, J. Gao and P. Cui, *J. Cleaner Prod.*, 2019, **213**, 480–490.

113 S. Yang, Y. Qian and S. Yang, *Ind. Eng. Chem. Res.*, 2016, **55**, 6186–6193.

114 J. Haider, M. A. Qyyum, A. Riaz, A. Naquash, B. Kazmi, M. Yasin, A.-S. Nizami, M. Byun, M. Lee and H. Lim, *Fuel*, 2022, **314**, 123064.

115 J. Jacquemin, P. Husson, A. A. Padua and V. Majer, *Green Chem.*, 2006, **8**, 172–180.

116 J. Li, Z. Dai, M. Usman, Z. Qi and L. Deng, *Int. J. Greenhouse Gas Control*, 2016, **45**, 207–215.

117 L. I. Tomé, V. Baião, W. da Silva and C. M. Brett, *Appl. Mater. Today*, 2018, **10**, 30–50.

118 A. Paiva, R. Craveiro, I. Aroso, M. Martins, R. L. Reis and A. R. C. Duarte, *ACS Sustain. Chem. Eng.*, 2014, **2**, 1063–1071.

119 B. B. Hansen, S. Spittle, B. Chen, D. Poe, Y. Zhang, J. M. Klein, A. Horton, L. Adhikari, T. Zelovich and B. W. Doherty, *Chem. Rev.*, 2020, **121**, 1232–1285.

120 D. O. Abranches, M. A. Martins, L. P. Silva, N. Schaeffer, S. P. Pinho and J. A. Coutinho, *Chem. Commun.*, 2019, **55**, 10253–10256.

121 Y. Liu, J. B. Friesen, J. B. McAlpine, D. C. Lankin, S.-N. Chen and G. F. Pauli, *J. Nat. Prod.*, 2018, **81**, 679–690.

122 L. Lomba, M. P. Ribate, E. Sangüesa, J. Concha, M. P. Garralaga, D. Errazquin, C. B. García and B. Giner, *Appl. Sci.*, 2021, **11**, 10061.

123 S. Sarmad, J. P. Mikkola and X. Ji, *ChemSusChem*, 2017, **10**, 324–352.

124 G. García, S. Aparicio, R. Ullah and M. Atilhan, *Energy Fuels*, 2015, **29**, 2616–2644.

125 M. Karibayev and D. Shah, *Energy Fuels*, 2020, **34**, 9894–9902.

126 H. S. Salehi, R. Hens, O. A. Moultos and T. J. Vlugt, *J. Mol. Liq.*, 2020, **316**, 113729.

127 E. Słupek, P. Makoś and J. Gębicki, *Energies*, 2020, **13**, 3379.

128 K. D. O. Vigier, G. Chatel and F. Jérôme, *ChemCatChem*, 2015, **7**, 1250–1260.

129 D. Deng, X. Liu and B. Gao, *Ind. Eng. Chem. Res.*, 2017, **56**, 13850–13856.

130 Y. Chen, B. Jiang, H. Dou, L. Zhang, X. Tantai, Y. Sun and H. Zhang, *Energy Fuels*, 2018, **32**, 10737–10744.

131 Y. Gu, Y. Hou, S. Ren, Y. Sun and W. Wu, *ACS Omega*, 2020, **5**, 6809–6816.

132 D. Jung, J. B. Jung, S. Kang, K. Li, I. Hwang, J. H. Jeong, H. S. Kim and J. Lee, *Green Chem.*, 2021, **23**, 1300–1311.

133 M. Hayyan, M. A. Hashim, A. Hayyan, M. A. Al-Saadi, I. M. AlNashef, M. E. Mirghani and O. K. Saheed, *Chemosphere*, 2013, **90**, 2193–2195.

134 M. Xiao, H. Liu, H. Gao, W. Olson and Z. Liang, *Appl. Energy*, 2019, **235**, 311–319.

135 S. J. Kumar, S. R. Prasad, R. Banerjee, D. K. Agarwal, K. S. Kulkarni and K. Ramesh, *Chem. Cent. J.*, 2017, **11**, 1–7.

136 P. L. McCarty, *In Situ Remediation of Chlorinated Solvent Plumes*, 2010, pp. 1–28.

137 W. W. Anku, M. A. Mamo and P. P. Govender, *Phenolic Compounds-Natural Sources, Importance and Applications*, 2017, pp. 419–443.

138 M. Saygun, A. Ekici, N. B. Muluk, A. Çakmak, T. Pinar, E. Dağ and M. Ekici, *Clinical and Investigative Medicine*, 2012, pp. E190–E205.

139 M. Jaishankar, T. Tseten, N. Anbalagan, B. B. Mathew and K. N. Beeregowda, *Interdiscip. Toxicol.*, 2014, **7**, 60.

140 H. Vanda, Y. Dai, E. G. Wilson, R. Verpoorte and Y. H. Choi, *C. R. Chim.*, 2018, **21**, 628–638.

141 Y. Chen and T. Mu, *Green Chem. Sci.*, 2021, **2**, 174–186.

142 R. Malolan, K. P. Gopinath, D.-V. N. Vo, R. S. Jayaraman, S. Adithya, P. S. Ajay and J. Arun, *Environ. Chem. Lett.*, 2021, **19**, 1001–1023.

143 B. Miller, in *Fossil Fuel Emissions Control Technologies*, ed. B. Miller, Butterworth-Heinemann, 2015, pp. 367–438, DOI: 10.1016/B978-0-12-801566-7.00008-7.

144 D. A. Bell, B. F. Towler and M. Fan, in *Coal Gasification and Its Applications*, ed. D. A. Bell, B. F. Towler and M. Fan, William Andrew Publishing, Boston, 2011, pp. 113–136, DOI: 10.1016/B978-0-8155-2049-8.10006-3.

145 A. K. Coker, in *Ludwig's Applied Process Design for Chemical and Petrochemical Plants*, ed. A. K. Coker, Gulf Professional Publishing, Boston, 4th edn, 2010, pp. 269–344, DOI: 10.1016/B978-0-7506-8366-1.10011-8.

146 B. G. Miller, in *Clean Coal Engineering Technology*, ed. B. G. Miller, Butterworth-Heinemann, 2nd edn, 2017, pp. 261–308, DOI: 10.1016/B978-0-12-811365-3.00006-5.

147 A. L. Kohl and R. B. Nielsen, in *Gas Purification*, ed. A. L. Kohl and R. B. Nielsen, Gulf Professional Publishing, Houston, 5th edn, 1997, pp. 40–186, DOI: 10.1016/B978-088415220-0/50002-1.

148 L. A. Pellegrini, M. Gilardi, F. Giudici and E. Spatolisano, *Energies*, 2021, **14**, DOI: 10.3390/en14206687.

149 S. Northrop, J. Seagraves, S. Ramkumar and T. Cullinane, ExxonMobil's Experience with Sour Gas Treating and Acid Gas Handling, in *Abu Dhabi International Petroleum Exhibition & Conference*, OnePetro, 2019.

150 J. Seagraves and G. Vorberg, OASE® sulfexxTM : The next generation of super selective solvents, in *GPA Europe Autumn Conference, Royal Ascot*, Gas Processors Association Europe, 2020, https://www.gpaeurope.com.

151 A. L. Kohl and R. B. Nielsen, in *Gas Purification*, ed. A. L. Kohl and R. B. Nielsen, Gulf Professional Publishing, Houston, 5th edn, 1997, pp. 330–414, DOI: 10.1016/B978-088415220-0/50005-7.

152 S. S. Hosseini and J. F. Denayer, *J. Environ. Chem. Eng.*, 2022, **10**, 107483.

153 O. D. Agboola and N. U. Benson, *Front. Environ. Sci.*, 2021, **9**, 167.

154 M. Atif, H. Z. Haider, R. Bongiovanni, M. Fayyaz, T. Razzaq and S. Gul, *Surf. Interfaces*, 2022, **31**, 102080.

155 H. Tang, J. Tao, A. Ruzsinszky and J. P. Perdew, *J. Phys. Chem. C*, 2019, **123**, 13748–13757.

156 S. Saini, J. Halldin Stenlid and F. Abild-Pedersen, *npj Comput. Mater.*, 2022, **8**, 163.

157 S. N. Kudahi, A. R. Noorpoor and N. M. Mahmoodi, *J. CO₂ Util.*, 2017, **21**, 17–29.

158 K.-J. Ko, H. Kim, Y.-H. Cho, K.-M. Kim and C.-H. Lee, *Sep. Purif. Technol.*, 2023, **305**, 122539.

159 N. N. Zulkefli, A. M. I. Noor Azam, M. S. Masdar and W. N. R. W. Isahak, *Materials*, 2023, **16**, 462.

160 N. Le-Minh, E. C. Sivret, A. Shammay and R. M. Stuetz, *Crit. Rev. Environ. Sci. Technol.*, 2018, **48**, 341–375.

161 H. Yildiz, H. Gülşen, Ö. Şahin, O. Baytar and S. Kutluay, *Int. J. Phytorem.*, 2023, 1–13.

162 S. E. Manahan, *Environmental Chemistry*, CRC Press, 2017.

163 J. Gopalan, A. Buthiyappan and A. A. A. Raman, *J. Ind. Eng. Chem.*, 2022, **113**, 72–95.

164 Y. Wang, R. Cui, H. Jiang, M. Bai, K. Lin, M. Zhang and L. Ren, *Processes*, 2022, **10**, 2016.

165 J.-H. Tsai, H.-M. Chiang, G.-Y. Huang and H.-L. Chiang, *J. Hazard. Mater.*, 2008, **154**, 1183–1191.

166 R. Ahmadi, M. S. Alivand, N. H. M. H. Tehrani, M. Ardjmand, A. Rashidi, M. Rafizadeh, A. Seif, F. Mollakazemi, Z. Noorpoor and J. Rudd, *Chem. Eng. J.*, 2021, **415**, 129076.

167 S. Wang, H. Nam and H. Nam, *J. Environ. Chem. Eng.*, 2020, **8**, 103683.

168 C. Yang, Y. Wang, H. Fan, G. de Falco, S. Yang, J. Shangguan and T. J. Bandosz, *Appl. Catal., B*, 2020, **266**, 118674.

169 C. Yang, M. Florent, G. de Falco, H. Fan and T. J. Bandosz, *Chem. Eng. J.*, 2020, **394**, 124906.

170 Y. Yuan, L. Huang, T. C. Zhang, L. Ouyang and S. Yuan, *Sep. Purif. Technol.*, 2021, **279**, 119686.

171 Y. Pan, M. Chen, Z. Su, K. Wu, Y. Zhang and D. Long, *Appl. Catal., B*, 2021, **280**, 119444.

172 L. Chen, J. Yuan, T. Li, X. Jiang, S. Ma, W. Cen and W. Jiang, *Sci. Total Environ.*, 2021, **768**, 144452.

173 S. Fakhraie, H. R. Rajabi, A. Rashidi, Y. Orooji, E. Ghasemy, A. S. Zeraati, R. Rahighi and A. Mirhashemi, *Appl. Surf. Sci.*, 2021, **559**, 149892.

174 Z. Yu, X. Wang, Y.-N. Hou, X. Pan, Z. Zhao and J. Qiu, *Carbon*, 2017, **117**, 376–382.

175 J. Wang, C. Ke, X. Jia, C. Ma, X. Liu, W. Qiao and L. Ling, *Appl. Catal., B*, 2021, **283**, 119650.

176 C. Xu, J. Chen, S. Li, Q. Gu, D. Wang, C. Jiang and Y. Liu, *J. Hazard. Mater.*, 2021, **403**, 123806.

177 H. Ou, M. Fang, M. Chou, H. Chang and T. Shiao, *J. Air Waste Manage. Assoc.*, 2020, **70**, 641–648.

178 H. Sawalha, M. Maghalseh, J. Qutaina, K. Junaidi and E. R. Rene, *Bioengineered*, 2020, **11**, 607–618.

179 Q. Dong, J. Wang, C. Ma, Y. Wu, W. Qiao and L. Ling, *Sep. Purif. Technol.*, 2024, **330**, 125152.

180 Y. Feng, J. Lu, J. Wang, J. Mi, M. Zhang, M. Ge, Y. Li, Z. Zhang and W. Wang, *J. Cleaner Prod.*, 2020, **273**, 123080.

181 P. R. Westmoreland and D. P. Harrison, *Environ. Sci. Technol.*, 1976, **10**, 659–661.

182 X. Zhang, Y. Tang, S. Qu, J. Da and Z. Hao, *ACS Catal.*, 2015, **5**, 1053–1067.

183 L. R. Pahalagedara, A. S. Poyraz, W. Song, C.-H. Kuo, M. N. Pahalagedara, Y.-T. Meng and S. L. Suib, *Chem. Mater.*, 2014, **26**, 6613–6621.

184 S. Cheah, D. L. Carpenter and K. A. Magrini-Bair, *Energy Fuels*, 2009, **23**, 5291–5307.

185 S. Sureshkumar, S. Rajakumari and R. Manonmani, *J. Iran. Chem. Soc.*, 2023, 1–16.

186 A. Marikutsa, A. A. Dobrovolskii, M. N. Rumyantseva, A. A. Mikhaylov, A. G. Medvedev, O. Lev and P. V. Prikhodchenko, *J. Alloys Compd.*, 2023, 169141.

187 Schlumberger, *H₂S Removal Adsorbents*, https://www.slb.com/-/media/files/mi/brochure/h2s-removal-absorbents-br.ashx, (accessed 28th February, 2023).

188 M. N. Hassankiadeh and A. Hallajisani, *J. Pet. Sci. Eng.*, 2020, **190**, 107131.

189 S. H. Orojlou, B. Zargar and S. Rastegarzadeh, *J. Nat. Gas Sci. Eng.*, 2018, **59**, 363–373.

190 Z. Pan, W. P. Chan, W. Da Oh, A. Veksha, A. Giannis, S. Kumaran, O. Tamilselvam, J. Lei, D. K. B. Mohamed and H. Wang, *Fuel Process. Technol.*, 2020, **201**, 106344.

191 S. Kim, N. K. Gupta, J. Bae and K. S. Kim, *J. Environ. Chem. Eng.*, 2021, **9**, 105216.

192 M. Wu, E. Guo, Q. Li, J. Mi and H. Fan, *Chem. Eng. J.*, 2020, **389**, 123750.

193 Y. Ahn, K. Pandi, M. Lee and J. Choi, *J. Cleaner Prod.*, 2020, **272**, 122849.

194 K. Morioka, S. Inaba, M. Shimizu, K. Ano and T. Sugiyama, *ISIJ Int.*, 2000, **40**, 280–285.

195 C. J. Heard, L. Grajciar, F. Uhlík, M. Shamzhy, M. Opanasenko, J. Čejka and P. Nachtigall, *Adv. Mater.*, 2020, **32**, 2003264.

196 J. Li, A. Corma and J. Yu, *Chem. Soc. Rev.*, 2015, **44**, 7112–7127.

197 M. Król, *Crystals*, 2020, **10**, 622.

198 M. W. Ackley, S. U. Rege and H. Saxena, *Microporous Mesoporous Mater.*, 2003, **61**, 25–42.

199 M. G. Rimoli, M. R. Rabaioli, D. Melisi, A. Curcio, S. Mondello, R. Mirabelli and E. Abignente, *Journal of Biomedical Materials Research Part A: An Official Journal of the Society for Biomaterials*, The Japanese Society for Biomaterials, and The Australian Society for Biomaterials and the Korean Society for Biomaterials, 2008, vol. 87, pp. , pp. 156–164.

200 Y. Li and J. Yu, *Nat. Rev. Mater.*, 2021, **6**, 1156–1174.

201 M. Ozekmekci, G. Salkic and M. F. Fellah, *Fuel Process. Technol.*, 2015, **139**, 49–60.

202 P. Bareschino, E. Mancusi, A. Forgione and F. Pepe, *Chem. Eng. Sci.*, 2020, **223**, 115744.

203 L. Barelli, G. Bidini, L. Micoli, E. Sisani and M. Turco, *Energy*, 2018, **160**, 44–53.

204 S. Bahraminia, M. Anbia and E. Koohsaryan, *Int. J. Hydrogen Energy*, 2020, **45**, 31027–31040.

205 M. Jafari, R. Zendehdel, A. Rafieepour, M. Nakhaei Pour, H. Irvani and S. Khodakarim, *Int. J. Environ. Sci. Technol.*, 2020, **17**, 187–194.

206 L. Song, X. Du, Y. Chen, Z. Yang, J. Ran, G. Yang, Q. Shi and Z. Xue, *Microporous Mesoporous Mater.*, 2021, **328**, 111495.

207 M. Florent and T. J. Bandosz, *Chem. Eng. J.*, 2020, **401**, 125986.

208 Z. Yan, S. Tang, X. Zhou, L. Yang, X. Xiao, H. Chen, Y. Qin and W. Sun, *Chin. J. Chem. Eng.*, 2019, **27**, 174–181.

209 A. G. Georgiadis, N. D. Charisiou, S. Gaber, K. Polychronopoulou, I. V. Yentekakis and M. A. Goula, *ACS Omega*, 2021, **6**, 14774–14787.

210 S. Kitagawa, *Chem. Soc. Rev.*, 2014, **43**, 5415–5418.

211 E. Sharmin and F. Zafar, in *Metal–Organic Frameworks*, IntechOpen, 2016.

212 T. R. Cook, Y.-R. Zheng and P. J. Stang, *Chem. Rev.*, 2013, **113**, 734–777.

213 Q. Liu, C. Bian, S. Ming, L. Guo, S. Zhang, L. Pang, P. Liu, Z. Chen and T. Li, *Appl. Catal., A*, 2020, **607**, 117865.

214 N. K. Gupta, S. Kim, J. Bae and K. S. Kim, *RSC Adv.*, 2021, **11**, 4890–4900.

215 N. K. Gupta, S. Kim, J. Bae and K. S. Kim, *Chem. Eng. J.*, 2021, **411**, 128536.

216 J. A. Zárate, E. Sánchez-González, T. Jurado-Vázquez, A. Gutiérrez-Alejandre, E. González-Zamora, I. Castillo, G. Maurin and I. A. Ibarra, *Chem. Commun.*, 2019, **55**, 3049–3052.

217 J. G. Flores, J. A. Zárate-Colín, E. Sanchez-Gonzalez, J. R. Valenzuela, A. Gutierrez-Alejandre, J. Ramirez, V. Jancik, J. Aguilar-Pliego, M. C. Zorrilla and H. A. Lara-García, *ACS Appl. Mater. Interfaces*, 2020, **12**, 18885–18892.

218 E. S. Grape, J. G. Flores, T. Hidalgo, E. Martínez-Ahumada, A. Gutiérrez-Alejandre, A. Hautier, D. R. Williams, M. O'Keeffe, L. Öhrström and T. Willhammar, *J. Am. Chem. Soc.*, 2020, **142**, 16795–16804.

219 J. Xu, T. Lawson, H. Fan, D. Su and G. Wang, *Adv. Energy Mater.*, 2018, **8**, 1702607.

220 T. N. L. T. Ngo and K.-Y. Chiang, *J. Environ. Chem. Eng.*, 2023, **11**, 109592.

221 Y. Liu, H. Cheng, M. Cheng, Z. Liu, D. Huang, G. Zhang, B. Shao, Q. Liang, S. Luo and T. Wu, *Chem. Eng. J.*, 2021, **417**, 127914.

222 J. O. Ighalo, S. Rangabhashiyam, C. A. Adeyanju, S. Ogunniyi, A. G. Adeniyi and C. A. Igwegbe, *J. Ind. Eng. Chem.*, 2022, **105**, 34–48.

223 A. A. Jameh, T. Mohammadi, O. Bakhtiari and M. Mahdyarfar, *J. Environ. Chem. Eng.*, 2019, **7**, 103058.

224 X. Liu, B. Wang, J. Cheng, Q. Meng, Y. Song and M. Li, *Sep. Purif. Technol.*, 2020, **250**, 117300.

225 L. Feng, K.-Y. Wang, G. S. Day, M. R. Ryder and H.-C. Zhou, *Chem. Rev.*, 2020, **120**, 13087–13133.

226 P. Lyu and G. Maurin, *ACS Appl. Mater. Interfaces*, 2021, **13**, 4813–4822.

227 A. J. Rieth, A. M. Wright and M. Dincă, *Nat. Rev. Mater.*, 2019, **4**, 708–725.

228 T. W. Clyne and D. Hull, *An Introduction to Composite Materials*, Cambridge University Press, 2019.

229 B. Zimmerli, M. Strub, F. Jeger, O. Stadler and A. Lussi, Composite materials: composition, properties and clinical applications. A literature review, *Schweizer Monatsschrift fur Zahnmedizin= Revue mensuelle suisse d'odonto-stomatologie= Rivista mensile svizzera di odontologia e stomatologia*, 2010, vol. 120, pp. 972–986.

230 K. N. Keya, N. A. Kona, F. A. Koly, K. M. Maraz, M. N. Islam and R. A. Khan, *Mater. Eng. Res.*, 2019, **1**, 69–85.

231 D. K. Rajak, D. D. Pagar, R. Kumar and C. I. Pruncu, *J. Mater. Res. Technol.*, 2019, **8**, 6354–6374.

232 N. K. Gupta, J. Bae, S. Kim and K. S. Kim, *Chemosphere*, 2021, **274**, 129789.

233 M. Wu, Q. Li, X. Wang and J. Mi, *Energy Fuels*, 2021, **35**, 2456–2467.

234 B. Lin, H. Chen, W. Wei, J. Zhang, M. Wu, W. Li, W. Zhu, Y. Zhang and Y. Wang, *Fuel*, 2024, **358**, 130318.

235 C. N. Okonkwo, C. Okolie, A. Sujan, G. Zhu and C. W. Jones, *Energy Fuels*, 2018, **32**, 6926–6933.

236 C. N. Okonkwo, J. J. Lee, A. De Vylder, Y. Chiang, J. W. Thybaut and C. W. Jones, *Chem. Eng. J.*, 2020, **379**, 122349.

237 C. N. Okonkwo, H. Fang, D. S. Sholl, J. E. Leisen and C. W. Jones, *ACS Sustain. Chem. Eng.*, 2020, **8**, 10102–10114.

238 S. Kasulla, S. Malik, S. Zafar and A. Saraf, *Int. J. Trend Sci. Res. Dev.*, 2021, **5**, 857–863.

239 S. Cimino, L. Lisi, A. Erto, F. Deorsola, G. de Falco, F. Montagnaro and M. Balsamo, *Microporous Mesoporous Mater.*, 2020, **295**, 109949.

240 Y. Pan, M. Chen, M. Hu, M. Tian, Y. Zhang and D. Long, *Appl. Catal., B*, 2020, **262**, 118266.

241 Y. Wang, P. Ning, R. Zhao, K. Li, C. Wang, X. Sun, X. Song and Q. Lin, *Front. Environ. Sci. Eng.*, 2021, **15**, 1–10.

242 N. N. Zulkefli, M. S. Masdar, W. N. R. Wan Isahak, J. Md Jahim, S. A. Md Rejab and C. Chien Lye, *PLoS One*, 2019, **14**, e0211713.

243 N. N. Zulkefli, M. S. Masdar, W. N. R. Wan Isahak, S. N. H. Abu Bakar, H. Abu Hasan and N. Mohd Sofian, *Catalysts*, 2021, **11**, 545.

244 V. Gasquet, B. Kim, L. Sigot and H. Benbelkacem, *Waste Biomass Valorization*, 2020, **11**, 5363–5373.

245 E. Surra, M. C. Nogueira, M. Bernardo, N. Lapa, I. Esteves and I. Fonseca, *Waste Manage.*, 2019, **94**, 136–145.

246 S. Liang, J. Mi, F. Liu, Y. Zheng, Y. Xiao, Y. Cao and L. Jiang, *Chem. Eng. Sci.*, 2020, **221**, 115714.

247 X. Kan, X. Chen, W. Chen, J. Mi, J.-Y. Zhang, F. Liu, A. Zheng, K. Huang, L. Shen and C. Au, *ACS Sustain. Chem. Eng.*, 2019, **7**, 7609–7618.

248 M. Sun, X. Wang, X. Pan, L. Liu, Y. Li, Z. Zhao and J. Qiu, *Fuel Process. Technol.*, 2019, **191**, 121–128.

249 S. A. Nicolae, P. Á. Szilágyi and M. M. Titirici, *Carbon*, 2020, **169**, 193–204.

250 C. Yang, S. Yang, H. Fan, Y. Wang and J. Shangguan, *J. Colloid Interface Sci.*, 2019, **555**, 548–557.

251 Z. Aslam, I. A. Hussein, R. A. Shawabkeh, M. A. Parvez, W. Ahmad and Ihsanullah, *J. Air Waste Manage. Assoc.*, 2019, **69**, 246–257.

252 F. Dashtestani, M. Nusheh, V. Siriwongrungson, J. Hongrapipat, V. Materic and S. Pang, *Fuel*, 2021, **295**, 120586.

253 N. K. Gupta, J. Bae and K. S. Kim, *Chem. Eng. J.*, 2022, **427**, 130909.

254 N. K. Gupta, J. Bae and K. S. Kim, *Sci. Rep.*, 2021, **11**, 14740.

255 M. Daraee, R. Saeedirad and A. Rashidi, *J. Solid State Chem.*, 2019, **278**, 120866.

256 M. Daraee, E. Ghasemy and A. Rashidi, *J. Environ. Chem. Eng.*, 2020, **8**, 104351.

257 M.-H. Lee, K. Vikrant, S. A. Younis, J. E. Szulejko and K.-H. Kim, *J. Cleaner Prod.*, 2020, **250**, 119486.

258 N. K. Gupta, J. Bae and K. S. Kim, *ACS Omega*, 2021, **6**, 25631–25641.

259 N. Bhoria, G. Basina, J. Pokhrel, K. S. K. Reddy, S. Anastasiou, V. V. Balasubramanian, Y. F. AlWahedi and G. N. Karanikolos, *J. Hazard. Mater.*, 2020, **394**, 122565.

260 J. Mi, F. Liu, W. Chen, X. Chen, L. Shen, Y. Cao, C. Au, K. Huang, A. Zheng and L. Jiang, *ACS Appl. Mater. Interfaces*, 2019, **11**, 29950–29959.

261 N. Hazrati, M. Abdouss, A. Vahid, A. Miran Beigi and A. Mohammadalizadeh, *Int. J. Environ. Sci. Technol.*, 2014, **11**, 997–1006.

262 Q. Geng, L.-J. Wang, C. Yang, H.-Y. Zhang, Y.-R. Zhao, H.-L. Fan and C. Huo, *Fuel Process. Technol.*, 2019, **185**, 26–37.

263 C. Yang, J. Kou, H. Fan, Z. Tian, W. Kong and J. Shangguan, *Langmuir*, 2019, **35**, 7759–7768.

264 G. Basina, D. A. Gaber, S. Al Yafei, V. Tzitzios, S. A. Gaber, I. Ismail, B. V. Vaithilingam, K. Polychronopoulou, S. Al Hashimi and Y. Al Wahedi, *Chem. Eng. J.*, 2020, **398**, 125585.

265 M. Daraee, E. Ghasemy and A. Rashidi, *J. Environ. Chem. Eng.*, 2020, **8**, 103836.

266 Q. Li, X. Liu, L. Du, B. Bai, Z. Fang, M. Jing and X. Li, *Energy Procedia*, 2013, **37**, 2505–2510.

267 M. J. Ledoux, S. Pham-Huu, N. Keller, J.-B. Nougayrède, S. Savin-Poncet and J. Bousquet, *Catal. Today*, 2000, **61**, 157–163.

268 F. Tari, M. Shekarriz, S. Zarrinpashne and A. Ruzbehani, *J. Nat. Gas Sci. Eng.*, 2018, **59**, 124–135.

269 H. Xu, D. Zhang, F. Wu, X. Wei and J. Zhang, *Fuel*, 2018, **225**, 104–110.

270 A. P. Reverberi, J. J. Klemeš, P. S. Varbanov and B. Fabiano, *J. Cleaner Prod.*, 2016, **136**, 72–80.

271 M. Sekhavatjou, R. Moradi, A. A. Hosseini and H. A. Taghinia, *Int. J. Environ. Res.*, 2014, **8**, 273–278.

272 B. Lal, D. B. Pal, C. Nayak, A. K. Gupta and A. Singh, *J. Inst. Eng. (India): Ser. E*, 2022, **103**(2), 357–363.

273 B. Lal, D. B. Pal, C. Nayak, A. K. Gupta and A. Singh, *J. Inst. Eng. (India): Ser. E*, 2022, **103**, 357–363.

274 H. R. Mahdipoor and H. Ganji, *Petroleum & Coal*, 2022, vol. 64, p. 1011.

275 B. Salomatov, Z. Azimova and S. Gaybullaev, *Eur. J. Innov. Nonform. Edu.*, 2022, **2**, 51–57.

276 W. Rouleau and J. Watson, *LO-CAT: A Flexible Hydrogen Sulphide Removal Process*, (accessed 3rd March, 2023).

277 L. Hardison and D. Kamshow, New developments in the LO-CAT hydrogen sulfide oxidation process, in *40th Annual laurance reid gas conditioning conference*, 1991.

278 A. Bassani, G. Bozzano, C. Pirola, C. Frau, A. Pettinau, E. Maggio, E. Ranzi and F. Manenti, *J. Sustain. Dev. Energy Water Environ. Syst.*, 2017, **6**, 210–226.

279 K. H. Al Hatmi, A. d. N. Al Mashrafi and M. S. Shaikh, An Innovative and Well-Demonstrated Approach Toward Achieving Zero-Flaring, in *ADIPEC*, OnePetro, 2022.

280 K. Gaj and K. Cichuta, *Energies*, 2023, **16**, 100.

281 M. J. Goodwin, O. M. Musa and J. W. Steed, *Energy Fuels*, 2015, **29**, 4667–4682.

282 S. P. Nunes and K.-V. Peinemann, *Membrane Technology*, Wiley Online Library, 2001.

283 S. N. Mithra and S. Ahankari, *Mater. Today Sustain.*, 2022, **19**, 100191.

284 X. He, I. Kumakiri and M. Hillestad, *Sep. Purif. Technol.*, 2020, **247**, 116993.

285 Y. Shi, B. Liang, R.-B. Lin, C. Zhang and B. Chen, *Trends Chem.*, 2020, **2**, 254–269.

286 R. S. K. Valappil, N. Ghasem and M. Al-Marzouqi, *J. Ind. Eng. Chem.*, 2021, **98**, 103–129.

287 Y. Han and W. W. Ho, *J. Membr. Sci.*, 2021, **628**, 119244.

288 W. F. Yong and H. Zhang, *Prog. Mater. Sci.*, 2021, **116**, 100713.

289 Y. Alqaheem, A. Alomair, M. Vinoba and A. Pérez, *Int. J. Polym. Sci.*, 2017, **2017**, 4250927.

290 G. George, N. Bhoria, S. AlHallaq, A. Abdala and V. Mittal, *Sep. Purif. Technol.*, 2016, **158**, 333–356.

291 X. He, *Energy Sustain. Soc.*, 2018, **8**, 1–14.

292 F. Sabbagh and B. S. Kim, *J. Controlled Release*, 2022, **341**, 132–146.

293 U. W. Siagian, A. Raksajati, N. F. Himma, K. Khoiruddin and I. Wenten, *J. Nat. Gas Sci. Eng.*, 2019, **67**, 172–195.

294 J. R. Klaehn, C. J. Orme and D. M. Ginosar, *Sep. Sci. Technol.*, 2022, 1–11.

295 L. M. Robeson, *J. Membr. Sci.*, 2008, **320**, 390–400.

296 L. Ansaloni and L. Deng, in *Recent Developments in Polymer Macro, Micro and Nano Blends*, Elsevier, 2017, pp. 163–206.

297 D. J. Jasim, T. J. Mohammed and M. F. Abid, *Eng. Technol. J.*, 2022, **40**, 441–450.

298 B. Wilks and M. E. Rezac, *J. Appl. Polym. Sci.*, 2002, **85**, 2436–2444.

299 M. Farnam, H. Bin Mukhtar and A. Bin Mohd Shariff, *ChemBioEng Rev.*, 2021, **8**, 90–109.

300 M. Klepić, K. Setničková, M. Lanč, M. Žák, P. Izák, M. Dendisová, A. Fuoco, J. C. Jansen and K. Friess, *J. Membr. Sci.*, 2020, **597**, 117623.

301 Y. Liu, Z. Liu, G. Liu, W. Qiu, N. Bhuwania, D. Chinn and W. J. Koros, *J. Membr. Sci.*, 2020, **593**, 117430.

302 D. J. Harrigan, J. A. Lawrence III, H. W. Reid, J. B. Rivers, J. T. O'Brien, S. A. Sharber and B. J. Sundell, *J. Membr. Sci.*, 2020, **602**, 117947.

303 Y. Yampolskii, L. Starannikova, N. Belov, M. Bermeshev, M. Gringolts and E. Finkelshtein, *J. Membr. Sci.*, 2014, **453**, 532–545.

304 M. Isanejad, N. Azizi and T. Mohammadi, *J. Appl. Polym. Sci.*, 2017, **134**, DOI: **10.1002/app.44531**.

305 E. G. Estahbanati, M. Omidkhah and A. E. Amooghin, *J. Ind. Eng. Chem.*, 2017, **51**, 77–89.

306 K. Amo, R. Baker, V. Helm, T. Hofmann, K. Lokhandwala, I. Pinnau, M. Ringer, T. Su, L. Toy and J. Wijmans, *Low-Quality Natural Gas Sulfur Removal/Recovery*, Federal Energy Technology Center Morgantown (FETC-MGN), Morgantown, WV …, 1998.

307 J. T. Vaughn and W. J. Koros, *J. Membr. Sci.*, 2014, **465**, 107–116.

308 A. P. Isfahani, M. Sadeghi, A. H. S. Dehaghani and M. A. Aravand, *J. Ind. Eng. Chem.*, 2016, **44**, 67–72.

309 G. Chatterjee, A. Houde and S. Stern, *J. Membr. Sci.*, 1997, **135**, 99–106.

310 Z. Si, H. Wu, P. Qin and B. Van der Bruggen, *Sep. Purif. Technol.*, 2022, 121612.

311 C. A. Scholes, G. W. Stevens and S. E. Kentish, *J. Membr. Sci.*, 2010, **350**, 189–199.

312 W. Robb, *Ann. N. Y. Acad. Sci.*, 1968, **146**, 119–137.

313 B. Bhide and S. A. Stern, *J. Membr. Sci.*, 1993, **81**, 209–237.

314 T. Merkel, R. Gupta, B. Turk and B. Freeman, *J. Membr. Sci.*, 2001, **191**, 85–94.

315 V. P. Babu, B. E. Kraftschik and W. J. Koros, *J. Membr. Sci.*, 2018, **558**, 94–105.

316 L. M. Robeson, Q. Liu, B. D. Freeman and D. R. Paul, *J. Membr. Sci.*, 2015, **476**, 421–431.

317 M. S. Shah, M. Tsapatsis and J. I. Siepmann, *Chem. Rev.*, 2017, **117**, 9755–9803.

318 Y. Yampolskii, *Macromolecules*, 2012, **45**, 3298–3311.

319 Z.-X. Low, P. M. Budd, N. B. McKeown and D. A. Patterson, *Chem. Rev.*, 2018, **118**, 5871–5911.

320 V. F. Cardoso, D. M. Correia, C. Ribeiro, M. M. Fernandes and S. Lanceros-Méndez, *Polymers*, 2018, **10**, 161.

321 B. Ameduri and H. Sawada, *Fluorinated Polymers: Volume 1: Synthesis, Properties, Processing and Simulation*, Royal Society of Chemistry, 2016.

322 D. J. Kim, M. J. Jo and S. Y. Nam, *J. Ind. Eng. Chem.*, 2015, **21**, 36–52.

323 T. C. Merkel and L. G. Toy, *Macromolecules*, 2006, **39**, 7591–7600.

324 A. Kusoglu and A. Z. Weber, *Chem. Rev.*, 2017, **117**, 987–1104.

325 L. Olivieri, H. Aboukeila, M. G. Baschetti, D. Pizzi, L. Merlo and G. C. Sarti, *J. Membr. Sci.*, 2017, **542**, 367–377.

326 M. De Angelis, S. Lodge, M. G. Baschetti, G. Sarti, F. Doghieri, A. Sanguineti and P. Fossati, *Desalination*, 2006, **193**, 398–404.

327 J. S. Chiou and D. R. Paul, *Ind. Eng. Chem. Res.*, 1988, **27**, 2161–2164.

328 V. Signorini, M. G. Baschetti, D. Pizzi and L. Merlo, *J. Membr. Sci.*, 2021, **640**, 119809.

329 H. Ohya, V. Kudryavsev and S. I. Semenova, *Polyimide Membranes: Applications, Fabrications and Properties*, Routledge, 2022.

330 R. Castro-Muñoz, V. Martin-Gil, M. Z. Ahmad and V. Fíla, *Chem. Eng. Commun.*, 2018, **205**, 161–196.

331 C. A. Scholes, G. Q. Chen, W. X. Tao, J. Bacus, C. Anderson, G. W. Stevens and S. E. Kentish, *Energy Procedia*, 2011, **4**, 681–687.

332 J. Hao, P. Rice and S. Stern, *J. Membr. Sci.*, 2002, **209**, 177–206.

333 J. Hao, P. Rice and S. Stern, *J. Membr. Sci.*, 2008, **320**, 108–122.

334 B. Kraftschik, W. J. Koros, J. Johnson and O. Karvan, *J. Membr. Sci.*, 2013, **428**, 608–619.

335 P. Goel, P. Mandal, E. Bhuvanesh, V. K. Shahi and S. Chattopadhyay, *Sep. Purif. Technol.*, 2021, **255**, 117730.

336 S. Willdorf-Cohen, A. N. Mondal, D. R. Dekel and C. E. Diesendruck, *J. Mater. Chem. A*, 2018, **6**, 22234–22239.

337 M. P. Chenar, M. Soltanieh, T. Matsuura, A. Tabe-Mohammadi and C. Feng, *Sep. Purif. Technol.*, 2006, **51**, 359–366.

338 M. Aguilar-Vega and D. Paul, *J. Polym. Sci., Part B: Polym. Phys.*, 1993, **31**, 1577–1589.

339 M. P. Chenar, H. Savoji, M. Soltanieh, T. Matsuura and S. Tabe, *Korean J. Chem. Eng.*, 2011, **28**, 902–913.

340 S. Fischer, K. Thümmler, B. Volkert, K. Hettrich, I. Schmidt and K. Fischer, Properties and applications of cellulose acetate, in *Macromolecular symposia*, Wiley Online Library, 2008, vol. 262(1), pp. 89–96.

341 A. Moghadassi, Z. Rajabi, S. Hosseini and M. Mohammadi, *J. Ind. Eng. Chem.*, 2014, **20**, 1050–1060.

342 C. S. Achoundong, N. Bhuwania, S. K. Burgess, O. Karvan, J. R. Johnson and W. J. Koros, *Macromolecules*, 2013, **46**, 5584–5594.

343 A. Houde, B. Krishnakumar, S. Charati and S. Stern, *J. Appl. Polym. Sci.*, 1996, **62**, 2181–2192.

344 R. W. Baker, *Membrane Technology and Applications*, John Wiley & Sons, 2012.

345 Y. Liu, Z. Liu, A. Morisato, N. Bhuwania, D. Chinn and W. J. Koros, *J. Membr. Sci.*, 2020, **601**, 117910.

346 H. Lu, L. Liu, S. Kanehashi, C. Scholes and S. Kentish, *J. Membr. Sci.*, 2018, **555**, 362–368.

347 M. Shahbaz, N. Rashid, J. Saleem, H. Mackey, G. McKay and T. Al-Ansari, *Fuel*, 2023, **332**, 126220.

348 B. Bhide, A. Voskericyan and S. Stern, *J. Membr. Sci.*, 1998, **140**, 27–49.

349 H. Maghsoudi and M. Soltanieh, *J. Membr. Sci.*, 2014, **470**, 159–165.

350 N. Gilani, J. T. Daryan, A. Rashidi and M. R. Omidkhah, *Appl. Surf. Sci.*, 2012, **258**, 4819–4825.

351 H. Lu, S. Kanehashi, C. Scholes and S. Kentish, *J. Membr. Sci.*, 2017, **539**, 432–440.

352 G. O. Yahaya, A. Hayek, A. Alsamah, Y. A. Shalabi, M. M. B. Sultan and R. H. Alhajry, *Sep. Purif. Technol.*, 2021, **272**, 118897.

353 J. A. Lawrence III, D. J. Harrigan, C. R. Maroon, S. A. Sharber, B. K. Long and B. J. Sundell, *J. Membr. Sci.*, 2020, **616**, 118569.

354 C. A. Scholes, G. Dong, J. S. Kim, H. J. Jo, J. Lee and Y. M. Lee, *Sep. Purif. Technol.*, 2017, **179**, 449–454.

355 J. Vaughn and W. Koros, *Macromolecules*, 2012, **45**, 7036–7049.

356 C. J. Orme, J. R. Klaehn and F. F. Stewart, *J. Membr. Sci.*, 2004, **238**, 47–55.

357 T. Mohammadi, M. T. Moghadam, M. Saeidi and M. Mahdyarfar, *Ind. Eng. Chem. Res.*, 2008, **47**, 7361–7367.

358 S. Niknejad, H. Savoji, M. Pourafshari Chenar and M. Soltanieh, *Int. J. Environ. Sci. Technol.*, 2017, **14**, 375–384.

359 Y.-I. Park, B.-S. Kim, Y.-H. Byun, S.-H. Lee, E.-W. Lee and J.-M. Lee, *Desalination*, 2009, **236**, 342–348.

360 P. J. Carvalho and J. A. Coutinho, *Energy Environ. Sci.*, 2011, **4**, 4614–4619.

361 X. Zhang, Z. Tu, H. Li, K. Huang, X. Hu, Y. Wu and D. R. MacFarlane, *J. Membr. Sci.*, 2017, **543**, 282–287.

362 O. Malykh, A. Y. Golub and V. Teplyakov, *Adv. Colloid Interface Sci.*, 2011, **164**, 89–99.

363 W. Heilman, V. Tammela, J. Meyer, V. Stannett and M. Szwarc, *Ind. Eng. Chem.*, 1956, **48**, 821–824.

364 R. Quinn and D. Laciak, *J. Membr. Sci.*, 1997, **131**, 49–60.

365 J. Pellegrino and P. Giarratano, *Gas Separation Using Ion Exchange Membranes for Producing Hydrogen from Synthesis Gas. Quarterly Report 22 Covering the Period October 1, 1991–December 31, 1991*, National Inst. of Standards and Technology, Boulder, CO (United States …), 1992.

366 R. Quinn, J. Appleby and G. Pez, *Sep. Sci. Technol.*, 2002, **37**, 627–638.

367 D. A. Nicol, *Whisky and Other Spirits*, 2022, pp. 247–270.

368 F. S. Taylor, *Ann. Sci.*, 1945, **5**, 185–202.

369 J. M. Chambers, Alcohol distillation process, *US pat.*, US2647078A, 1953.

370 J. H. Cho and B. Hariharan, On the efficacy of knowledge distillation, in *Proceedings of the IEEE/CVF international conference on computer vision*, 2019, pp. 4794–4802.

371 T. He, Z. Liu, H. Son, T. Gundersen and W. Lin, *J. Cleaner Prod.*, 2023, **383**, 135264.

372 T. N. A. Tengku Hassan, A. M. Shariff, M. M. i. Mohd Pauzi, M. S. Khidzir and A. Surmi, *Molecules*, 2022, **27**, 1424.

373 D. Clodic and M. Younes, A new method for CO_2 capture: frosting CO_2 at atmospheric pressure, in *Greenhouse gas control technologies-6th international conference*, Elsevier, 2003, pp. 155–160.

374 D. Berstad, R. Anantharaman and P. Nekså, *Int. J. Refrig.*, 2013, **36**, 1403–1416.

375 D. Clodic, R. El Hitti, M. Younes, A. Bill and F. Casier, CO_2 capture by anti-sublimation Thermo-economic process evaluation, in *4th annual conference on carbon capture and sequestration*, Citeseer, 2005, pp. 2–5.

376 X. Pan, D. Clodic and J. Toubassy, *Greenhouse Gases: Sci. Technol.*, 2013, **3**, 8–20.

377 M.-O. Schach, B. Oyarzún, H. Schramm, R. Schneider and J.-U. Repke, *Energy Procedia*, 2011, **4**, 1403–1410.

378 C. Song, Q. Liu, S. Deng, H. Li and Y. Kitamura, *Renewable Sustainable Energy Rev.*, 2019, **101**, 265–278.

379 R. Haut, R. Denton and E. Thomas, *SPE Prod. Eng.*, 1989, **4**, 265–271.

380 B. Kelley, J. Valencia, P. Northrop and C. Mart, *Energy Procedia*, 2011, **4**, 824–829.

381 T. E. Rufford, S. Smart, G. C. Watson, B. Graham, J. Boxall, J. D. Da Costa and E. May, *J. Pet. Sci. Eng.*, 2012, **94**, 123–154.

382 J. Nichols, B. Friedman, A. Nold, S. McCutcheon and A. Goethe, Processing technologies for CO2 rich gas, in *Proceedings of the 88th Annual Convention of the Gas Processors Association*, San Antonio, TX, USA, 2009, pp. 8–11.

383 P. S. Northrop and J. A. Valencia, *Energy Procedia*, 2009, **1**, 171–177.

384 J. A. Valencia, S. D. Kelman, A. K. Nagavarapu and D. W. Maher, The controlled freeze zone technology for the commercialization of sour gas resources, in *IPTC 2014: International Petroleum Technology Conference*, European Association of Geoscientists & Engineers, 2014, pp. cp-395-00180.

385 H. Tan, Z. Ding and N. Wen, *Appl. Therm. Eng.*, 2022, **214**, 118903.

386 C. Font-Palma, D. Cann and C. Udemu, *C*, 2021, **7**, 58.

387 M. Tuinier, M. van Sint Annaland and J. Kuipers, *Int. J. Greenhouse Gas Control*, 2011, **5**, 694–701.

388 A. Ali, K. Maqsood, N. Syahera, A. B. Shariff and S. Ganguly, *Chem. Eng. Technol.*, 2014, **37**, 1675–1685.

389 M. J. Tuinier and M. van Sint Annaland, *Ind. Eng. Chem. Res.*, 2012, **51**, 5552–5558.

390 M. Tuinier, M. van Sint Annaland, G. J. Kramer and J. Kuipers, *Chem. Eng. Sci.*, 2010, **65**, 114–119.

391 Q. Fu, C. Song, Y. Liu, M. Ishizuka and A. Tsutsumi, *Energy Procedia*, 2014, **61**, 1673–1676.

392 A. Hart and N. Gnanendran, *Energy Procedia*, 2009, **1**, 697–706.

393 R. Amin, A. T. Jackson and T. Kennaird, The Cryocell: an advanced gas sweetening technology, *International Petroleum Technology Conference*, 2005, IPTC-10106-MS.

394 S. Iglauer, C. Pentland and A. Busch, *Water Resour. Res.*, 2015, **51**, 729–774.

395 J. Park, S. Yoon, S.-Y. Oh, Y. Kim and J.-K. Kim, *Energy*, 2021, **214**, 118844.

396 H. Ababneh, A. AlNouss, I. A. Karimi and S. A. Al-Muhtaseb, *Energies*, 2022, **15**, 5286.

397 H. Li, R. Zhang, T. Wang, X. Sun, C. Hou, R. Xu, Y. Wu and Z. Tang, *Carbon Capture Sci. Technol.*, 2022, **3**, 100012.

398 D. Haldar, N. Bhattacharjee, A. M. Shabbirahmed, G. S. Anisha, A. K. Patel, J.-S. Chang, C.-D. Dong and R. R. Singhania, *Biomass Bioenergy*, 2023, **173**, 106804.

399 R. A. Sheldon, *Chem. Commun.*, 2008, 3352–3365.

400 M. Becker, S. Lütz and K. Rosenthal, *Molecules*, 2021, **26**, 573.

401 P. Anastas and N. Eghbali, *Chem. Soc. Rev.*, 2010, **39**, 301–312.

402 J. B. Zimmerman, P. T. Anastas, H. C. Erythropel and W. Leitner, *Science*, 2020, **367**, 397–400.

403 H. Zhang, L. Chen, Y. Chen and Z. Wang, *Braz. J. Chem. Eng.*, 2023, 1–35.

404 F. Li, A. Laaksonen, X. Zhang and X. Ji, *Ind. Eng. Chem. Res.*, 2022, **61**, 2643–2671.

405 B. H. Lipshutz, N. A. Isley, J. C. Fennewald and E. D. Slack, *Angew. Chem., Int. Ed.*, 2013, **52**, 10952–10958.

406 B. Wu, W. Liu, Y. Zhang and H. Wang, *Chem.–Eur. J.*, 2009, **15**, 1804–1810.

407 S. I. Abu-Eishah, *Ionic Liquids-Classes and Properties*, 2011, pp. 239–272.

408 S. Ravula, N. E. Larm, M. A. Mottaleb, M. P. Heitz and G. A. Baker, *ChemEngineering*, 2019, **3**, 42.

409 E. Maria Siedlecka, M. Czerwicka, S. Stolte and P. Stepnowski, *Curr. Org. Chem.*, 2011, **15**, 1974–1991.

410 A. S. Berenblyum, E. A. Katsman and Y. Z. Karasev, *Appl. Catal., A*, 2006, **315**, 128–134.

411 R. Abro, A. A. Abdeltawab, S. S. Al-Deyab, G. Yu, A. B. Qazi, S. Gao and X. Chen, *RSC Adv.*, 2014, **4**, 35302–35317.